Title
Signal recognition particler dependent protein targeting in yeast (Saccharomyces cerevisiae)

Author
Ogg, Stephen C.

Publication Date
1995

Peer reviewed|Thesis/dissertation

Signal Recognition Particle Dependent Protein Targeting in Yeast
(Saccharomyces cerevisiae)

by

Stephen C. Ogg

DISSERTATION

Submitted in partial satisfaction of the requirements for the degree of

DOCTOR OF PHILOSOPHY

in

Cell BIOLOGY

in the

GRADUATE DIVISION

of the

UNIVERSITY OF CALIFORNIA

San Francisco

This work is dedicated to my parents,

and to my family.

Acknowledgments

I've heard that this is the easiest part of the thesis to write. If I were to thank everyone who made this possible, however, the list would be endless. So with apologies to those who contributed, but are not explicitly acknowledged, here goes. I'll begin with Peter, who has been a terrific advisor. He has an uncanny knack of taking raw data and turning it into a testable model that is more often than not, correct. He has taught me to keep in mind that understanding the biology of the problem is the ultimate goal. I have gained a great appreciation from this holistic view of the cell. I also appreciate the success that Peter has had in maintaining a socially enjoyable atmosphere in the lab.

I would also like to thank the other members of my thesis committee for their comments and investment of time and energy into this project. Henry Bourne is a wonderful scientist, I thank him for his practicality, for his down to earth demeanor and sincere sense of humor. Randy Schekman has provided many insights during our discussions and always shows a genuine interest with seemingly endless suggestions for new avenues of approach, just in case.

I am deeply indebted to Dr. Marvin Wickens for starting me in this business. His encouragement, unfailing enthusiasm, and suggestion that I should consider UCSF as one of my graduate school choices can not be fully compensated. Another person who deserves mention is Jodi Nunnari, her friendship is one of the things I will take with me, when (if ever) I leave UCSF. A constant badger, she has helped me with too many things to list, suffice it to say that without her I wouldn't be able to transform binding data into a Scatchard plot. In addition, I have had the pleasure of working closely

with several other members of the Walter lab. Byron Hann was my role model for how much time a graduate student should spend in the lab. Mark Poritz was my initial mentor in the Walter lab, and it was his work that set the stage for this thesis.

I would also like to specifically thank members of the Walter lab who provided all of the advice, support, and reagents necessary for a graduate student to complete a thesis. I am thankful to Sandy Wolin and Davis Ng for putting up with me as bay mates; Josh Miller for his room at 250 Kirkham; Dieter Zopf for much helpful advice about cloning; Jeremy Brown for the Scottish yeast expertise he brought to the lab; Jeff Cox, Jan Moskaug, Caroline Shamu for sharing advice, strains and plasmids.

Without the close knit community that is UCSF, I would have foundered at the outset of my graduate career. Many thanks go to the members of the Herskowitz and Guthrie lab members for providing reagents, plates, and expertise on yeast that was lacking in the Walter lab. The overcrowded working space that was endured on a day to day basis, was also the source of one of the most enticing features of UCSF–the ability to obtain help and expertise in many areas was always within easy walking distance. In addition I would like to thank Aaron Neiman for introducing me to Thompson canyon.

Finally, I thank my family. My father and mother have nourished my zeal for curiosity. I cannot thank them enough for their years of faith, support and encouragement. Thanks also go to my daughter, Madison, for keeping my life exciting. Last but not least thank you Amy, for your ability to endure this crazy time in our lives.

ABSTRACT

Signal Recognition Particle Dependent Protein Targeting in *Saccharomyces cerevisiae*

Stephen C. Ogg

As cells grow, they must accurately target proteins from the cytosol into or across the membrane of the endoplasmic reticulum (ER). A mammalian *in vitro* model system has identified two factors important for the targeting of nascent proteins; the signal recognition particle (SRP), and the SRP receptor (SR). In this work, we have identified and characterized the SR homolog in the yeast *Saccharomyces cerevisiae*. Using a reverse genetic approach, we identified and cloned genes encoding both subunits of the heterodimeric SR (encoded by *SRP101* and *SRP102*). Consistent with the notion that the proteins encoded by these genes are important for protein targeting in yeast, depletion of either one of these two gene products results in impaired translocation into the ER. Like their mammalian counterparts, both yeast subunits are localized to the ER and can be isolated as a heterodimeric complex. Additionally, both subunits are predicted by sequence analogy to be GTPases. Cells grown for long periods in the absence of either Srp101p or Srp102p no longer show pronounced protein translocation defects. This adaptation is a physiological process and is strain dependent.

In a separate approach, we investigated the SRP–ribosome interaction in the yeast *S. cerevisiae*. Using the observation that cycloheximide can suppress the temperature-sensitive defects of *sec65-1* (encoding the *S. cerevisiae* SRP19 homologue) as a starting point, we propose that SRP cycles

on and off translating ribosomes at a specific steps during translation elongation cycle to inspect all nascent chains for the presence of a signal sequence.

Cells deleted for either SR subunit have a reduced growth rate, and introduction of a complementing plasmid into these strains does not result in an increased growth rate. Unexpectedly, protein expressed from the plasmid is correctly localized and forms a heterodimeric SR complex. The same plasmid, however, when placed into a diploid cell heterozygous for the deletion for one of the SR subunits, is able to complement the growth rate after sporulation of the heterozygous diploid into a haploid strain containing both the gene deletion and the plasmid. To explain this observation, we postulate that preexisting SR is required for the conversion of newly synthesized SR into functional SR.

Peter Walter 6/13/95

TABLE OF CONTENTS

List of figures

(exclusive of chapter 2)

Chapter 3

Chapter 4

Chapter 5

Chapter 1

Introduction

Background

To be eucaryotic means to be compartmentalized. Although compartmentalization provides the answers to some of life's problems, it also creates special problems itself. As permeability barriers, membranes prevent the passage of hydrophilic molecules, yet subcellular organelles (bounded by one or more membranes) must be provided with all the components necessary for organellar function. Thus, the cell must have a means of directing proteins to their correct subcellular address. Most proteins synthesized in eucaryotic cells, however, begin their life as precursors on ribosomes in the cytosol. How then do those proteins that need to gain access to one of the other cellular compartments do so? Commonly, the cell uses two mechanisms for achieving this goal. A protein can either enter the secretory pathway in a co-translational mode and be targeted to an organelle in a vesicle mediated manner, or it can be imported into an organelle directly from the cytosol in a post-translational mode (e.g. mitochondria (Maccecchini et al., 1979), chloroplasts (Dobberstein et al., 1977), peroxisomes (Goldman and Blobel, 1978)). Proteins that are destined to enter the secretory pathway are initially targeted to the endoplasmic reticulum (ER) by virtue of an amino terminal signal sequence. ER targeting is a two step process achieved by interaction of this signal sequence, with a cytosolic ER targeting factor, signal recognition particle (SRP), and subsequent interaction of the SRP-ribosome-nascent chain complex with the SRP receptor (SR) in the membrane of the ER. Once inside the ER, proteins may undergo N-linked core glycosylation, oligomerization, and further maturation. The proteins may then travel in membrane bound vesicles from the ER to the Golgi complex, where they can undergo further carbohydrate modification and maturation. In the trans

Golgi network, lysosomal proteins are sorted and targeted to the lysosome, while secretory proteins are delivered to the cell's surface.

The process of co-translational translocation; i.e. the process of selecting a protein from the entire translational pool, and delivering the selected protein to the membrane of the ER– is the subject of this thesis.

In the Beginning

In 1975, Blobel and Dobberstein introduced the signal sequence hypothesis (Blobel and Dobberstein, 1975). They proposed that secretory proteins whose biogenesis originates in the cytoplasm contain information in the form of a hydrophobic "signal sequence" that is necessary and sufficient to direct the protein into the secretory pathway. Although now taken for granted, we still do not understand some of the basic questions of this hypothesis. For instance, the signal sequence (~15-20 amino acids) usually consists of a amino-terminal hydrophobic core flanked by charged residues. How can the relatively low information content contained in these few amino acids be sufficient to direct the targeting of the protein to the export pathway?

In *in vitro* assays developed from mammalian cells, a cytoplasmic particle (SRP) was identified that interacted with signal sequences and promoted translocation of nascent secretory proteins into microsomal vesicles derived from the ER membrane (Walter and Blobel, 1980). Purified on the basis of promoting translocation activity into these microsomes, SRP was shown to consist of six proteins (named according to their molecular weight in kilodaltons: SRP9, SRP14, SRP19, SRP54, SRP68, and SRP72) and one RNA molecule (7SL RNA) (Walter and Blobel, 1980; Walter and Blobel,

1982; Ullu et al., 1982). Extensive characterization of purified SRP *in vitro* led to a model of its function (Walter et al., 1984; updated in Walter and Johnson, 1994). Scanning all ribosomes synthesizing polypeptides, SRP only interacts productively with those ribosome-nascent chain complexes synthesizing preproteins destined to be targeted to the ER membrane (Walter et al., 1981). This "high affinity" binding occurs through an interaction between SRP and the signal sequence of the nascent protein. Because signal sequences are usually amino-terminal, they are the first feature to emerge from the ribosome, providing a binding site for SRP prior to the nascent chain's completion. In the presence of a signal sequence, SRP's affinity for the ribosome increases by three orders of magnitude, and translational elongation of the nascent protein is temporarily suspended (Walter and Blobel, 1981). Another required component of translocation identified with the in vitro assay was the SR (Gilmore et al., 1982; Meyer et al., 1982). Interaction of SRP with SR (composed of a 69 kDa α-subunit (SRα) and a 30 kDa β-subunit (SRβ)) (Tajima et al., 1986) in the membrane of the ER results in targeting of the nascent chain-ribosome complex to the ER. Once targeted, the ribosome-nascent chain complex is released from the SRP/SR (Gilmore and Blobel, 1983) complex and becomes productively engaged with components forming the translocation pore (translocon). Finally, SRP is released from the SRP receptor and is free to perform another round of targeting. SRP thus functionally couples protein translation in the cytosol to protein translocation on the cytosolic face of the ER membrane.

Towards the Middle

The translocation problem in yeast was initially approached in the same manner. Experiments to reconstitute yeast translocation in vitro

revealed differences from the hypothesis obtained from work in the mammalian system. It seemed that, for at least some proteins, translocation into the ER could be performed post-translationally (Hansen et al., 1986; Rothblatt and Meyer, 1986; Waters et al., 1986). Prepro-α-factor and carboxypeptidase Y could be fully translated, released from the ribosomes, and post-translationally imported into yeast microsomes in an ATP dependent manner (Hansen, et al., 1986; Rothblatt and Meyer, 1986; Waters, et al., 1986). Cytosolic chaperones in the form of the Hsp70p's were also shown to stimulate this post-translational translocation (Waters and Blobel, 1986; Chirico et al., 1988; Deshaies et al., 1988). Invertase, however, could only be translocated into yeast microsomes in a co-translational mode (Hansen and Walter, 1988).

Genetic selections in *S. cerevisiae* designed to identify proteins involved in translocation had failed to identify components of an SRP. *SEC61*, *SEC62*, and *SEC63* were identified and shown to be required for the translocation of prepro-α-factor, carboxypeptidase Y and invertase (Deshaies and Schekman, 1987; Rothblatt et al., 1989). The products encoded by these genes have been shown to be integral membrane proteins of the ER (Deshaies and Schekman, 1989; Deshaies and Schekman, 1990). In addition, genetic schemes from *E. coli* had also identified a number of proteins important for translocation into the periplasm (topologically equivalent to the mammalian ER) (reviewed in Deshaies, et al., 1988; Bieker et al., 1990; Schatz and Beckwith, 1990). Again none of these genetically identified components (*secY*, *secE*, *secA*, *secB*) resembled anything like an SRP constituent.

Balanced against mounting evidence that *S. cerevisiae* and *E. coli* have a fundamentally different targeting pathway from mammalian cells, was

evidence identifying SRP RNA homologs from yeast, archae, and procaryotic species (Struck et al., 1988; Poritz et al., 1988b). These RNAs were identified on the basis of a phylogenetically conserved stem-loop structure. In *E. coli*, the 4.5S RNA (*ffs*) is a minimal SRP RNA resembling only the most highly conserved loop of the SRP RNA (Poritz, et al., 1988b). Structural SRP RNA homologs from both *Schizosaccharomyces pombe* and *Yarrowia lipolytica* have also been identified (Poritz et al., 1988a).

Most Recently

In the end, the route to identifying the SRP pathway in *S. cerevisiae* was unexpected. Cloning of the mammalian *SRP54* gene was underway when I joined the laboratory. Experiments demonstrating that SRP54 was the subunit responsible for signal sequence binding (Krieg et al., 1986; Kurzchalia et al., 1986) had resulted in a flurry of activity in our lab as well as the lab of Bernhard Dobberstein. Simultaneously, the two groups published the sequence of the protein encoded by SRP54 (Bernstein et al., 1989; Römisch et al., 1989). In this case the sequence revealed a plethora of information about the protein's possible function. The amino terminal half of the protein contained a GTPase domain, while the carboxy-terminal portion of the protein was unusually–rich in methionine. Subsequent analysis has shown that the methionine rich domain binds to signal sequences as well as to the SRP RNA (Zopf et al., 1990; Römisch et al., 1990). Database searches to find homologous proteins revealed that the GTPase domain of SRP54 diverged enough from canonical GTPase sequences to be considered a separate sub-family in the *ras* superfamily. Unexpectedly, SRα, a known GTP-binding protein (Connolly and Gilmore, 1989), was also found to belong to the same sub-family of GTPases. In addition, two *E. coli* proteins, Ffh (fifty-four

homolog) and FtsY were found to be similar to SRP54 and SRα, respectively (Bernstein et al., 1989; Römisch et al., 1989). This discovery opened the door for our lab to identify and clone all of the components from an SRP-dependent targeting pathway in the yeast *Saccharomyces cerevi*siae (Hann et al., 1989; Hann and Walter, 1991; Hann et al., 1992; Ogg et al., 1992; Ogg and Walter, 1995b; Brown et al., 1994). We chose *S. cerevisiae* to characterize the role of SRP in vivo for many reasons. It has well documented procedures to take advantage of both biochemical and genetic approaches towards understanding the role of SRP *in vivo*.

Conserved regions between SRP54 and Ffh, as well as regions conserved between SRα and FtsY were used to design degenerate primers, and then used with the polymerase chain reaction (PCR) to identify the genes in *S. cerevisiae* that were homologous to the mammalian SRP54 and SRα. Chapter 2 contains the identification of the *S. cerevisiae* SRα homolog (encoded by the *SRP101* gene) using this technique (Ogg, et al., 1992). Subsequent work by Byron Hann in our lab showed that the *S. cerevisiae* SRP RNA homolog was the previously identified *SCR1* RNA (Hann and Walter, 1991). Purification of a particle containing these two components led to the cloning of the rest of the SRP subunits (Brown, et al., 1994). When I began this work the degenerate primers used in identifying the *S. cerevisiae SRP54* and SRα homologs had just been synthesized.

The goal of this thesis was to identify and characterize the yeast SRP receptor. After the initial success of cloning the homolog to the SRα subunit (Srp101p), several approaches were taken to identify the yeast SRβ homolog. I reasoned that suppression of a conditional allele of *SRP101* would identify components with which it interacted, leading to the identification of SRβ, and

perhaps other interacting components. Attempts to obtain a temperature sensitive allele of *SRP101* by random chemical induced mutagenesis were unsuccessful, and I resorted to a biochemical scheme in order to identify SRβ. I raised antibodies against Srp101p, and began using these antibodies in an attempt to indirectly immunoprecipitate the yeast SRβ homolog by virtue of its interaction with Srp101p. These efforts were thwarted, however, by the inability of our α-Srp101p antibodies, raised against SDS-denatured Srp101p, to recognize the native form of Srp101p. At this point, I focused my attention on an observation that was to become Chapter 4 of this work (see below). The cloning of the yeast SRβ homolog would have to wait for the yeast genome sequencing project to progress. Recent identification of the mammalian SRβ gene (Miller et al., 1995) illustrates how far yeast genetics has come in the last five years. Instead of a laborious reverse genetic approach employed for identification of the yeast SRα, SRβ was already in the sequence database, and mapped to chromosome XI as an unidentified open reading frame, thanks to the yeast genome sequencing project. Chapter 3 describes the cloning and subsequent characterization of the yeast SRβ, (encoded by *SRP102*) as well as some characteristics of the whole yeast SR (Ogg and Walter, 1995b).

Recent convergence of the reverse genetic approach taken by our lab, and a more traditional genetic approach (selecting for mutants) has allowed the identification of one of the subunits of SRP. *SEC65*, originally isolated in a selection for the mislocalization of a protein targeted to the ER (Stirling et al., 1992), is also the homolog to the mammalian SRP19 (Stirling and Hewitt, 1992; Hann, et al., 1992). Chapter 4 describes how, using an observation specific to Sec65p, we obtain *in vivo* evidence for an SRP sampling model

during the initial selection of ribosomes from the cytoplasmic translational pool (Ogg and Walter, 1995a).

A divergence from the characterization of the SRP-dependent protein targeting pathway in yeast is presented in Chapter 5. I describe how an unusual observation concerning the SR genes in yeast may lead to evidence in favor of the hypothesis that cellular membranes are endowed with spatial, temporal, and functional continuity.

REFERENCES

Bernstein, H. D., Poritz, M. A., Strub, K., Hoben, P. J., Brenner, S. and Walter, P. (1989). Model for signal sequence recognition from amino-acid sequence of 54k subunit of signal recognition particle. Nature *340*, 482-486.

Bieker, K. L., Philips, G. J. and Silhavy, T. (1990). The *sec* and *prl* genes of E. coli. J. Bioenerg. Biomem. *22*, 291-310.

Blobel, G. and Dobberstein, B. (1975). Transfer of proteins across the membrane. I. Presence of proteolytically processed and unprocessed nascent immunoglobulin light chains on membrane-bound ribosomes of murine myeloma. J. Cell Biol. *67*, 835-851.

Brown, J. D., Hann, B. C., Medzihradszky, K. F., Niwa, M., Burlingame, A. L. and Walter, P. (1994). Subunits of the *Saccharomyces cerevisiae* signal recognition particle required for its functional expression. EMBO J. *13*, 4390-4400.

Chirico, W. J., Waters, M. G. and Blobel, G. (1988). 70K heat shock related proteins stimulate protein translocation into microsomes. Nature *332*, 805-10.

Connolly, T. and Gilmore, R. (1989). The signal recognition particle receptor mediates the GTP-dependent displacement of SRP from the signal sequence of the nascent polypeptide. Cell *57*, 599-610.

Deshaies, R. J., Koch, B. D., Werner, W. M., Craig, E. A. and Schekman, R. (1988). A subfamily of stress proteins facilitates translocation of secretory and mitochondrial precursor polypeptides. Nature *332*, 800-805.

Deshaies, R. J. and Schekman, R. (1987). A yeast mutant defective at an early stage in import of secretory protein precursors into the endoplasmic reticulum. J. Cell Biol. *105*, 633-45.

Deshaies, R. J. and Schekman, R. (1989). SEC62 encodes a putative membrane protein required for protein translocation into the yeast endoplasmic reticulum. J. Cell Biol. *109*, 2653-2664.

Deshaies, R. J. and Schekman, R. (1990). Structural and functional dissection of Sec62p, a membrane-bound component of the yeast endoplasmic reticulum protein import machinery. Mol. Cell. Biol. *10*, 6024-6035.

Dobberstein, B., Blobel, G. and Chua, N.-H. (1977). In vitro synthesis and processing of a putative precursor for the small subunit of ribulose-1,5-bisphosphate carboxylase of *Chlamydomonas reinhardtii*. Proc. Natl. Acad. Sci. USA *74*, 1082-1085.

Gilmore, R. and Blobel, G. (1983). Transient involvement of signal recognition particle and its receptor in the microsomal membrane prior to protein translocation. Cell *35*, 677-685.

Gilmore, R., Walter, P. and Blobel, G. (1982). Protein translocation across the endoplasmic reticulum. II. Isolation and characterization of the signal recognition particle receptor. J. Cell Biol. *95*, 470-477.

Goldman, B. L. and Blobel, G. (1978). Biogenesis of peroxisomes: intracellular site of synthesis of catalase and uricase. Proc. Natl. Acad. Sci. USA *75*, 5066-5070.

Hann, B., Stirling, C., J. and Walter, P. (1992). *SEC65* gene product is a subunit of the yeast signal recognition particle required for its integrity. Nature *356*, 532-533.

Hann, B. C., Poritz, M. A. and Walter, P. (1989). *Saccharomyces cerevisiae* and *Schizosaccharomyces pombe* Contain a Homologue to the 54-kD Subunit of The Signal Recognition Particle That in *S. cerevisiae* Is Essential for Growth. J. Cell Biol. *109*, 3223-3230.

Hann, B. C. and Walter, P. (1991). The Signal Recognition Particle in *S. cerevisiae*. Cell *67*, 131-144.

Hansen, W., Garcia, P. D. and Walter, P. (1986). In vitro protein translocation across the yeast endoplasmic reticulum: ATP-dependent post-translational translocation of the prepro-α factor. Cell *45*, 397-406.

Hansen, W. and Walter, P. (1988). Prepro-carboxypeptidase Y and a truncated form of pre-invertase, but not full-length pre-invertase, can be

posttranslationally translocated across microsomal vesicle membranes from *Saccharomyces cerevisiae*. J. Cell Biol.*106*, 1075-1081.

Krieg, U. C., Walter, P. and Johnson, A. E. (1986). Photocrosslinking of the signal sequence of nascent preprolactin to the 54-kilodalton polypeptide of the signal recognition particle. Proc. Natl. Acad. Sci. USA *83*, 8604-8608.

Kurzchalia, T. V., Wiedmann, M., Girshovich, A. S., Bochkareva, E. S., Bielka, H. and Rapoport, T. A. (1986). The signal sequence of nascent preprolactin interacts with the 54K polypeptide of the signal recognition particle. Nature *320*, 634-636.

Maccecchini, M. L., Rudin, Y. and Schatz, G. (1979). Transport of proteins across the mitochondrial outer membrane. A precursor form of the cytoplasmically made intermembrane enzyme cytochrome c peroxidase. J. Biol. Chem. *254*, 7468-7471.

Meyer, D. I., Krause, E. and Dobberstein, B. (1982). Secretory protein translocation across membranes- the role of the docking protein. Nature *297*, 647-650.

Miller, J. D., Tajima, S., Lauffer, L. and Walter, P. (1995). The β-subunit of the signal recognition particle receptor is a transmembrane GTPase that anchors the α-subunit, a peripheral membrane GTPase, to the endoplasmic reticulum membrane. J. Cell Biol.*128*, 273-282.

Ogg, S., Poritz, M. and Walter, P. (1992). The signal recognition particle receptor is important for growth and protein secretion in *Saccharomyces cerevisiae*. Mol. Biol. Cell *3*, 895-911.

Ogg, S. C. and Walter, P. (1995a). SRP interacts with ribosomes at a specific step during translational elongation. Cell *In press*,

Ogg, S. C. and Walter, P. (1995b). The Saccharomyces cerevisiae Signal Recognition Particle receptor consists of two interacting subunits both of which are GTPases. J. Cell Biol. in preparation

Poritz, M. A., Siegel, V., Hansen, W. J. and Walter, P. (1988a). Small ribonucleoproteins in Schizosaccharomyces pombe and Yarrowia lipolytica homologous to signal recognition particle. Proc. Natl. Acad. Sci. USA *85*, 4315-4319.

Poritz, M. A., Strub, K. and Walter, P. (1988b). Human SRP RNA and E. coli 4.5S RNA contain a highly homologous structural domain. Cell *55*, 4-6.

Römisch, K., Webb, J., Herz, J., Prehn, S., Frank, R., Vingron, M. and Dobberstein, B. (1989). Homology of the 54K Protein of signal recognition particle, docking protein, and two E. coli proteins with putative GTP-binding domains. Nature *340*, 478-482.

Römisch, K., Webb, J., Lingelbach, K., Gausepohl, H. and Dobberstein, B. (1990). The 54-kD protein of signal recognition particle contains a methionine-rich RNA binding domain. J. Cell Biol. *111*, 1793-1802.

Rothblatt, J. A., Deshaies, R. J., Sanders, S. L., Daum, G. and Schekman, R. (1989). Multiple Genes are Required for Proper Insertion of Secretory Proteins Into the Endoplasmic Reticulum in Yeast. J. Cell Biol. *72*, 61-68.

Rothblatt, J. A. and Meyer, D. I. (1986). Secretion in yeast: Translocation and glycosylation of prepro-α factor in vitro can occur via ATP-dependent post-translational mechanism. EMBO J. *5*, 1031-1036.

Schatz, P. J. and Beckwith, J. (1990). Genetic analysis of protein export in Escherichia coli. Ann. Rev. Genet. *24*, 215-248.

Stirling, C. J. and Hewitt, E. W. (1992). The *Saccharomyces cerevisiae SEC65* gene encodes a component of the yeast signal recognition particle with homology to human SRP19. Nature *356*, 534-537.

Stirling, C. J., Rothblatt, J., Hosobuchi, M., Deshaies, R. and Schekman, R. (1992). Protein translocation mutants defective in the insertion of integral membrane proteins into the endoplasmic reticulum. Mol. Biol. Cell *3*, 129-142.

Struck, J. C. R., Toschka, H. Y., Specht, T. and Erdmann, V. A. (1988). Common structural features between eukaryotic 7SL RNAs, eubacterial 4.5S RNA and scRNA and archaebacterial 7S RNA. Nuc. Acids Res. *16*, 7740.

Tajima, S., Lauffer, L., Rath, V. L. and Walter, P. (1986). The signal recognition particle receptor is a complex that contains two distinct polypeptide chains. J. Cell Biol. *103*, 1167-1178.

Ullu, E., Murphy, S. and Melli, M. (1982). Human 7SL RNA consists of a 140 nucleotide middle-repetitive sequence inserted in an Alu sequence. Cell *29*, 195-202.

Walter, P. and Blobel, G. (1980). Purification of membrane-associated protein complex required for protein translocation across the endoplasmic reticulum. Proc. Natl. Acad. Sci. USA *77*, 7112-7116.

Walter, P. and Blobel, G. (1981). Translocation of proteins across the endoplasmic reticulum. III. Signal recognition protein (SRP) causes signal sequence and site specific arrest of chain elongation that is released by microsomal membranes. J. Cell Biol. *91*, 557-561.

Walter, P. and Blobel, G. (1982). Signal recognition particle contains a 7S RNA essential for protein translocation across the endoplasmic reticulum. Nature *299*, 691-698.

Walter, P., Gilmore, R. and Blobel, G. (1984). Protein translocation across the endoplasmic reticulum. Cell *38*, 5-8.

Walter, P., Ibrahimi, I. and Blobel, G. (1981). Translocation of proteins across the endoplasmic reticulum I. Signal Recognition Protein (SRP) binds to in

vitro assembled polysomes synthesizing secretory protein. J. Cell Biol. *91*, 545-550.

Walter, P. and Johnson, A. E. (1994). Signal Sequence Recognition and Protein Targeting to the Endoplasmic Reticulum Membrane. Ann. Rev. Cell Biol.*10*, 87-119.

Waters, G. and Blobel, G. (1986). Secretory protein translocation in a yeast cell free system can occur post-translationally and requires ATP hydrolysis. J. Cell Biol. *102*, 1543-1550.

Waters, M. G., Chirico, W. J. and Blobel, G. (1986). Protein translocation across the yeast microsomal membrane is stimulated by a soluble factor. J. Cell Biol. *103*, 2629-2636.

Zopf, D., Bernstein, H. D., Johnson, A. E. and Walter, P. (1990). The methionine-rich domain of the 54 kd protein subunit of the signal recognition particle contains an RNA binding site and can be crosslinked to a signal sequence. EMBO J. *9*, 4511-4517.

Chapter 2

Signal Recognition Particle Receptor Is Important for Cell Growth and Protein Secretion in *Saccharomyces cerevisiae*

Molecular Biology of the Cell
Vol. 3, 895-911, August 1992

Signal Recognition Particle Receptor is Important for Cell Growth and Protein Secretion in *Saccharomyces cerevisiae*

Stephen C. Ogg, Mark A. Poritz, and Peter Walter

Department of Biochemistry and Biophysics, University of California, Medical School, San Francisco, California 94143-0448

Submitted March 24, 1992; Accepted June 17, 1992

In mammalian cells, the signal recognition particle (SRP) receptor is required for the targeting of nascent secretory proteins to the endoplasmic reticulum (ER) membrane. We have identified the *Saccharomyces cerevisiae* homologue of the α-subunit of the SRP receptor (SRα) and characterized its function in vivo. *S. cerevisiae* SRα is a 69-kDa peripheral membrane protein that is 32% identical (54% chemically similar) to its mammalian homologue and, like mammalian SRα, is predicted to contain a GTP binding domain. Yeast cells that contain the SRα gene (*SRP101*) under control of the *GAL1* promoter show impaired translocation of soluble and membrane proteins across the ER membrane after depletion of SRα. The degree of the translocation defect varies for different proteins. The defects are similar to those observed in SRP deficient cells. Disruption of the *SRP101* gene results in an approximately sixfold reduction in the growth rate of the cells. Disruption of the gene encoding SRP RNA (*SCR1*) or both *SCR1* and *SRP101* resulted in an indistinguishable growth phenotype, indicating that SRP receptor and SRP function in the same pathway. Taken together, these results suggest that the components and the mechanism of the SRP-dependent protein targeting pathway are evolutionarily conserved yet not essential for cell growth. Surprisingly, cells that are grown for a prolonged time in the absence of SRP or SRP receptor no longer show pronounced protein translocation defects. This adaptation is a physiological process and is not due to the accumulation of a suppressor mutation. The degree of this adaptation is strain dependent.

INTRODUCTION

Mammalian signal recognition particle (SRP)[1] acts to target ribosomes that synthesize secretory and membrane proteins to the endoplasmic reticulum (ER) membrane where they are translocated across the membrane into the ER lumen. In vitro assays have allowed the development of a detailed model describing the function of SRP in mammalian cells (Walter and Lingappa, 1986, for review). In brief, signal sequences that are expressed as part of a nascent protein chain emerging from the ribosome bind to SRP in a binding site contained on the 54-kDa SRP subunit (SRP54) (Krieg *et al.*, 1986; Kurzchalia *et al.*, 1986). This interaction causes SRP to bind tightly to the ribosome, effecting an elongation arrest or pause in the translation of the nascent secretory protein. Interaction of the engaged SRP with the SRP receptor, a heterodimeric membrane protein, that is anchored in the ER membrane (Gilmore *et al.*, 1982a; Meyer *et al.*, 1982; Tajima *et al.*, 1986) releases the translational arrest and allows the ribosome that is synthesizing the protein chain to become bound to other components in the ER membrane. These components, collectively termed a "translocon," allow the transfer of the growing protein chain across the membrane, presumably through a transient aqueous pore in the membrane (Gilmore and Blobel, 1985; Simon and Blobel, 1991). SRP and SRP receptor act catalytically in this

[1] *Abbreviations used:* bp, base pair; CPY, carboxypeptidase Y; DPAP-B, dipeptidyl aminopeptidase-B; DTT, dithiothreitol; ER, endoplasmic reticulum; HEPES, *N*-2-hydroxyethylpiperazine-*N*'-ethanesulfonic acid; kb, kilobase; PCR, polymerase chain reaction; SDS-PAGE, sodium dodecyl sulfate-polyacrylamide gel electrophoresis; SRα, SRP receptor α-subunit; SRβ, SRP receptor β-subunit; SRP, signal recognition particle; SRP54, 54-kDa subunit of SRP; Tris, tris-(hydroxymethyl)aminomethane.

process; they are not part of the ribosome-membrane junction that mediates the transfer of the protein chain across the lipid bilayer. Rather, they function to bring the ribosome to the correct target membrane and are then released from the ribosome (Gilmore and Blobel, 1983).

Interestingly, SRP54 and the α-subunit of the SRP receptor (SRα) both contain a GTPase domain (G-domain) (Bernstein *et al.*, 1989; Connolly and Gilmore, 1989; Römisch *et al.*, 1989). The G-domains of SRP54 and SRα are homologous to one another and define a new family of GTPases. The β-subunit of the SRP receptor (SRβ) also contains a GTPase domain, which is structurally distinct from those of SRP54 and SRα (Miller and Walter, unpublished data). The precise mechanistic role of each of the three GTPase domains that interact during the SRP-dependent protein targeting reaction remains to be elucidated. Cycles of GTP hydrolysis by SRP54 and SRP receptor may control the assembly of the SRP-signal sequence-ribosome complex and the assembly of components of the translocon. Thus, GTP hydrolysis may enhance the fidelity of and provide unidirectionality to the targeting reaction. Point mutations in the GTP binding sites of SRP54 and SRα block the translocation of proteins across the ER membrane (Rapiejko and Gilmore, 1992; Bernstein and Walter, unpublished data), indicating that both GTP binding sites are functionally important in the pathway.

Recently, components of a SRP have been identified and characterized in *Saccharomyces cerevisiae* (Hann and Walter, 1991; Hann *et al.*, 1992; Stirling and Hewitt, 1992). The yeast SRP is a 16S cytoplasmic ribonucleoprotein that is important for the targeting of membrane and secretory proteins to the ER membrane. *S. cerevisiae* SRP is not essential for cell growth, although cells in which SRP is genetically disrupted grow poorly. The translocation of a number of soluble and membrane proteins into the lumen of the ER is impaired in SRP deficient cells. Surprisingly, different proteins show translocation defects of varying severity. After SRP depletion, the membrane integration of dipeptidyl aminopeptidase B (DPAP-B) is inhibited by over 90%, the translocation of preKAR2p is inhibited by ~50%, and the translocation of preprocarboxypeptidase Y (preproCPY) is not affected. Thus, in the absence of SRP, proteins are targeted via an SRP-independent pathway to the ER membrane and are translocated in sufficient amounts to sustain cell growth. Some proteins, however, cannot efficiently use the SRP-independent pathway.

The approach that lead to the first identification of the yeast SRP took advantage of the phylogenetic conservation of the primary structure of the mammalian SRP54 and its prokaryotic homologue, the product of the *ffh* gene of *Escherichia coli*. Comparison of these evolutionary distant sequences allowed the identification of conserved blocks of amino acids that were used in a polymerase chain reaction (PCR)-based approach to isolate the gene (*SRP54*) encoding the corresponding protein from *S. cerevisiae* (Hann *et al.*, 1989). Here we have used a similar method to identify an SRα homologue in *S. cerevisiae*.

MATERIALS AND METHODS

Strains, Antibodies, and General Methods

Yeast strains used in this study are listed in Table 1. Genetic techniques were performed as described by Sherman *et al.* (1974), except where noted. Anti-DPAP-B serum was kindly provided by Tom Stevens, Institute of Molecular Biology, University of Oregon, Eugene; anti-KAR2p by Mark Rose, Biology Department, Princeton University, Princeton, NJ; anti-invertase, anti-CPY, anti-Sec61p, and anti-prepro-α-factor by Randy Schekman, Division of Biochemistry and Molecular Biology, University of California at Berkeley; and anti-$F_1\beta$ATPase by M. Yaffe, Department of Biology, University of California, San Diego. Recombinant DNA techniques were performed as described in Maniatis *et al.* (1982). Oligonucleotides were synthesized on a Milligen/Biosearch Cyclone Plus DNA synthesizer (Milligen/Biosearch, Division of Millipore, Novato, CA) and purified according to the manufacturer's instructions. Sodium dodecyl sulfate-polyacrylamide gel electrophoresis (SDS-PAGE) was performed on 10–15% gradient gels and all Western blots were visualized by enhanced chemiluminescence (Amersham, Arlington Heights, IL) according to the instructions of the manufacturer.

PCR and Cloning of SRP101

PCR was performed on *S. cerevisiae* genomic DNA as described (Saiki *et al.*, 1988; Hann *et al.*, 1989; Kamb *et al.*, 1989). The oligonucleotide "A" had the sequence 5'-GGTGTNAA(T/C)GGNGTNGGNAA-3' (20mer, 512-fold degenerate) and encoded the amino acid sequence GVNGVGK. The reverse complement of oligonucleotide "B" with the sequence 5'-CN(G/C)CNGCNC(G/T)(A/G)AANGT(A/G)TC-3' (20mer, 4096-fold degenerate) encoded the amino acids DTFRAGA (Hann *et al.*, 1989). PCR products were separated on a 6% polyacrylamide gel. A 110-base pair (bp) band was excised from the gel and sequenced as described by Hann *et al.* (1989).

A genomic clone of the *SRP101* gene was isolated by screening a plasmid library of *S. cerevisiae* strain AB320 (Nasmyth and Tatchell, 1980) in the vector YEp13 using either the gel purified *S. cerevisiae* PCR product or, in later rounds of screening, an oligonucleotide derived from the PCR sequence. The complete 4.6-kilobase (kb) genomic insert together with flanking (pBR322 derived) vector sequences was excised by digestion with *Eco*RI and *Sal* I and cloned into Bluescript II SK (+) and SK (−) (Stratagene, La Jolla, CA) to generate plasmids pSRP101(+) and pSRP101(−), respectively. A series of deletions from the 5' end of the insert was generated using the method of Henikoff (1984) (using the Stratagene Exo-Mung kit) for the pSRP101(+) clone (Henikoff, 1984); a series of deletions from the 3' end was generated using the Kilo-sequencing method of Barnes (1987) for the pSRP101(−) clone (Barnes, 1987). Dideoxysequencing using Sequenase (United States Biochemicals, Cleveland, OH), ^{35}S-dATP, and electrolyte gradient gels (Sheen and Seed, 1988) was carried out on single stranded phagemid DNA isolated according to Stratagene protocols. Gaps in the sequence were filled by sequencing from synthetic oligonucleotide primers. Base number 1 of the DNA sequence deposited in Genbank (accession no. M77274) is the A of the presumptive initiating AUG codon.

Gene Disruption and Rescue

We constructed a DNA fragment suitable for gene disruption of the *SRP101* locus by PCR. A 2320-bp DNA fragment of the *ADE2* locus (bases 273–2593 [Stotz and Linder, 1990]) was amplified by PCR using two primers that each contained 27 bases of *ADE2* sequence at their

3′ ends (bases 273–300 and 2566–2593 of the *ADE2* sequence [Stotz and Linder, 1990]) and 72 bases of *SRP101* sequence at their 5′ ends (bases −1 to −72 and 1780–1846 of the *SRP101* sequence [Figure 5A]), respectively. The resulting 2474-bp fragment was introduced into an *ade2* diploid strain (strain W303) by one step gene replacement (Orr-Weaver *et al.*, 1981) using the LiOAc transformation procedure (Ito *et al.*, 1983). Yeast genomic DNA was prepared (Davis *et al.*, 1980) from Ade$^+$ transformants and was screened by PCR using oligonucleotides corresponding to bases −404 to −385 and 2136–2153 (Figure 5A, regions Y and Z) of the *SRP101* locus. The *ADE2* gene was found to be correctly integrated at the *SRP101* locus in 1 of 16 isolated Ade$^+$ transformants.

Disruption of the *SCR1* gene was performed exactly as in Hann and Walter (1991), except that the W303 strain was used. The disruption was confirmed by Southern hybridization as described (Hann and Walter, 1991). Because loss of either *SCR1* or *SRP101* yields only rho$^-$ cells, a diploid heterozygote resulting from a cross of these two deletions is also rho$^-$ and, consequently, unable to sporulate. Thus, we could not construct a strain bearing the double deletion of *SCR1* and *SRP101* by crossing strains bearing the single deletions. The double deletion was therefore constructed by the following procedure. A rho$^-$ haploid strain (SOY60, but MAT**a**) containing *scr1-Δ2* (*SCR1::HIS3*) was crossed with a rho$^+$ strain (SOY48) containing *srp101-Δ1* (*SRP101::ADE2*) complemented by plasmid pSO210 (see below). After selection on His$^-$, Ade$^-$, Ura$^-$ plates, diploids were scored for loss of pSO210 by growth on plates containing 5-fluoroorotic acid. The resulting diploid, heterozygous for both gene deletions, was sporulated and dissected by standard procedures.

Rescue of the haploid strain containing the *SRP101* deletion (*srp101-Δ1*) was performed by moving the complete genomic SRα insert of plasmid pSRP101(+) on a 7.0-kb *Pvu* I fragment into the *CEN6 ARS4*-containing *Pvu* I fragment of plasmids pRS316 and pRS314 (Sikorski and Heiter, 1989) to yield plasmids pSO210 and pSO220, respectively. Plasmid pSO210 contains *URA3* as a selectable marker, and pSO220 contains *TRP1* as a marker. These plasmids were transformed into the *SRP101/srp101-Δ1* diploid strain SOY34 by selecting for Ura$^+$ or Trp$^+$ transformants. Transformants were sporulated and tetrads dissected and tested by standard procedures (Sherman *et al.*, 1974).

Preparation of Antibodies to SRα

Antiserum was raised against a fusion protein expressed in *E. coli*, containing glutathione-S-transferase from *S. Japonicum* as the N-terminal domain linked to a fragment of SRα. This fusion protein was generated by a three step subcloning procedure. First, pUC5′Δ242 was generated by subcloning a 2.0-kb *Xba* I-*Hin*dIII fragment from pSRP101(+) encoding the C-terminal 379 amino acids of *SRP101* into the *Xba* I-*Hin*dIII sites of pUC18. Second, pUCSRP101 was constructed by subcloning a 740-bp PCR fragment encoding the first 242 amino acids of *SRP101* into the *Bam*HI-*Xba* I site of pUC5′Δ242. This regenerated the entire coding sequence of *SRP101* and removed all the DNA sequence information upstream of the start codon. Finally, subcloning a 950-bp *Bam*HI-*Hpa*I fragment from pUCSRP101 into the *Bam*HI-*Eco*RI site of pGEX-3X created the fusion protein plasmid, pGEXSRP101 (Smith and Johnson, 1988).

A 60-kDa fusion protein, containing amino acids 1–317 from SRα, was overproduced in *E. coli*. The protein was insoluble and was therefore solubilized in urea before further purification by differential centrifugation and preparative SDS-PAGE (Schloss *et al.*, 1988). Polyclonal rabbit antiserum against the SDS denatured fusion protein was prepared by Caltag (South San Francisco, CA).

The antibodies were purified by affinity chromatography. The fusion protein was coupled to CNBr activated Sepharose Cl-4B (Pharmacia, Piscataway, NJ) at a concentration of 6 mg/ml according to the manufacturers instructions. Bound antibodies were eluted as described (Walter and Blobel, 1983). Affinity purified antibodies were concentrated by precipitation with ammonium sulfate, resuspended in phosphate-buffered saline containing 50% glycerol and 0.02% NaN_3 at a concentration of 4 mg/ml, and stored at −80°C.

Cell Fractionation

Subcellular localization of SRα was performed essentially as in Deshaies and Schekman (1990). Briefly, strain W303 was grown to 2.0 OD_{600}/ml, and cells were harvested by centrifugation in a clinical centrifuge. After one wash in buffer A (100 mM tris(hydroxymethyl)aminomethane [Tris]-HCl, pH 9.4, 10 mM dithiothreitol (DTT), 10 mM NaN_3), cells were resuspended to a concentration of 20 OD_{600} cell equivalents per ml in buffer A and incubated for 10 min at 24°C. Cells were then pelleted and resuspended in spheroplast buffer (25 mM *N*-2-hydroxyethylpiperazine-*N*′-2-ethanesulfonic acid [HEPES]/KOH, pH 7.5, 20 mM DTT, 5 mM $MgCl_2$, 10 mM NaN_3) containing 1.3 M sorbitol to a concentration of 50 OD_{600} cell equivalents/ml. After adding 25 U/OD_{600} of lyticase (Sigma Chemicals, St. Louis, MO), cells were incubated with shaking at 30°C for 30 min. Spheroplasts were centrifuged through a cushion consisting of spheroplast buffer without DTT containing 1.9 M sorbitol at 8000 × *g* (7250 rpm) in a Beckman (Fullerton, CA) JS-13 rotor for 5 min at 4°C. Spheroplasts were resuspended in lysis buffer (200 mM sorbitol, 10 mM HEPES-KOH, pH 7.5, 100 mM NaCl, 5 mM $MgCl_2$, 1 mM EDTA, 1 mM phenylmethylsulfonyl fluoride, 2 μg/ml each of the protease inhibitors pepstatin A, leupeptin, chymostatin, and antipain) to a concentration of 100 OD_{600} cell equivalents/ml. Lysis of the cells was achieved by gently vortexing (setting 3 on a scale of 1 to 10) the cell suspension three times in the presence of three-fourths volume zirconium oxide beads (Biospec Products, Bartlesville, OK). Each round of lysis consisted of 15 s of vortexing followed by 30 s incubation at 4°C.

The supernatant fraction was transferred to a new tube, and the beads were washed one time with one volume of lysis buffer. The supernatant and wash fractions were combined and adjusted to a final concentration of the cell lysate of 50 OD_{600} cell equivalents/ml. The cell lysate was subjected to a low-speed centrifugation of 200 × *g* (1200 rpm) in a Beckman JS-13 rotor for 4 min at 4°C.

The resulting supernatant fraction was further fractionated by centrifugation in a Beckman TL100 ultracentrifuge at 96 600 × *g* (50 000 rpm) in a TLA100 rotor for 25 min at 4°C. Mock extraction of the low-speed supernatant fraction was performed by addition of one fifth of the final volume of lysis buffer, incubation at 4°C for 20 min, and separation into pellet and supernatant fractions by centrifugation at 96 600 × *g* as described above. Extraction of the low-speed supernatant was performed by the addition of one fifth of the final volume of either 8 M urea, 3 M KOAc, or 2.5% Triton X-100. Samples were incubated for 20 min at 4°C and then separated into pellet and supernatant fractions by centrifugation at 96 600 × *g*. Sodium carbonate extraction was performed by the addition of the low-speed supernatant to 100 volumes of ice-cold 100 mM Na_2CO_3 (pH 11.5), incubation at 4°C for 30 min, and separation into pellet and supernatant fractions by centrifugation at 103 040 × *g* (50 000 rpm) in a Beckman TLA100.2 rotor.

Conditional Expression of SRP101

The plasmid pSO400 that contains *SRP101* under the control of the *GAL1* promoter was produced by a two-step subcloning procedure. A 2.6-kb *Bam*HI-*Hin*dIII fragment from pUCSRP101 (containing the entire coding sequence of *SRP101* but lacking all of the 5′ control region; see above for construction details) was subcloned into the *Bam*HI-*Hin*dIII site of pRS316 (Sikorski and Heiter, 1989), generating plasmid pSO213. In a second step, a 685-bp *Bam*HI fragment containing the *GAL1* promoter was inserted into the *Bam*HI site of pSO213, generating the plasmid pSO400. The *GAL1* shut-off, ^{35}S-methionine labeling, and denaturing immunoprecipitations were performed as described in Hann and Walter (1991).

Protease Protection Assay and Pulse-Chase Analysis

Protease protections were performed essentially as described by Deshaies and Schekman (1990). *S. cerevisiae* strain SOY46 and control cells were metabolically labeled for 7 min with ^{35}S-methionine after

Table 1. Yeast strains used in this study

Strain	Genotype	Reference
W303	*ade2-1/ade2-1 trp1-1/trp1-1 leu2-3, 112/leu2-3, 112 his3-11/his3-11 ura3-1/ura3-1 can1-100/can1-100* MAT**a**/MATα	Deshaies and Schekman (1990)
SOY34	*ade2-1/ade2-1 trp1-1/trp1-1 leu2-3, 112/leu2-3, 112 his3-11/his3-11 ura3-1/ura3-1 can1-100/can1-100 SRP101/srp101::ADE2 (srp101-Δ1)* MAT**a**/MATα	This study (see MATERIALS AND METHODS)
SOY35	*ade2-1 trp1-1 leu2-3, 112 his3-11 ura3-1 can1-100* MATα *SRP101* (Ade$^-$)	This study
SOY36	*ade2-1 trp1-1 leu2-3, 112 his3-11 ura3-1 can1-100* MAT**a** *srp101-Δ1* (Ade$^+$)	This study
SOY37	*ade2-1 trp1-1 leu2-3, 112 his3-11 ura3-1 can1-100* MAT**a** *srp101-Δ1* (Ade$^+$)	This study
SOY38	*ade2-1 trp1-1 leu2-3, 112 his3-11 ura3-1 can1-100* MATα *SRP101* (Ade$^-$)	This study
SOY46	*ade2-1 trp1-1 leu2-3, 112 his3-11 ura3-1 can1-100* MATα *srp101-Δ1* [pSO400]	This study
SOY48	*ade2-1 trp1-1 leu2-3, 112 his3-11 ura3-1 can1-100* MATα *srp101-Δ1* [pSO210]	This study
SOY53	*ade2-1 trp1-1 leu2-3, 112 his3-11 ura3-1 can1-100* MAT**a** *srp101-Δ1* [pSO220]	This study
SOY60	*ade2-1 trp1-1 leu2-3, 112 his3-11 ura3-1 can1-100 scr1-Δ2* MATα	This study
SOY61	*ade2-1 trp1-1 leu2-3, 112 his3-11 ura3-1 can1-100 srp101-Δ1* MATα	This study
SOY62	*ade2-1 trp1-1 leu2-3, 112 his3-11 ura3-1 can1-100 scr1-Δ2 srp101-Δ1* MATα	This study
SOY64	*ade2-1/ade2-1 trp1-1/trp1-1 leu2-3, 112/leu2-3, 112 his3-11/his3-11 ura3-1/ura3-1 can1-100/can1-100 srp101-Δ1/srp101-Δ1* MAT**a**/MATα [pSO400]	This study
SOY70	SOY46 [rho$^-$]	This study
RSY457	*sec65-1 ura3-52 ade2-1 trp1-Δ1 leu2-3, 112 his3* MATα	Stirling *et al.* (1992)
MYY147	*mas1-1 leu2-3,112 his3 ura3-52* MAT**a**	Witte *et al.* (1988)

repression of SRα synthesis for 20 h. Cell extracts were prepared as described above. Extracts were digested with proteinase K (0.5 mg/ml) for 20 min on ice and terminated by the addition of phenylmethylsulfonyl fluoride to a final concentration of 10 mM. In the mock digestion, proteinase K was preincubated with phenylmethylsulfonyl fluoride for 20 min at 4°C and then added to the extracts. Samples were precipitated by addition of an equal volume of 20% trichloroacetic acid. Pellets derived from 1 OD_{600} equivalents of cells were resuspended in 40 μl of a solution of 3% SDS, 100 mM Tris base, 3 mM DTT, incubated for 5 min at 100°C, frozen in liquid nitrogen, and stored at −80°C. Subsequent denaturing immunoprecipitations and pulse-chase analysis were performed as in Hann and Walter (1991).

Strain Constructions of SOY64 and SOY70

SOY64 was constructed by crossing SOY53 with SOY46 (see Table 1). Before the cross, SOY46 was repeatedly streaked over a 4-wk period onto plates containing glucose to allow the cells to undergo adaptation. Ura$^+$, Trp$^-$, Ade$^+$ diploids were selected on Ura$^-$, Ade$^-$, Trp$^-$ plates containing galactose as the carbon source, allowing SRα expression from pSO400. Approximately 95% of these cells were rho$^-$, whereas the remaining 5% were rho$^+$. One rho$^+$ colony was chosen for further strain construction. This colony was streaked onto rich plates containing 2% galactose to allow loss of pSO220. Single colonies from this plate were tested for growth in the absence of Trp. Several colonies were found that were Trp auxotrophs but still prototrophs for Ura, suggesting that these cells had lost pSO220 but still retained pSO400. These cells were designated strain SOY64. After sporulation, tetrads were dissected onto YEP plates containing 2% galactose and 2% sucrose as the carbon sources. One tetrad was chosen in which all four spores formed colonies with normal growth rates. Cells derived from each spore were Trp$^-$ and Ade$^-$, but Ura$^+$. These cells were used for the analysis shown in Figure 12A.

SOY70 was made by streaking out SOY46 onto a rich plate containing 2% glucose as well as 2 μg/ml of ethidium bromide. Individual colonies were tested for growth on YEP glycerol/ethanol plates; SOY70 was unable to grow on carbon sources requiring respiration.

RESULTS

Yeast SRP101 Gene Encodes an SRα Homologue

Although the G-domains of mammalian SRα and SRP54 are similar, sequence alignments reveal regions in which the G-domains of both proteins are more closely related to their corresponding prokaryotic homologues, FtsY and Ffh, than to one another. We therefore used the alignment of all four G-domains to identify short contiguous blocks of amino acid sequence that are either highly conserved across all four sequences or that are unique to the SRα/FtsY and SRP54/Ffh subfamilies (Bernstein *et al.*, 1989; Römisch *et al.*, 1989). These sequences allowed us to design oligonucleotide probes that could be used in PCR to identify genes encoding putative SRα homologues in yeast.

For this purpose, we synthesized two pools of degenerate oligonucleotides. One pool encoded a seven amino acid stretch (designated A in Figure 1) that is conserved between mammalian SRα and FtsY but distinct from eukaryotic SRP54 (both mammalian and yeast) and Ffh. A second pool contained the reverse complements of sequences encoding a seven amino acid stretch (designated B in Figure 1) that is conserved between SRα and FtsY, as well as SRP54 from mammals and yeast. We used PCR to amplify DNA products from genomic DNA of both *Schizosaccharomyces pombe* and *S. cerevisiae* using the two oligonucleotide pools as primers. Because the spacing between regions A and B is conserved between mammalian SRα and FtsY, we predicted that amplification of the desired yeast genes would yield products of 110 bp. Indeed, both PCRs yielded abundant products of the expected size as part of a complex mixture. The 110-bp PCR products were purified by gel electrophoresis and sequenced directly as described (Hann *et al.*, 1989) (see also MATERIALS AND METHODS and Figure 1). The DNA amplified from both yeast species predicted protein sequences in

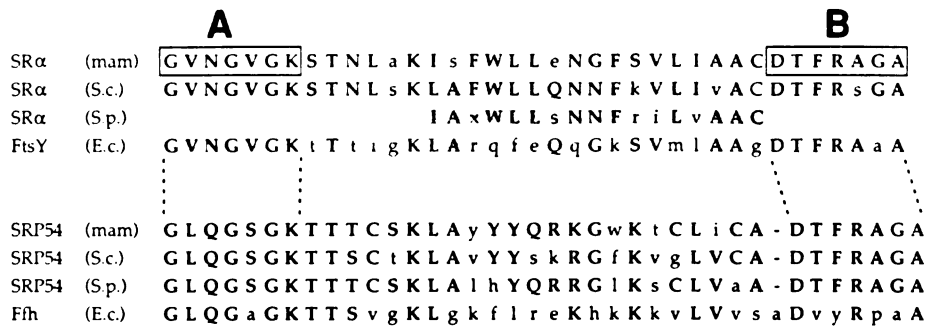

Figure 1. PCR strategy for SRα cloning. The sequences (single letter amino acid code) of the relevant portions of the SRα and SRP54 protein families are aligned. The amino acid sequences used to design the degenerate PCR oligonucleotides A and B are boxed. The amino acid sequences that could be unambiguously determined from the PCR products are shaded; the *S. cerevisiae* sequence includes amino acids determined from the genomic clone (outside the shaded area, see Figure 2). The x in the *S. pombe* sequence could not be determined. Capital letters indicate two or more identical amino acid residues in a given position (SRα and SRP54 related sequences are treated independently in this analysis). The nucleotide sequences that could be determined from the PCR fragments are: 5' AAAGCTAGCG TTTTGGTTAC TGCAAAATAA TTTCAAGGTC TTAATTGTTG CTTG 3' (*S. cerevisiae*) and 5' AAATCGCGTN TTGGCTTTTA TCTAACAACT TTCGAATCTT AGTTGCTGCC TGCGACA 3' (*S. pombe*; N could not be determined unambiguously). The sequences of mammalian SRα (mam) and mammalian SRP54 (mam) are identical in this region between different species (canine and human for SRα and canine and mouse for SRP54). The quest for a complete SRα gene from *S. pombe* was not further pursued as part of this study.

the expected orientation and reading frame (shaded in Figure 1) that were similar to the corresponding region of mammalian SRα and FtsY. Moreover, the amino acid sequences were distinct from known sequences of SRP54 in *S. cerevisiae* and *S. pombe* (Figure 1). This suggested that the amplified DNA segments were derived from genes encoding protein homologues of SRα in both yeast species.

We proceeded to isolate a genomic clone of the *S. cerevisiae* gene using the 110-bp PCR product as a hybridization probe to screen a plasmid library. Sequence analysis of the cloned *S. cerevisiae* gene revealed a 621 amino acid open reading frame (predicted molecular mass of 69.25 kDa) with 44% sequence identity (67% chemical similarity) to mammalian SRα in the G-domain and 19% identity (41% chemical similarity) in the amino terminal domain (Figure 2). We refer to the gene as *SRP101* and to its protein product as SRα.

Yeast SRα is a Peripheral Membrane Protein

To identify SRα in yeast cells, we raised rabbit antibodies to a fusion protein containing a portion of SRα linked to glutathione transferase (see MATERIALS AND METHODS). The antibodies specifically recognized SRα as a single protein of the predicted molecular mass in lysates from wild-type cells but not in lysates from cells in which the *SRP101* gene had been genetically disrupted (*srp101-Δ1* cells, see below) (Figure 3).

To characterize the intracellular localization of SRα, we fractionated yeast cell homogenates by differential centrifugation. Samples from each fraction were subjected to SDS-PAGE followed by Western blot analysis with anti-SRα and a control antibody to a known ER membrane protein, Sec61p (Stirling *et al.*, 1992) (Figure 4A). After low-speed centrifugation, SRα and Sec61p were each equally distributed between the pellet fraction (Figure 4A, lane 3) and the supernatant fraction (Figure 4A, lane 2). The presence of the two proteins in the low-speed pellet is presumably due to incomplete cell lysis. On further centrifugation at 100 000 × *g*, SRα and Sec61p were quantitatively recovered in the pellet fraction (Figure 4A, lane 5), suggesting that both proteins were associated with intracellular membranes.

The physical association of SRα with intracellular membranes was examined by extracting the low-speed supernatant fraction with various reagents known to perturb protein-membrane interactions. After centrifugation of the extracts at 100 000 × *g*, supernatant and pellet fractions were subjected to SDS-PAGE and immunoblotted with anti-SRα and anti-Sec61p (Figure 4B). SRα remained associated with the membrane fraction after treatment with 1.6 M urea (Figure 4B, lanes 3 and 4) or high salt (Figure 4B, lanes 5 and 6). In contrast, when membranes were disrupted with non-ionic detergent, most of SRα was released into the 100 000 × *g* supernatant fraction (compare lanes 7 and 8). The presence of a portion of Sec61p in the 100 000 × *g* detergent pellet may be due to its association with other proteins in the ER that remain insoluble after detergent extraction.

To test whether SRα is an integral membrane protein, we diluted the low-speed supernatant with a large excess of a solution of sodium carbonate at pH 11.5 and centrifuged as above. Under alkaline conditions peripheral, but not integral, membrane proteins are ex-

Mammal
S. cer.
Mammal
S. cer.
Mammal
S. cer.
E. coli
Mammal
S. cer.
E. coli
Mammal
S. cer.
E. coli
G
Mammal
S. cer.
E. coli
I
Mammal
S. cer.
E. coli
Mammal
S. cer.
E. coli
II
Mammal
S. cer.
E. coli
III
Mammal
S. cer.
E. coli

tracted from membranes (Fujiki *et al.*, 1982). SRα was quantitatively recovered in the supernatant fraction, whereas Sec61p remained in the pellet fraction (Figure 4B, lanes 9 and 10). These extraction properties of SRα are consistent with the view that yeast SRα, like its mammalian homologue, is a peripheral ER membrane protein. Mammalian SRα is thought to be anchored in the ER membrane through an interaction with SRβ, which contains a bona fide transmembrane domain (Miller, Tajima, Lauffer, and Walter, unpublished data). Yeast SRα does not contain any obvious hydrophobic amino acid stretches characteristic of transmembrane regions. Moreover, in yeast cells in which the yeast SRα is overexpressed, a large portion of the protein is found soluble in a high-speed supernatant, indicating that attachment sites to the membrane are limiting. From the data shown, we can conclude that SRα is membrane associated; however, due to the intrinsic limitations of the fractionation scheme, we presently cannot conclude with certainty that SRα is associated with the ER. Attempts to show an ER localization of SRα in yeast cells directly by immunofluorescence have been unsuccessful, presumably due to the low abundance of the protein.

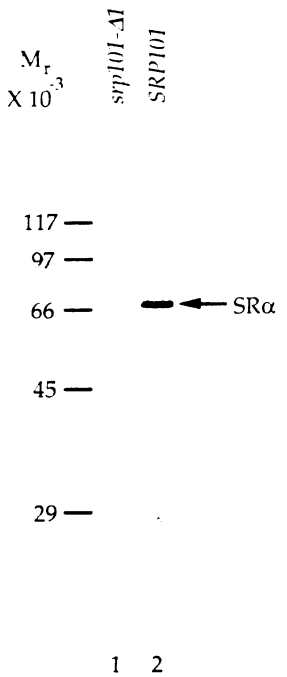

Figure 3. Characterization of anti-SRα. Cell lysates (0.2 OD_{600} cell equivalents per lane) were probed by Western blot analysis using affinity purified anti-SRα. Lane 1 contains lysate from cells deleted for the *SRP101* gene (SOY36), and lane 2 contains lysate from wild-type cells (W303). The positions of molecular weight standards and SRα are indicated.

Yeast Cells Require SRP101 for Efficient Growth

To analyze the physiological role of SRα, we constructed a strain in which the *SRP101* gene was deleted using a one-step gene replacement (Rothstein, 1983). The entire coding region of *SRP101* was replaced with a selectable marker, the *ADE2* gene (schematically shown in Figure 5A). In brief, we used a novel approach based on PCR to construct a linear DNA fragment containing the *ADE2* gene flanked by DNA sequences derived from the 5′ and 3′ flanking regions of the *SRP101* locus (Figure 5A, PCR step). This DNA was introduced into diploid *ade2*$^-$cells (strain W303) by transformation and selection of Ade$^+$ colonies (Figure 5A, gene replacement step). Integration of the *ADE2* gene at the *SRP101* locus was confirmed by PCR analysis (Figure 5B, compare lanes 1 and 2). For this analysis, oligonucleotides corresponding to regions Y and Z in Figure 5A, which lie outside the regions of homology used for integration (W and X in Figure 5A), were used in an amplification reaction of genomic DNA from wild-type cells (W303) or from an Ade$^+$ transformant (strain SOY34). As expected, amplification of DNA containing the wild-type *SRP101* locus (Figure 5B, lanes 1 and 2) yielded a predicted 2.4-kb PCR product. Integration of the *ADE2* gene into the *SRP101* locus (*srp101-Δ1*) was revealed by the presence of a larger 3.0-kb PCR product (Figure 5B, lane 2). The identity of these PCR products was confirmed by restriction analysis. Sporulation of diploid SOY34 (*SRP101/srp101-Δ1*) cells produced tetrads containing two to four viable spores. PCR analysis of the four colonies produced from spores of a single tetrad confirmed that the deletion allele *srp101-Δ1* cosegregated with the *ADE2* gene (Figure 5B).

All *SRP101* spores were Ade$^-$, formed normal colonies on plates, and grew in culture with a doubling time similar to that of the parent W303 strain (~80 min). In

Figure 2. Alignment of the amino acid sequences of SRα homologues. The deduced amino acid sequence of mammalian SRα (canine; Lauffer *et al.*, 1985), *S. cerevisiae* SRα (this work), and FtsY (*E. coli*; Gill *et al.*, 1986) are aligned. Two or more identical amino acids at a single position are shown in capital letters. Amino acids of similar chemical properties are boxed (Dayhoff *et al.*, 1972) as described by Bernstein *et al.* (1989) and Hann *et al.* (1989). Gaps are indicated with dashes. The positions of three regions matching GTP-binding consensus sequences are indicated above the alignment by roman numerals (Dever *et al.*, 1987). The amino acid sequence of the third conserved motif SKxD (box III) predicted to contact the guanine ring of GTP differs by a conservative substitution in *S. cerevisiae* SRα from the consensus TKxD defined for all other known members of the SRP54/SRα subfamily of GTPases. The beginning of the G-domain, as defined by Bernstein *et al.* (1989), is marked. The primary structures of SRα homologues from two additional species are known but for clarity omitted from this alignment. These proteins are the products of the *PilA* gene from *Neisseria gonorrhoeae* (Taha *et al.*, 1991) and the *SSO* gene from *Sulfolobus solfataricus* (Ramirez and Matheson, 1991). As for *E. coli* FtsY and eukaryotic SRα, the primary structures of these proteins are very similar in the G-domain but diverge in N-terminal regions.

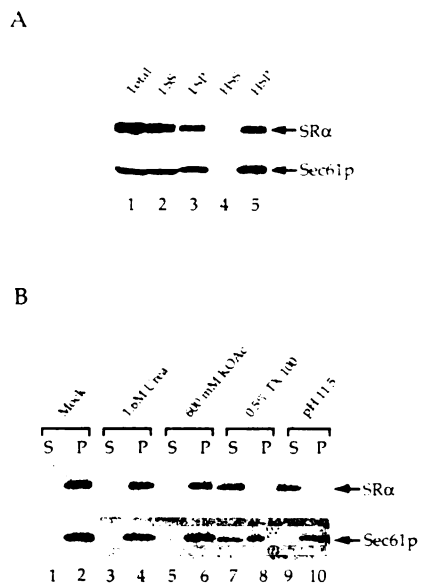

Figure 4. Subcellular localization of SRα. (A) Wild-type cell extracts were fractionated as detailed in MATERIALS AND METHODS. Cell fractions were analyzed by Western blot using affinity purified anti-SRα and anti-Sec61p. Each lane contains 0.2 OD_{600} cell equivalents of the fraction: lane 1, cell lysate; lane 2, low-speed supernatant; lane 3, low-speed pellet; lane 4, high-speed supernatant; lane 5, high-speed pellet. (B) A portion of the low-speed supernatant (as shown in lane 3 of A) was diluted with lysis buffer (lanes 1 and 2) or adjusted to final concentrations of 1.6 M urea (lanes 3 and 4), 0.6 M KOAc (lanes 5 and 6), 0.5% Triton X-100 (lanes 7 and 8), or 0.1 M Na_2CO_3, pH 11.5 (lanes 9 and 10). The samples were centrifuged at 100 000 × *g* and the supernatant fractions (lanes 1, 3, 5, 7, and 9) and pellet fractions (lanes 2, 4, 6, 8, and 10) were analyzed by Western blot using affinity purified anti-SRα and anti-Sec61p. Only the relevant portions of each immunoblot are shown. SRα was frequently observed as a doublet, presumably due to some proteolysis that occurred during cell fractionation. Note that no doublet was observed when cell extracts were prepared rapidly and under denaturing conditions (see Figure 3).

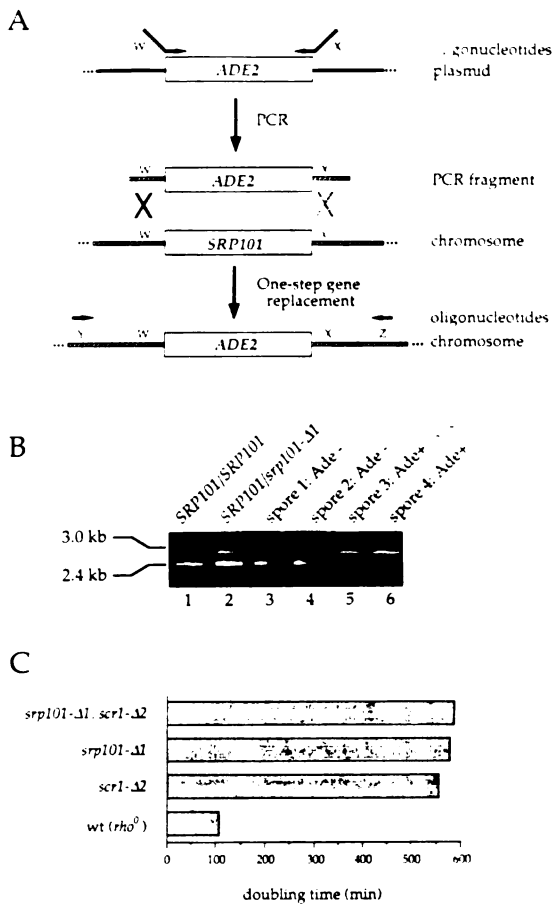

Figure 5. Gene disruption of *SRP101*. (A) The gene disruption procedure is depicted (see MATERIALS AND METHODS). Oligonucleotides composed of sequences from both the *ADE2* gene and sequences from regions W and X of the *SRP101* gene were used in a PCR reaction to generate a DNA fragment (PCR fragment) containing the *ADE2* gene of *S. cerevisiae* flanked at either end by sequences from the 5′ and 3′ untranslated regions of the *SRP101* locus. Upon transformation, the end sequences directed the integration of the linear DNA fragment into the *SRP101* gene (one-step gene replacement). PCR confirming the gene disruption was performed on yeast genomic DNA using the oligonucleotides corresponding to regions Y and Z. (B) PCR reactions confirming the gene disruption were performed on genomic DNA from the wild-type parent strain (lane 1), SOY34, the diploid transformant heterozygous for *SRP101*, and the *srp101::ADE2* gene disruption (*srp101-Δ1*; lane 2) or cells derived from the surviving spores of a single tetrad that are either Ade⁺ (lanes 5 and 6) or Ade⁻ (lanes 3 and 4). The PCR products were separated on a 1% agarose gel and visualized by ethidium bromide staining. (C) Growth rates in YEPD medium of strains in which the chromosomal copies of *SRP101*, *SCR1* (see MATERIALS AND METHODS), or both *SCR1* and *SRP101* have been disrupted.

contrast, all *srp101-Δ1* spores were Ade⁺, formed unusually small colonies on plates, were unable to grow on carbon sources requiring respiration, and grew about sixfold slower in liquid culture when compared with an isogenic *SRP101* rho⁰ strain (Figure 5C).

To show that the genomic clone of *SRP101* is functional in vivo, we transformed the SOY34 (*SRP101/srp101-Δ1*) cells with a centromeric yeast vector carrying both the *URA3* and *SRP101* genes (pSO210; see MATERIALS AND METHODS). Ura⁺ transformants were sporulated and dissected. We recovered Ade⁺ Ura⁺ colonies with wild-type growth rates indicating that the *srp101-Δ1* allele was complemented by the plasmid carrying the cloned *SRP101* gene. As expected, every Ade⁺ spore that grew at the wild-type rate was also Ura⁺. Southern analysis revealed that *SRP101* is present in

single copy in the haploid yeast genome. Taken together, these results indicate that SRα is encoded by a single gene that is important but not essential for cell growth. Low stringency Southern blots, however, performed with a probe derived from the *SRP54* gene encoding a structurally related protein failed to detect any *SRP101* sequences. Likewise, no *SRP54* sequences were detected using *SRP101* sequences as a probe. Thus, it remains possible that other distantly related homologues of the SRα/SRP54 subfamily of GTPases exist in yeast.

If SRP and SRα function in sequential steps of a common protein targeting pathway, then the absence of both SRP and SRα should be no more detrimental to cell growth than the absence of either component alone. To test this directly, we constructed strain SOY60 in which the SRP RNA gene was deleted (*scr1-Δ2*) and strain SOY62 in which the genes encoding SRP RNA and SRα were both deleted (*srp101-Δ1/scr1-Δ2*). SOY60 and SOY62 were both constructed in the same strain background (W303) used elsewhere in this study. The results depicted in Figure 5C show that cells bearing the double gene deletion grow with a doubling time that is comparable with that of cells bearing either gene deletion alone.

Conditional Expression of SRα

To characterize the molecular nature of the defects in SRα deficient cells, we constructed a strain (SOY46) that allows the conditional expression of SRα. SOY46 is a haploid strain bearing the *srp101-Δ1* deletion allele that is complemented by a plasmid (pSO400) containing *SRP101* under control of the *GAL1* promoter. SOY46 cells grew as well as wild-type cells when galactose was used as a carbon source (Figure 6A, early time points). Under these conditions, the level of SRα was ~50-fold higher than found in wild-type cells, as estimated from an immunoblot analysis using anti-SRα antibodies (Figure 6B, compare lanes 1 and 7). The level of SRα decreased rapidly, when SOY46 cells were switched to growth medium containing glucose. After 16 h of growth on glucose containing medium, the amount of SRα was approximately equal to the amount found in wild-type cells (Figure 6B, compare lanes 4 and 7). By 19 h, SRα had fallen below wild-type levels and by 32 h was barely detectable by immunoblot analysis (Figure 6B, lanes 5 and 6; also see Figure 11B, lane 1). Concomitant with the drop of SRα levels, SOY46 cells began to grow at a slower rate (Figure 6A), rapidly approaching the growth rate of *srp101-Δ1* cells with a doubling time of ~10 h.

Yeast SRα is Required for Efficient Protein Translocation Across the ER Membrane

To test whether yeast SRα performs a function in facilitating protein translocation similar to that of its mammalian homologue, we depleted cells of SRα and

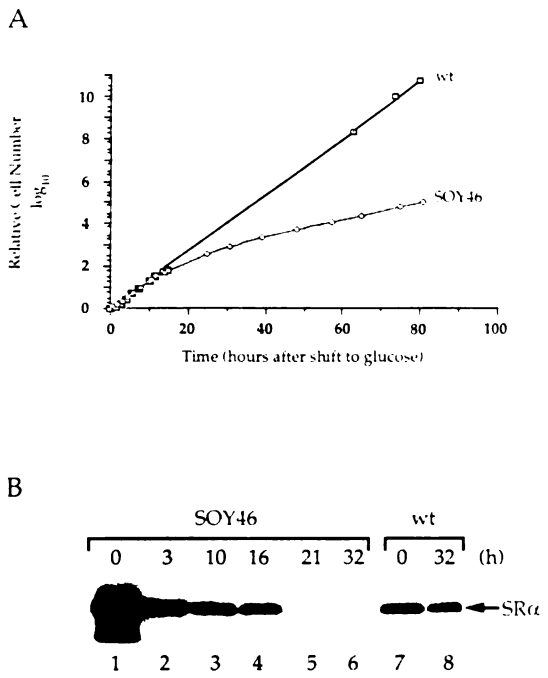

Figure 6. Growth curves and immunoblot analysis of SRα depletion. (A) The growth curves of SOY48 (*SRP101* expressed from its own promoter, labeled wt) and SOY46 (*SRP101* expressed from the *GAL1* promoter) are shown. At time 0, the carbon source was changed from galactose to glucose as detailed in Hann and Walter (1991). (B) Cellular SRα was monitored by Western blot analysis. Lanes 1–6 contain cell lysates prepared from SOY46 cells and lanes 7 and 8 contain lysate prepared from SOY48 cells at the indicated times after switch to glucose medium. The position of SRα is indicated.

monitored the maturation of several newly synthesized soluble and membrane proteins known to be translocated across the ER membrane. SOY46 cells were pulse labeled for 7 min with ^{35}S-methionine at various time points after the repression of SRα synthesis. Cell extracts were prepared from the labeled cells, and individual proteins were immunoprecipitated with specific antibodies and analyzed by SDS-PAGE. This allowed us to monitor the efficiency with which different proteins were translocated into the ER. For all substrates analyzed, translocation across the ER is accompanied by well-characterized modifications (signal sequence cleavage and/or glycosylation) that alter their gel mobility.

Figure 7 shows the results of such an analysis at time points during the course of SRα depletion. Under these conditions, four of the five proteins analyzed showed an accumulation of cytoplasmic precursor forms, indicating that protein translocation was perturbed as a consequence of the reduced SRα level. The degree to

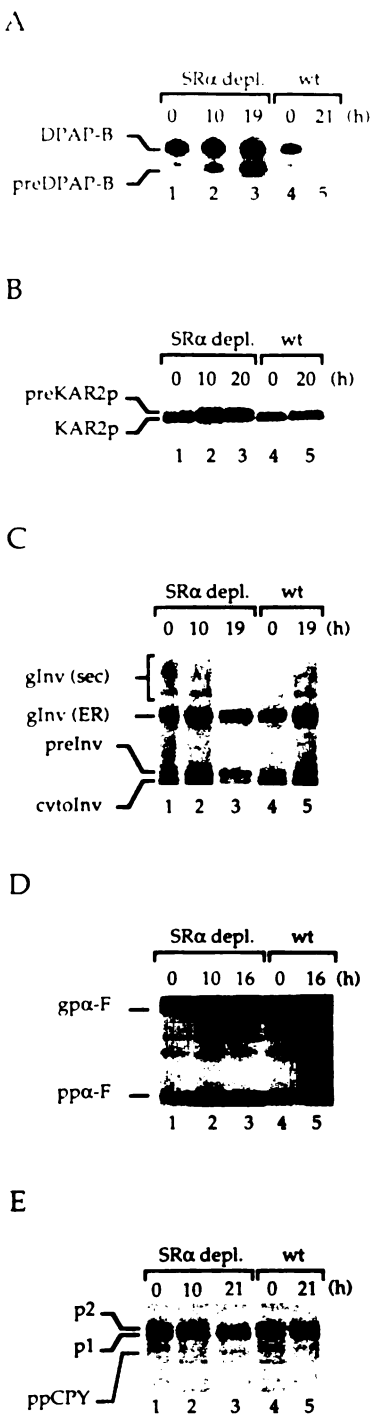

which translocation was affected, however, varied among the different proteins. KAR2p, a soluble ER resident protein, and DPAP-B, a vacuolar integral membrane protein, showed the greatest defect. In the case of KAR2p, the translocation defect is inferred from the accumulation of a more slowly migrating band representing preKAR2p, which contains the uncleaved signal sequence (Figure 7B, lanes 2 and 3, preKAR2p); in the case of DPAP-B, the defect is inferred from the accumulation of a faster migrating band representing unglycosylated DPAP-B (Figure 7A, lanes 2 and 3, preDPAP-B). At the later time point, 20 or 21 h after repressing the synthesis of SRα, about one half of the KAR2p or DPAP-B synthesized remained untranslocated. The translocation of invertase and prepro-α-factor were affected to a lesser extent, but for both proteins significant amounts of precursor forms (Figure 7, C, lanes 2 and 3, preInv, and D, lanes 2 and 3, ppαF) accumulated after repression of SRα synthesis. In contrast to the four translocation substrates discussed above, CPY showed no detectable translocation defect on SRα depletion as indicated by the absence of a band migrating in the position of its cytoplasmic unglycosylated prepro-form (Figure 7E, ppCPY). No effect was observed on the translocation of any of the four substrates when an isogenic strain carrying *SRP101* controlled by its own promoter was switched from galactose to glucose (Figure 7, A, B, D, and E, wt lanes).

Note that translocation defects were already apparent at the first timepoint in the analysis shown in Figure 7, which was taken 10 h after switch of the SOY46 cells from galactose to glucose, yet at this time the intracellular SRα level as judged by Western analysis was still above that found in wild-type cells (Figure 6B). This apparent paradox can be reconciled if we assume that in SOY46 cells (which overproduce SRα from the *GAL1* promoter) only a portion of the SRα is properly assembled at the membrane and functional, whereas another portion remains unassembled and nonfunctional. As discussed above, fractionation of SOY46 cells grown on galactose indicated that a large portion of SRα remained

Figure 7. Precursor protein accumulation on depletion of SRα. SOY46 cells (*GAL1* promoter regulated *SRP101*) and SOY48 cells (wild-type *SRP101*) were grown as described in Figure 6A. Before (0 h) and at the indicated times after changing the carbon source from galactose to glucose cells were pulse labeled for 7 min with ^{35}S-methionine. Cell extracts were prepared and immunoprecipitations were performed using antibodies against the following proteins. (A) Dipeptidyl aminopeptidase-B; mature DPAP-B and the nonglycosylated precursor preDPAP-B are indicated. (B) KAR2p; mature KAR2p and precursor preKAR2p (containing the uncleaved signal sequence) are indicated. (C) Invertase; cytoplasmic cytoInv, precursor preInv (containing the uncleaved signal sequence and lacking carbohydrate attachment), core glycosylated ER form gInv (ER), and secreted outer chain glycosylated gInv (sec) forms are indicated. (D) α-Factor; precursor pp-αF and core-glycosylated gp-αF forms are indicated. (E) Carboxypeptidase Y. ER glycosylated p1 and Golgi modified p2 forms are indicated, as well as the predicted location of preproCPY ppCPY.

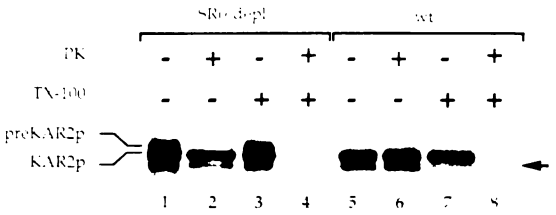

Figure 8. Accessibility of accumulated preKAR2p to protease. SOY46 cells (*GAL1* promoter regulated *SRP101*) and SOY48 cells (wild-type *SRP101*) were grown as described in Figure 6 and pulse labeled at 20 h after the shift from galactose to glucose. Extracts were prepared under nondenaturing conditions (see MATERIALS AND METHODS) from SRα depleted (lanes 1–4) and wild-type cells (lanes 5–8) and either digested with 0.5 mg/ml proteinase K (PK) or mock digested in the presence (lanes 3, 4, 7, and 8) or absence (lanes 1, 2, 5, and 6) of 0.5% Triton X-100. After inactivation of the protease, immunoprecipitations were performed with anti-KAR2p antibodies followed by SDS-PAGE. The position of mature KAR2p and preKAR2p are indicated. A protected fragment of KAR2p (indicated with an arrow) migrates slightly faster than the mature form of KAR2p.

in a cytoplasmic supernatant. Accordingly, upon SRα depletion, only a portion of the SRα remaining in the cells as detected in Figure 6B may be functional. Alternatively, SRα expression from SOY46 cells could be nonuniform during the depletion experiment, giving rise to cell populations that are heterogeneous with respect to their levels of SRα. At the 10-h timepoint then, there could exist a population of cells that contain higher than wild-type levels of SRα and show no translocation defect, in addition to a population of cells that contain lower than wild-type levels of SRα and show a defect in protein translocation. The Western blot shown in Figure 6B would not distinguish these two populations.

The data presented suggest that the SRα facilitates protein translocation across the membrane of the ER. Because translocation was assayed indirectly in the experiments shown in Figure 7, we used a protease protection assay to ask whether the precursor proteins detected were retained in the cytoplasm or had, in fact, entered the ER. To this end, control cells or SOY46 cells (taken 20 h after SRα synthesis had been repressed), were pulse labeled, and crude cell extracts were prepared. The extracts were treated with proteinase K. PreKAR2p that was present in SOY46 cell extracts (Figure 8, lane 1, preKAR2p) but not in the control cell extracts (Figure 8, lane 5) was completely digested by proteinase K (Figure 8, lane 2). In contrast, mature KAR2p was resistant to proteolysis (Figure 8, lanes 2 and 6, KAR2p), presumably because it was sequestered within ER membrane vesicles. When membrane vesicles in the extract were disrupted with detergent, KAR2p became accessible to protease and was digested under these conditions (Figure 8, lanes 4 and 8). Thus, we conclude that preKAR2p accumulated in the cytoplasm in SRα depleted cells.

The accumulation of preKAR2p in the cytoplasm could be explained in two ways. First, cellular depletion of SRα could cause a kinetic delay in the targeting of preKAR2p to the ER membrane. The precursor observed after the pulse labeling would then represent an intermediate in the translocation process and would be expected eventually to reach the lumen of the ER. Alternatively, the depletion of SRα could impair the efficiency of targeting rather than the rate of the process, allowing only a portion of the nascent preproteins to become productively engaged with the translocation machinery. To distinguish between these possibilities, we performed a pulse-chase analysis. Both control and SOY46 cells were pulse labeled for 2 min with ^{35}S-methionine 20 h after repressing the synthesis of SRα, followed by addition of a large excess of nonradioactive methionine. The forms of KAR2p were examined by immunoprecipitation at timepoints during a 16-min chase period. The results are presented in Figure 9. From the quan-

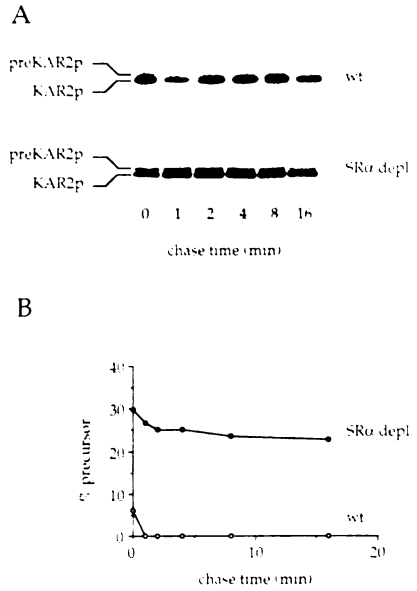

Figure 9. Pulse-chase of preKAR2p after SRα depletion. Twenty hours after switch from galactose to glucose medium, SOY48 cells (wild-type *SRP101*) and SOY46 cells (*GAL1* promoter regulated *SRP101*) were pulse labeled for 2 min with ^{35}S-methionine and chased for 0, 1, 2, 4, 8, or 16 min after the addition of excess unlabeled methionine. (A) Extracts prepared from each time point were subjected to immunoprecipitation with anti-KAR2p antibodies, followed by SDS-PAGE and autoradiography. The position of mature KAR2p and preKAR2p are indicated. (B) The data in A were quantitated using a Phosphorimager (Molecular Dynamics, Sunnyvale, CA). Note that the percent translocation, as calculated from the ratio of preKAR2 and KAR2, was less in this experiment than during the corresponding SRα depletion experiments shown in Figure 7. This is due to the longer pulse time used in Figure 7, which allowed more preKAR2p to accumulate.

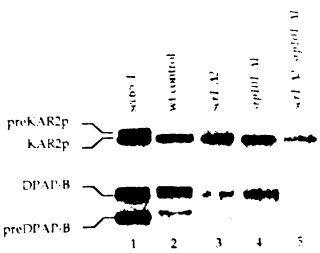

Figure 10. Precursor proteins do not accumulate in SRα (*srp101-Δ1*) or SRP RNA (*scr1-Δ2*) deletion strains. Strains (SOY60, SOY61, SOY62) containing the indicated chromosomal gene deletions and a wild-type strain were pulse labeled for 7 min with ^{35}S-methionine. Cell extracts were prepared and immunoprecipitations were performed using antibodies against KAR2p and DPAP-B. Precursor and mature forms of each protein are indicated. Sec63-1 cells were similarly labeled and immunoprecipitated to provide markers for the gel mobility of preKAR2p and preDPAP-B.

titative analysis of the data (Figure 9B), it is apparent that most of the accumulated preKAR2p did not chase into the mature form during the chase period. These data suggest that the translocation defect observed after removal of SRα is not due to a kinetic delay but represents a reduction of the efficiency with which preproteins can be translocated. This analysis identifies two distinct pools of KAR2p: one portion that was translocated and processed to mature KAR2p during the time of the pulse and one portion, the accumulated preKAR2p, that was rendered translocation incompetent.

Cells can Adapt to the Absence of SRα and SRP

The defects in protein translocation demonstrated in Figures 7–9 were observed in cells in which SRα was progressively depleted after repression of its synthesis. To determine the effects of long-term SRα depletion, we performed similar experiments to monitor translocation defects in *srp101-Δ1* mutant cells. Surprisingly, we detected no translocation defects in *srp101-Δ1* cells when ^{35}S-methionine pulse-labeled extracts were immunoprecipitated with anti-KAR2 and anti-DPAP-B antibodies (Figure 10, lane 4). This result was unexpected because the corresponding experiment performed with yeast SRP, a component of the same pathway, showed only minor amelioration of translocation defects in deletion strains (Hann and Walter, 1991). Because a different strain (TR1) was used in the previous study, we repeated the experiment with cells containing a deletion of the SRP RNA gene, *SCR1*, in the W303 strain background used in this study (SOY60). In these cells and in cells containing the double deletion *scr1-Δ2* and *srp101-Δ1* (SOY62), translocation defects of both KAR2p and DPAP-B are barely detectable (Figure 10, lanes 3 and 5).

Thus, it appears that W303 cells are capable of adapting efficiently to the absence of SRα. Translocation defects were observed when SRα was depleted from cells rapidly after shutoff of its synthesis yet were not apparent when cells bearing the genetic disruption of SRα were grown for a prolonged time in the absence of SRα. To show this adaptation directly, we grew SOY46 (*SRP101* under control of the *GAL1* promoter) for an extended time on plates containing glucose, i.e., under conditions that repress SRα synthesis from the *GAL1* promoter. Analogous to the phenotype of *srp101-Δ1* cells, neither preDPAP-B nor preKAR2p were detected above the level found in wild-type control cells (Figure 11A). Thus, the translocation defects that are maximal between 10 and 20 h after shutoff of SRα synthesis (Figure 7, A and B, lanes 2 and 3) are no longer apparent after growth in the absence of SRα for a prolonged time. This reduction in the translocation defects was not due to increased SRα levels. Western blot analysis confirmed that the intracellular SRα level remained depressed even after prolonged growth on glucose plates (Figure 11B, lane 3).

Curiously, although cells grown for prolonged time in the absence of SRα are able to diminish their apparent protein translocation defects, they do not increase their growth rate as a result of this adaptation (compare Figure 6A and 5C).

To distinguish whether the adaptation was due to the accumulation of a simple suppressor mutation or was due to a reversible physiological change on SRα depletion, we performed a back cross experiment. Haploid SOY46 cells were grown on glucose plates to allow adaptation to occur. These cells were then mated with the strain SOY53 that, like SOY46, contains the chromosomal *srp101-Δ1* deletion but a different plasmid (pSO220) bearing *SRP101* under control of its own pro-

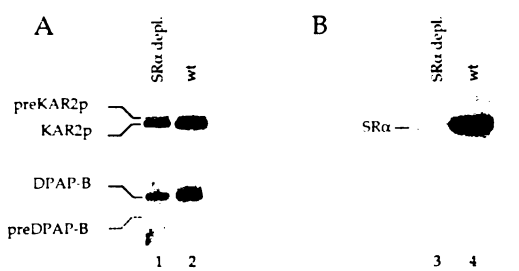

Figure 11. Precursor proteins do not accumulate after extended depletion of SRα. After prolonged growth in glucose medium, SOY48 cells (wild-type *SRP101*) and SOY46 cells (*GAL1* promoter regulated *SRP101*) were assayed for both levels of SRα protein and precursor protein accumulation. Before the assay, cells were maintained for ~10 wk on glucose Ura$^-$ plates. (A) Cells were pulse labeled with ^{35}S-methionine for 7 min. Cell extracts were prepared and immunoprecipitations performed using antibodies against KAR2p and DPAP-B. The positions of both precursor and mature forms of each protein are indicated. (B) Cellular SRα levels in SOY46 and SOY48 cells were monitored by Western blot as described in Figure 3. The position of SRα is indicated.

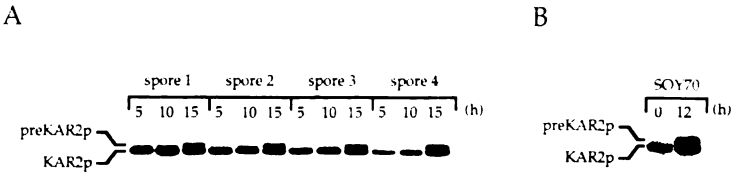

Figure 12. Genetic suppression or loss of respiratory function are not the cause of adaptation. Cells were pulse labeled with ^{35}S-methionine for 7 min. Cell extracts were prepared and immunoprecipitations performed using antibodies against KAR2p. The positions of both precursor and mature forms of KAR2p are indicated. (A) Cells from the four spores of a single tetrad (labeled spore 1 through spore 4) after sporulation of SOY64 were pulse labeled at the indicated times after repression of expression of SRα. (B) SOY70 cells were pulse labeled at the indicated times after repression of SRα synthesis.

moter. In contrast to the SOY46 cells used in the mating, SOY53 cells had never been depleted of SRα, were not adapted, and were still rho$^+$. Once mating had occurred, cells (SOY64; see MATERIALS AND METHODS) were isolated from the resulting diploid strain (homozygous for the *srp101-Δ1* deletion and containing the plasmids pSO220 and pSO400) that had lost pSO220 and thus only contained *SRP101* under control of the *GAL1* promoter. After sporulation and tetrad dissection, cells were maintained on galactose-containing media allowing expression of SRα. If adaptation results from a suppressor mutation, then we would predict that the adapted phenotype would segregate two-to-two when four spores from a single tetrad are analyzed. If, on the other hand, adaptation is a reversible event, we would expect that none of the four spores from a single tetrad would show the adapted phenotype. We assessed the adaptation of cells derived from the four spores obtained from a single tetrad by repressing the expression of SRα after shift to glucose-containing media. As shown in Figure 12A, the amount of preKAR2p that accumulated in cells derived from each spore at different timepoints after repression of SRα synthesis was identical. Thus, we conclude that adaptation is not due to a single suppressor mutation but is caused by a reversible alteration of cellular physiology.

Accumulation of Mitochondrial Precursors

We previously observed that cells in which SRP was genetically disrupted rapidly lost the ability to grow on fermentable carbon sources (Felici *et al.*, 1989; Hann and Walter, 1991). Furthermore, we showed that mitochondrial precursor proteins accumulate in SRP-depleted cells (Hann and Walter, 1991). We thus asked whether similar phenotypes would be observed in SRα deficient cells. Similar to the results obtained for SRP mutant cells, we found that all strains containing deletions of SRP101 were rho$^-$, indicating that mitochondrial function in these cells was impaired. As shown in Figure 13, at late timepoints during the SRα depletion, we observed a defect in the import of the β-subunit of the F_1-ATPase ($F_1\beta$) into the mitochondrial matrix space. As with KAR2p and DPAP-B, no import defect was observed in *srp101-Δ1* cells.

To test whether the loss of respiratory function causes adaptation, we constructed strain SOY70, which is rho$^-$ (see MATERIALS AND METHODS) and allows regulated expression of SRα from the *GAL1* promoter. As shown in Figure 12B, preKAR2p accumulated after repression of SRα synthesis in SOY70 cells, indicative of the nonadapted phenotype. Thus, we conclude that the acquisition of the rho$^-$ phenotype, which occurs after growth of cells in the absence of SRα, is not the cause for the observed adaptation.

DISCUSSION

We have isolated a gene from *S. cerevisiae* that encodes a homologue of the mammalian SRα protein. Several lines of evidence suggest that the yeast SRα not only shares structural similarities with its mammalian counterpart but also serves an analogous function. First and most important, yeast cells in which SRα has been depleted show defects in the translocation of proteins across the ER membrane. Second, the growth defects of *srp101-Δ1* cells and the severity to which different proteins are compromised in their translocation across the ER in SRα deficient cells resemble that of cells in which SRP has been disrupted (Hann and Walter, 1991).

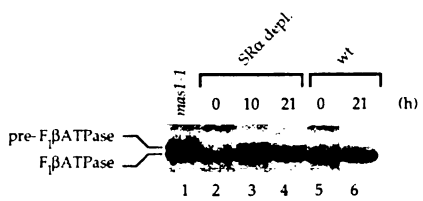

Figure 13. Mitochondrial precursor accumulation on SRα depletion. SOY46 (*GAL1* promoter regulated *SRP101*), SOY48 (wild-type *SRP101*), and MYY147 (*mas1-1*) cells were grown and labeled as described in Figure 7. Cell extracts were subjected to immunoprecipitation with antibodies to the β-subunit of the F_1 ATPase, followed by SDS-PAGE. Precursor (pre-$F_1\beta$ATPase) and mature ($F_1\beta$ATPase) forms are indicated.

Furthermore, cells lacking both SRP and SRα show a growth defect indistinguishable from cells in which either component alone was deleted. This suggests that yeast SRα and SRP function in the same pathway. Third, its subcellular localization is consistent with the notion that yeast SRα, like its mammalian homologue, is a peripheral ER membrane protein. Taken together, these findings suggest that the mechanism and the components mediating SRP/SRP receptor dependent protein targeting are evolutionarily conserved.

Structural Features of Yeast SRα

Mammalian SRα is attached to the ER membrane presumably through an interaction with SRβ that, based on its primary structure, is a bona fide integral membrane protein (Miller, Tajima, Lauffer, and Walter, unpublished data). Based on proteolytic dissection studies, this interaction is thought to be mediated by regions of SRα that are located proximal to its N-terminus (Lauffer *et al.*, 1985). Sequence comparison of yeast and mammalian SRα reveals a striking similarity that extends across the entire coding sequence. This extensive homology and the similarity in the extraction conditions that allow the release of yeast and mammalian SRα from the membrane suggest that yeast SRα may also be complexed to a putative yeast SRβ chain in the ER membrane. Thus, in cells overproducing SRα, only a portion of the protein may assemble into a functional heterodimeric SRP receptor. Oligomeric assembly in the ER membrane may be limited by the number of available SRβ chains. The sequence similarity between yeast and mammalian SRα is strongest in the G-domain and includes the consensus sequences that, as predicted from the known x-ray structures of H-ras and EF-Tu, form loops on the surface of the domain that contact the bound GTP (Bourne *et al.*, 1991). The strong phylogentic sequence conservations in the G-domain reaffirm the notion that the GTPase function of SRα is important for its biological activity.

Role of SRα in Elongation Arrest Release

SRα was originally purified from mammalian cells (Gilmore *et al.*, 1982b) based on its activity to release the SRP mediated translation arrest of presecretory proteins (Walter and Blobel, 1981). These in vitro studies led to the notion that SRα is required for releasing SRP-induced translational arrest. In the absence of SRα, protein synthesis would not proceed beyond a short "arrested fragment" of the presecretory protein. To date, such a tight arrest has only been observed in in vitro assays composed of heterologous components, e.g., mammalian SRP and a wheat germ translation system. In assays composed of exclusively mammalian components, the SRP-induced elongation arrest is transient, thus causing a kinetic delay in protein elongation (Wolin and Walter, 1989). We previously have speculated that the effects of SRP on presecretory protein synthesis may help to maintain proteins in a translocation competent state and/or may provide a potential regulatory point to couple translation to the secretory needs of the cell.

In the experiments described here, presecretory protein synthesis is not detectably reduced as compared with overall protein synthesis when SRα is depleted from cells. We therefore conclude that the lack of SRP receptor in vivo does not lead to a tight elongation arrest that is not released in the absence of SRα. In future studies, it will be interesting to measure directly the elongation rates of presecretory protein synthesis in SRα-depleted cells to test whether yeast SRP causes elongation pausing in vivo as observed in the mammalian in vitro system. Interestingly, in a different yeast, *Yarrowia lipolytica*, it recently was shown that mutations in SRP RNA can cause an inhibition of the translation of a secretory protein (He *et al.*, 1992; Yaver *et al.*, 1992).

Functional Role of Yeast SRα in ER Targeting

From previous studies of SRP, we concluded that in yeast, protein targeting to the ER can occur by redundant pathways (Hann and Walter, 1991). The data presented here for the SRP receptor confirm this notion. In the absence of SRP and SRP receptor, proteins must be targeted to and translocated across the ER membrane by alternative SRP and SRP receptor independent targeting pathways. Although the translocation of some proteins is severely impaired on disruption of the SRP/SRP receptor dependent targeting pathway, the mutant cells are viable. Thus, every protein that has to cross the ER membrane during its biogenesis and that is essential for cell viability can use an alternate targeting pathway sufficiently well to sustain cell growth.

Most of the proteins analyzed were impaired in their translocation across the ER membrane in SRP and/or SRP receptor depleted cells. We consider it likely that these proteins are cotranslationally targeted by SRP and SRP receptor to the ER membrane in wild-type cells and that they become rerouted into alternative targeting pathways only in the mutant cells lacking SRP and/or SRP receptor function. Some preproteins, e.g., preproCPY, that can be targeted as efficiently in the absence of SRP as in its presence may have evolved signal sequences that do not interact efficiently with SRP. Thus, preproCPY may not use the SRP dependent targeting pathway even in wild-type cells (Bird *et al.*, 1987; Hann and Walter, 1991).

The molecular details of alternative targeting pathways in these mutant cells are presently unclear. There are two conceptually distinct but not mutually exclusive possibilities. First, SRP/SRP receptor independent targeting could occur posttranslationally; precursor proteins are released from ribosomes and maintained soluble and translocation competent by interactions with cytosolic chaperonins and other putative targeting fac-

tors. The folding characteristics of a particular preprotein may thus determine how efficiently it can be maintained in a translocation competent form. This could explain why translocation defects observed in SRP and SRP receptor deficient cells vary in magnitude for different proteins. Consistent with this hypothesis, in vitro studies have shown that some fully synthesized precursor proteins can be translocated efficiently across yeast microsomal membranes. Prepro-α-factor, for example, can be efficiently translocated posttranslationally in vitro and shows only minor translocation defects in SRP and SRP receptor depleted cells in vivo.

According to a second hypothesis, SRP/SRP receptor independent targeting could occur cotranslationally; ribosomes synthesizing precursor proteins engage with the ER membrane independent of SRP and SRP receptor but before termination of protein synthesis. If cotranslational targeting is obligate for a given precursor protein, then the kinetics of its elongation would affect the efficiency of its membrane translocation. If elongation is slow, for example, then a longer time window would be available for the nascent precursor protein to engage with the ER membrane before it is completed and released from the ribosome.

The pulse-chase data in Figure 9 show that in SRα-depleted cells, the accumulated pool of cytosolic preKAR2p molecules is not translocation competent. Although we cannot rule out that some of these preKAR2p molecules are translocated very slowly, such slow kinetics could not account for the rapid appearance of translocated KAR2p at the earliest time point. Similar kinetic data were previously obtained in SRP-depleted cells (Hann and Walter, 1991). These data are consistent with either model outlined above. The observed translocation of preKAR2p may occur by a rapid posttranslational mechanism, and a factor mediating this reaction may be limiting. Therefore, only a portion of the precursor proteins would be able to interact with this factor and be translocated. The other portion would be rapidly rendered translocation incompetent. Alternatively, it is possible that preKAR2p requires cotranslational targeting and cannot be maintained translocation competent if released from the ribosome. In this case, the translocated portion of the KAR2p molecules would be synthesized exclusively by ribosomes that are engaged with the ER membrane during KAR2p synthesis.

Growth and translocation defects of SRα-depleted cells resemble those observed in SRP-depleted cells (Hann and Walter, 1991). After shutoff of SRα or SRP54 synthesis, the translocation of KAR2p and DPAP-B was severely impaired, the translocation of invertase and pro-α-factor showed intermediate defects, and the translocation of preproCPY was not affected. There are some quantitative differences in the relative magnitudes of the translocation defects. The translocation of DPAP-B, for example, was impaired to >90% in SRP-depleted cells (Hann and Walter, 1991), yet only impaired to ~50% in SRα-depleted cells (Figure 7). Most likely these differences arose because different strains were used in these studies.

Cells that have been grown in the absence of SRP or SRP receptor for a prolonged time "adapt" to the lack of these components. In the W303 strain used in this study, the adaptation results in almost undetectable translocation defects among the preproteins examined. In the TR1 strain used previously (Hann and Walter, 1991), a similar adaptation was observed that was less pronounced. SRα-depleted cells in which translocation defects are no longer detectable grow with a sixfold increased doubling time, indicating that the adaptation process cannot restore cell physiology to a wild-type state. The molecular nature of the adaptation process is presently unknown. From the presented data, we can rule out, however, that the adaptation is a direct consequence of a suppressor mutation or of the rho$^-$ phenotype that cells acquire after growth in the absence of SRα. According to the two models discussed above, translocation in adapted cells could be enhanced either because limiting components mediating alternate targeting pathways are induced and/or because the rate of protein elongation is reduced. The latter possibility would provide a plausible mechanism by which translocation can be improved but cell growth remains impaired. More efficient protein translocation would be obtained at the expense of efficient protein synthesis. Further studies of the molecular nature of the adaptation process are required to distinguish between these possibilities and may provide valuable information as to the mechanism of SRP/SRP receptor independent protein targeting. From the available data, it is still conceivable that the efficiency of protein translocation only appears to be improved in adapted cells. Cells may have improved a "housekeeping" pathway that allows mislocalized precursor proteins to be degraded more rapidly. This would change the precursor to product ratio that presently is the only measure for translocation efficiency.

Surprisingly, the import of the β-subunit of the F_1-ATPase ($F_1\beta$) into mitochondria was impaired in SRα-depleted cells. A similar phenotype was observed in SRP-depleted cells. As discussed previously (Hann and Walter, 1991), the impaired mitochondrial import could be an indirect consequence of cumulative defects in cells after disruption of the SRP/SRP receptor dependent targeting pathway. Alternatively, it remains possible that SRP and SRα are directly involved in mitochondrial protein import. Models entertaining this latter notion would need to explain, however, how SRα, which is thought to be restricted in its intracellular localization to the ER membrane, could also participate in mitochondrial import. At present, the available data do not allow us to distinguish conclusively between different possibilities. On SRα or SRP depletion, cells rapidly acquired a rho phenotype (see RESULTS; Felici *et al.*,

1989; Hann and Walter, 1991). This loss of mitochondrial function could be a direct consequence of the impaired protein import.

ACKNOWLEDGMENTS

We thank Mark Rose, Randy Schekman, Tom Stevens, and Mike Yaffe for strains and antibodies. We thank Jodi Nunnari for suggesting the novel gene replacement scheme and Ray Deshaies, Byron Hann, Tim Stearns, and Debbie Zimmerman for comments on the manuscript. This work was supported by a predoctoral fellowship from the HHMI to S.C.O. and by grants from the Alfred P. Sloan Foundation and the NIH to P.W. The Genbank accession number for the *SRP101* sequence is M77274.

REFERENCES

Barnes, W.M. (1987). Sequencing DNA with dideoxyribonucleotides as chain terminators: hints and strategies for big projects. Methods Enzymol. *152*, 538–556.

Bernstein, H.D., Poritz, M.A., Strub, K., Hoben, P.J., Brenner, S., and Walter, P. (1989). Model for signal sequence recognition from amino-acid sequence of 54k subunit of signal recognition particle. Nature *340*, 482–486.

Bird, P., Gething, M.J., and Sambrook, J. (1987). Translocation in yeast and mammalian cells: not all signal sequences are functionally equivalent. J. Cell Biol. *105*, 2905–2914.

Bourne, H.R., Sanders, D.A., and McCormick, F. (1991). The GTPase superfamily: conserved structure and molecular mechanism. Nature *349*, 117–127.

Connolly, T., and Gilmore, R. (1989). The signal recognition particle receptor mediates the GTP-dependent displacement of SRP from the signal sequence of the nascent polypeptide. Cell *57*, 599–610.

Davis, R.W., Thomas, M., Cameron, J., St. John, T.P., Scherer, S., and Padgett, R.A. (1980). Rapid DNA isolations for enzymatic and hybridization analysis. Methods Enzymol. *65*, 404–406.

Dayhoff, M.O., Eck, R.V., and Park, C.M. (1972). Atlas of Protein Sequence and Structure. Bethesda, MD: National Biomedical Research Foundation.

Deshaies, R.J., and Schekman, R. (1990). Structural and functional dissection of Sec62p, a membrane-bound component of the yeast endoplasmic reticulum protein import machinery. Mol. Cell. Biol. *10*, 6024–6035.

Dever, T.E., Glynias, M.J., and Merrick, W.C. (1987). GTP-binding domain: three consensus sequence elements with distinct spacing. Proc. Natl. Acad. Sci. USA *84*, 1814–1818.

Felici, F., Cesareni, G., and Hughes, J.M.X. (1989). The most abundant small cytoplasmic RNA of *Saccharomyces cerevisiae* has an important function required for normal cell growth. Mol. Cell. Biol. *9*, 3260–3268.

Fujiki, Y., Hubbard, A.L., Fowler, S., and Lazarow, P.B. (1982). Isolation of intracellular membranes by means of sodium carbonate treatment: application to endoplasmic reticulum. J. Cell Biol. *93*, 97–102.

Gill, D.R., Hatfull, G.F., and Salmond, G.P.C. (1986). A new cell division operon in *Escherichia coli*. Mol. Gen. Genet. *205*, 134–145.

Gilmore, R., and Blobel, G. (1983). Transient involvement of signal recognition particle and its receptor in the microsomal membrane prior to protein translocation. Cell *35*, 677–685.

Gilmore, R., and Blobel, G. (1985). Translocation of secretory proteins across the microsomal membrane occurs through an environment accessible of aqueous perturbants. Cell *42*, 497–505.

Gilmore, R., Blobel, G., and Walter, P. (1982a). Protein translocation across the endoplasmic reticulum. I. Detection in the microsomal membrane of a receptor for the signal recognition particle. J. Cell Biol. *95*, 463–469.

Gilmore, R., Walter, P., and Blobel, G. (1982b). Protein translocation across the endoplasmic reticulum. II. Isolation and characterization of the signal recognition particle receptor. J. Cell Biol. *95*, 470–477.

Hann, B.C., Poritz, M.A., and Walter, P. (1989). *Saccharomyces cerevisiae* and *Schizosaccharomyces pombe* contain a homologue to the 54-kD subunit of the signal recognition particle that in *S. cerevisiae* is essential for growth. J. Cell Biol. *109*, 3223–3230.

Hann, B.C., Stirling, C.J., and Walter, P. (1992). *SEC65* gene product is a subunit of the yeast signal recognition particle required for its integrity. Nature *356*, 532–533.

Hann, B.C., and Walter, P. (1991). The signal recognition particle in *S. cerevisiae*. Cell *67*, 131–143.

He, F., Beckerich, J.-M., and Gaillardin, C. (1992). A mutant of 7SL RNA in *Yarrowia lipolytica* affecting the synthesis of a secreted protein. J. Biol. Chem. *267*, 1932–1937.

Henikoff, S. (1984). Unidirectional digestion with exonuclease III creates targeted breakpoints for DNA sequencing. Gene *28*, 351–359.

Ito, H., Fukuda, Y., Murata, K., and Kimura, A. (1983). Transformation of intact yeast cells treated with alkali cations. J. Bacteriol. *153*, 163–168.

Kamb, A., Weir, M., Rudy, B., Varmus, H., and Kenyon, C. (1989). Identification of genes from pattern formation, tyrosine kinase, and potassium channel families by DNA amplification. Proc. Natl. Acad. Sci. USA *86*, 4372–4376.

Krieg, U.C., Walter, P., and Johnson, A.E. (1986). Photocrosslinking of the signal sequence of nascent preprolactin to the 54-kilodalton polypeptide of the signal recognition particle. Proc. Natl. Acad. Sci. USA *83*, 8604–8608.

Kurzchalia, T.V., Wiedmann, M., Girshovich, A.S., Bochkareva, E.S., Bielka, H., and Rapoport, T.A. (1986). The signal sequence of nascent preprolactin interacts with the 54K polypeptide of the signal recognition particle. Nature *320*, 634–636.

Lauffer, L., Garcia, P.D., Harkins, R.N., Coussens, L., Ullrich, A., and Walter, P. (1985). Topology of the SRP receptor in the endoplasmic reticulum membrane. Nature *318*, 334–338.

Maniatis, T., Fritsch, E.F., and Sambrook, J. 1982. Molecular Cloning: A Laboratory Manual. Cold Spring Harbor, NY: Cold Spring Harbor Laboratory.

Meyer, D.I., Krause, E., and Dobberstein, B. (1982). Secretory protein translocation across membranes—the role of the docking protein. Nature *297*, 647–650.

Nasmyth, K.A., and Tatchell, K. (1980). The structure of transposable yeast mating type loci. Cell *19*, 753–764.

Orr-Weaver, T.L., Szostak, J.W., and Rothstein, R.J. (1981). Yeast transformation: a model for the study of recombination. Proc. Natl. Acad. Sci. USA *78*, 6354–6358.

Ramirez, C., and Matheson, A.T. (1991). A gene in the archaebacterium *Sulfolobus solfataricus* that codes for a protein equivalent to the alpha subunits of the signal recognition particle receptor in eukaryotes. Mol. Microbiol. *5*, 1687–1693.

Rapiejko, P.J., and Gilmore, R. (1992). Protein translocation across the endoplasmic reticulum requires a functional GTP binding site in the α-subunit of the signal recognition particle receptor. J. Cell Biol. *117*, 493–503.

Römisch, K., Webb, J., Herz, J., Prehn, S., Frank, R., Vingron, M., and Dobberstein, B. (1989). Homology of the 54K protein of signal-rec-

ognition particle, docking protein, and two *E. coli* proteins with putative GTP-binding domains. Nature *340*, 478–482.

Rothstein, R.J. (1983). One-step gene disruption in yeast. Methods Enzymol. *101*, 202–211.

Saiki, R.K., Gelfand, D.H., Stoffel, S., Scharf, S.J., Higuchi, R., Horn, G.T., Mullis, K.B., and Erlich, H.A. (1988). Primer-directed enzymatic amplification of DNA with a thermostable DNA polymerase. Science *239*, 487–494.

Schloss, P., Hermans-Borgmeyer, I., Betz, H., and Gundelfinger, E.D. (1988). Neuronal acetylcholine receptors in *Drosophila*: the ARD protein is a component of a high-affinity alpha-bungarotoxin binding complex. EMBO J. *7*, 2889–2894.

Sheen, J.Y., and Seed, B. (1988). Electrolyte gradient gels for DNA sequencing. Biotechniques *6*, 942–944.

Sherman, F., Fink, G., and Lawrence, C.W. (1974). Methods in Yeast Genetics. Cold Spring Harbor, NY: Cold Spring Harbor Laboratory.

Sikorski, R.S., and Heiter, P. (1989). A system of shuttle vectors and yeast host strains designed for efficient manipulation of DNA in *Saccharomyces cerevisiae*. Genetics *122*, 19–27.

Simon, S.M., and Blobel, G. (1991). A protein-conducting channel in the endoplasmic reticulum. Cell *65*, 371–380.

Smith, D.B., and Johnson, K.S. (1988). Single-step purification of polypeptides expressed in *Escherichia coli* as fusions with glutathione S-transferase. Gene *67*, 31–40.

Stirling, C.J., and Hewitt, E.W. (1992). The *Saccharomyces cerevisiae SEC65* gene encodes a component of the yeast signal recognition particle with homology to human SRP19. Nature *356*, 534–537.

Stirling, C.J., Rothblatt, J., Hosobuchi, M., Deshaies, R., and Schekman, R. (1992). Protein translocation mutants defective in the insertion of integral membrane proteins into the endoplasmic reticulum. Mol. Biol. Cell *3*, 129–142.

Stotz, A., and Linder, P. (1990). The *ADE2* gene from *Saccaromuces cerevisiae*: sequence and new vectors. Gene *95*, 91–98.

Taha, M.K., Dupuy, B., Saurin, W., So, M., and Marchal, C. (1991). Control of pilus expression in *Neisseria gonorrhoeae* as an original system in the family of two-component regulators. Mol. Microbiol. *5*, 137–148.

Tajima, S., Lauffer, L., Rath, V.L., and Walter, P. (1986). The signal recognition particle is a complex that contains two distinct polypeptide chains. J. Cell Biol. *103*, 1167–1178.

Walter, P., and Blobel, G. (1981). Translocation of proteins across the endoplasmic reticulum. III. Signal recognition protein (SRP) causes signal sequence and site specific arrest of chain elongation that is released by microsomal membranes. J. Cell Biol. *91*, 557–561.

Walter, P., and Blobel, G. (1983). Subcellular distribution of signal recognition particle and 7SL-RNA determined with polypeptide specific antibodies and complementary DNA probe. J. Cell Biol. *97*, 1693–1699.

Walter, P., and Lingappa, V.R. (1986). Mechanism of protein translocation across the endoplasmic reticulum membrane. Annu. Rev. Cell Biol. *2*, 499–516.

Witte, C., Jensen, R.E., Yaffe, M., and Schatz, G. (1988). MAS1, a gene essential for yeast mitochondrial assembly, encodes a subunit of the mitochondrial processing protease. EMBO J. *7*, 1439–1447.

Wolin, S., and Walter, P. (1989). Signal recognition particle mediates a transient elongation arrest of preprolactin in reticulocyte lysate. J. Cell Biol. *109*, 2617–2622.

Yaver, D.S., Matoba, S., and Ogrydziak, D.M. (1992). A mutation in the signal recognition particle 7S RNA of the yeast *Yarrowia lipolytica* preferentially affects synthesis of the alkaline extracellular protease: *in vivo* evidence for translational arrest. J. Cell Biol. *116*, 605–616.

Chapter 3

Saccharomyces Cerevisiae Signal Recognition Particle Receptor Consists of Two Interacting Subunits, Both of which Are GTPases

ABSTRACT

Database searches revealed an open reading frame on chromosome XI of the yeast *Saccharomyces cerevisiae* that is homologous to the mammalian SRP receptor beta subunit (SRβ). The yeast SRβ gene (*SRP102*) encodes a 30 kDa protein with similarity to GTPases, and is important for nascent secretory protein translocation into the endoplasmic reticulum (ER). Deletion of *SRP102* results in slow growing cells that are only marginally compromised in their ability to translocate proteins into the ER. This phenotype is identical to that of other SRP pathway gene disruptions. Deletion of the SRβ gene in combination with the gene for the SRP receptor alpha subunit (SRα; *SRP101*) results in cells that grow slowly, but no worse than either single gene deletion alone. A point mutation in one of the conserved GTP binding residues (K51I) results in temperature sensitive growth of the cells, and accumulation of precursors to secretory proteins at the non-permissive temperature. Taken together, these results suggest that the yeast SRβ functions as a GTPase in the SRP dependent targeting and translocation of nascent secretory proteins into the ER.

In cells deleted for SRβ, SRα is not found in its normal membrane containing fraction, instead it behaves as a cytosolic protein. This suggests a possible role of SRβ in the anchoring of SRα in the ER membrane. Further, SRα can be coimmunoprecipitated with SRβ from detergent solubilized membranes using antibodies directed against an epitope tagged SRβ. Consistent with the notion that SRβ is required for proper SRα membrane association, the membrane localization of SRα is perturbed in the temperature sensitive allele of *SRP102, SRP102-K51I*. Further, the growth defect of *SRP102-K51I* can be suppressed by overexpression of SRα. These

biochemical and genetic data support the notion that the yeast SRP receptor, like its mammalian counterpart, consists of two directly interacting subunits.

INTRODUCTION

Localization of proteins to their correct subcellular compartments is required for eucaryotic cells to maintain the high degree of order compatible with life. From studies of a mammalian in vitro system, a model was proposed whereby protein translocation across the ER membrane occurrs in a strictly co-translational manner (Walter et al., 1984). Secretory protein synthesis initiates on cytoplasmic ribosomes, and terminates only after those ribosomes have been targeted to the endoplasmic reticulum (ER). After targeting, the ribosome-nascent chain is assembled into a complex capable of translocating the nascent protein across the ER membrane concomitant with the completion of its synthesis. A small ribonucleoprotein, signal recognition particle (SRP) initially selects ribosomes for targeting if they are synthesizing nascent polypeptides containing signal sequences. These signal sequences, as they emerge from the ribosome, bind tightly to SRP effecting an elongation arrest or transient pause in the translation of the nascent secretory protein (Walter and Johnson, 1994). Targeting of this complex to the ER occurs via an interaction between SRP and its receptor (SR) (Meyer et al., 1982; Gilmore et al., 1982b; Gilmore et al., 1982a), a heterodimeric protein anchored in the ER membrane. While this interaction results in localization of the nascent protein to the ER, it also releases the SRP induced translational arrest and allows the nascent chain/ribosome complex to dissociate from SRP/SR dimer and assemble with other components required for translocation in the ER membrane (known as a translocon). The translocon is a proteinaceous structure through which the nascent polypeptide can cross the hydrophobic environment of the lipid bilayer (Gilmore and Blobel, 1983; Simon and Blobel, 1992; Görlich and Rapoport, 1993; Crowley et al., 1994). SRP and SR are

required for the initial targeting of the ribosome/nascent chain to the ER, and for proper ribosome/ translocon junction formation. Thus, SRP and SR act as a system that couples cytoplasmic translation to the translocation of proteins across the lipid bilayer of the ER membrane.

Studies in yeast suggest that there are at least two pathways by which a protein can be targeted to the ER membrane (Hann and Walter, 1991; Ogg et al., 1992). In addition to an SRP dependent pathway, some proteins can also become translocated in the abence of SRP. Two pieces of evidence led us to this conclusion. A number of integral membrane and soluble proteins have been assayed for their ability to acheive proper localization in yeast cells expressing condtional alleles of SRP genes. Different proteins are blocked in ER translocation to different degrees. Some proteins, such as predipeptidylaminopeptidase-B (DPAP-B), and preKar2p are rather dependent on the presence of components of the SRP dependent pathway for translocation into the ER,while other proteins, such as preprocarboxypeptidase Y (CPY) and prepro-α-factor, can attain their proper localization even in the absence of components of the SRP dependent pathway. In addition, yeast cells deleted for any of the known componenets of the SRP dependent targeting pathway can survive, and therefore must be able to translcoate all essential proteins via an SRP independent targeting pathway.

Both SRP and SR are multisubunit complexes: SRP consists of six protein subunits and a small RNA component (Walter and Blobel, 1980; Walter and Blobel, 1982); SR is a heterodimeric ER membrane protein consisting of a 69 kDa, peripheral membrane protein (SRα), and a 30kDa, integral membrane protein (SRβ) (Tajima et al., 1986). Much is known of one

SRP subunit, SRP54. It contains both the signal sequence binding activity of SRP, interacts with the SRP RNA, and mediates binding of SRP to SR (Brown et al., 1994; Krieg et al., 1986; Kurzchalia et al., 1986). In addition, SRP54 contains a functional GTPase domain (Miller et al., 1993). Although SR is less well characterized than SRP54 functionally, both subunits of SR contain GTPase domains (Miller et al., 1995; Connolly and Gilmore, 1986). The GTPase domains of SRP54 and SRα are related, defining a subfamily in the GTPase superfamily (Bourne et al., 1991; Bernstein et al., 1989; Römisch et al., 1989). That these two proteins are similar and interact with each other may reflect evolutionary divergence from an originally homotypic interaction. Work in our laboratory has sought to elucidate the relative contributions of each of these GTPases in protein targeting to the ER membrane. A model has been proposed for the cycle of GTP binding and hydrolysis of SRP54 (Miller, et al., 1993). As SRP binds to the signal sequence of a nascent secretory protein, SRP54 becomes stabilized in a nucleotide free state. Targeting of this complex to the ER membrane, and interaction of SRP with its receptor effects GTP binding to SRP54. Change in conformation of SRP54 to its GTP-bound state results in release of the signal sequence from SRP. The ribosome/nascent chain complex is thus free to interact with components of the translocon. SRP remains associated with SR after release of the ribosome/nascent chain complex. Hydrolysis of GTP contained either in SRP54 or SRa results in dissociation of SRP from SR and is thus able to reenter the cytoplasm and target another nascent secretory protein to the ER membrane. Recent results indicate that SRP54 and SRα act as GAPs for each other while they are in the GTP bound state.

In previous work, we showed that yeast contains a homologue of SRα encoded by the *SRP101* gene. Recently, the β subunit of the mammalian SR was characterized (Miller, et al., 1995). Here we present the first characterization on the SRβ subunit of the yeast SR, encoded by the *SRP102* gene. Although the precise role of SRβ remains enigmatic, we show that at least one role for SRβ is to anchor SRα to the membrane of the ER. Like its mammalian homologue, the sequence of the yeast SRβ predicts an integral membrane GTPase, related to Sar1p. Extensive site directed mutagenesis of residues in the highly conserved GTP binding domains of SRβ was performed. With one exception, these mutations are silent when placed in vivo. The high frequency of silent mutations suggests that the effects of mutations in SRβ cannot be readily predicted by analogy to other GTPases.

MATERIALS AND METHODS

strains, antibodies, materials, and general methods

Yeast strains are listed in Table I. Genetic techniques are performed as described previously, except where noted (Sherman and Lawrence, 1974). Yeast transformation was performed by the lithium acetate procedure (Ito et al., 1983). Yeast DNA for Southern analysis was prepared according to Davis et al. (1980). Recombinant DNA techniques, and Southern blots were performed as described by Sambrook et al. (1989). Western blots were visualized using enhnced chemiluminescence ("ECL", Amersham, Arlington Heights, IL) as described by the manufacturer. Oligonucleotides were synthesized on a Milligen/Biosearch Cyclone Plus DNA synthesizer (Milligen/Biosearch, Division of Millipore, Novato, CA) and purified according to the manufacturer's instructions. Sodium dodecyl sulfate-

Table 1 **Yeast Strains and plasmids Used in This Study**

Strain	Genotype	Reference
W303	*ade2-1/ade2-1 trp1-1/trp1-1 leu2-3, 112/leu2-3, 112 his3-11/his3-11 ura3-1/ura3-1 can1-100/can1-100* MAT***a***/MATα	Deshaies and Schekman, 1991
SOY133	W303 *SRP102/srp102::HIS3*	This study (see methods)
SOY162	W303 MATα *srp102::HIS3*	This study
SOY246	SOY162 [pSO462]	This study
SOY283	SOY162 [pSO460]	This study
SOY219	SOY162 [pSO457]	This study
SOY223	SOY162 [pSO459]	This study
SOY201	SOY162 [pSO454]	This study
SOY264	SOY162 [pSO462] [pSO211]	This study
SOY268	SOY162 [pSO462] [pSO400]	This study

Plasmid	Markers	Backbone	reference
pSO452	*URA3, SRP102, CEN6/ARSH4*	pRS316	Sikorski and Heiter, 1989
pSO454	*TRP1, SRP102, CEN6/ARSH4*	pRS314	Sikorski and Heiter, 1989
pSO457	*TRP1, SRP102*-myc, *REP3* (2μ)	YEplac112	Geitz and Sugino, 1988
pSO459	*TRP1, SRP102*-HA, *CEN6/ARSH4*	pRS314	Sikorski and Heiter, 1989
pSO460	*URA3*, p*GAL-SRP102*-myc, *CEN4/ARS1*	YCp50	Rose et al., 1987
pSO462	*TRP1, srp102(K51I)*-HA, *CEN6/ARSH4*	pRS314	Sikorski and Heiter, 1989
pSO211	*URA3, SRP101, CEN6/ARSH4*	pRS316	Sikorski and Heiter, 1989
pSO400	*URA3*, p*GAL1/10-SRP101, CEN6/ARSH4*	pRS316	Sikorski and Heiter, 1989

polyacrylamide gel electrophoresis was performed on 10%-15% gradient gels. Both high and low copy yeast shuttle vectors used are as described (Christianson et al., 1992; Sikorski and Heiter, 1989)unless otherwise indicated. Chemicals are from Sigma Chemicals (St. Louis, MO) unless otherwise noted. The plasmid library used for cloning *SRP102* was obtained from the ATCC (catalog # 37415). Anti-Kar2p serum was prepared in our laboratory using Kar2p overexpressed in *E. coli* from a clone kindly provided by Joe Vogel and Mark Rose (Rose et al., 1989). One-half a microliter of anti-Kar2p serum was used per OD_{600} in non-native immunoprecipitations. Fluorochrome coupled anti-rabbit and anti-mouse secondary antibodies are from Jakson Immuno Research (West Grove, PE). Anti- SRα is used as described in Ogg et al. (1992). Monoclonal 12CA5 (anti-HA) and 9E10 (anti-myc) were purchased from BAbCo (Berkeley, CA), and used at a dilution of 1:10,000 on Western blots. DNA sequencing was performed using an ABS A220 fluorescent DNA sequencer and cycle sequencing.

Cloning of SRP102

Initial attempts to clone *SRP102* using PCR from genomic DNA, and the known sequence to design oligonucleotides resulted in the clones having multiple sequence errors, presumably from inaccurate PCR. Therefore a genomic clone of *SRP102* was isolated by screening a plasmid library prepared from *S. Cerevisiae* strain GRF88 in the vector YCp50 using one of the PCR obtained clones as a probe to screen the library (Rose et al., 1987). pSO440, one of the plasmids obtained in the initial PCR attempt to clone *SRP102* was random primed using the "Ready To Go" DNA labeling kit according to the manufacturer's instructions (Pharmacia, Piscataway, NJ). pSO440 was constructed by ligating the *Hind* III/*Xba* I restricted PCR product from a

reaction using genomic DNA prepared from strain W303 and oligonucleotides oSRP102-1 (5′-CTAGAAAGCTTCTTTTTTCATCTAGTGGCGG-3′; corresponding to nt -175 to nt -156 where the A of the presumed initiation codon is nt 1 and 733 is the T in the ochre stop codon) and oSRP102-2 (5′-CTTTCTCTGCGTACGGAATC-3′; corresponding to nt 821 to nt 802, again from the presumed A of the initiation codon) into pBluescript II SK (+) (Strtagene, LaJolla, CA) that had been restricted with *Hind* III and *Xba* I. Three plasmids were isolated (designated pSO451a,b, and c) that contained identical inserts, and the 2966 bp *Eco* RI fragment predicted to contain *SRP102* was subcloned into the *Eco* RI sites of pRS314, pRS316, and pRS426 yielding plasmids pSO454, pSO452, and pSO453 repsectively. Both strands of the insert in pSO452 were sequenced from nt -175 (using oSRP102-1 as a sequencing primer) through nt 821 (using oSRP102-2 as a sequencing primer) and this sequence agreed with the published genomic sequence. Confirmation that these plasmids contained a functional open reading frame was obtained by complementation of the *SRP102* gene disruption.

Gene Disruption

We generated a null allele of *SRP102* in a two step fashion. First we used PCR to generate DNA fragments corresponding to the 5′ and 3′ flanking regions of *SRP102* and cloned these in a three piece ligation into pBluescript II SK (+) (Stratagene, LaJolla, CA) generating pSO445. Briefly, the 5′ flanking fragment was generated using W303 genomic DNA as the template and oSRP102-1 (see above for sequence) plus oSRP102-7 (5′-TCCCCCGGGGGATGCCTTTTGCACTGC-3′, corresponding to nt 81 to nt 64) to polymerize a 256 nt fragment corresponding to nt -175 to nt 81 of

SRP102. The 3′ flanking fragment was generated in a similar manner except that oSRP102-2 (see above for sequence) and oSRP102-8 (5′-TCCCCCGGGTCACTGCAAGACCACCATC-3′, corresponding to nt 476 to nt 494) were used as primers during PCR. This generated a 345 nt fragment corresponding to nt 476 to nt 821 of the *SRP102* gene. Note that the coding sequence ends at 733. Thus the 3′ flanking fragment also contains coding sequences for the ultimate 85 amino acids (out of 244). These two PCR products were digested with *Sma*I and *Hind*III (5′ flanking region fragment) or *Sma*I and *Xba*I (3′ flanking region fragment) purified by agarose gel electrophoresis and ligated into *Xba*I and *Hind*III restricted pBluescript II SK (+) to generate pSO445. In a second step, the *S. cerevisiae HIS3* gene was obtained by restriction digest of pRS303 with *Ssp*I. The 1621 nt fragment carrying the *HIS3* gene was ligated into pSO445 that had been digested with *Sma*I, generating pSO446, now carrying the *HIS3* gene between the 5′ and 3′ flanking regions of *SRP102*. A linear fragment carrying the *SRP102* disruption allele was generated by digesting pSO446 with *Xba*I and *Sal*I and agarose gel purifying the 2.1 Kb fragment. The diploid yeast strain W303 was transformed to His^+ prototrophy using this 2.1 Kb *Xba*I/*Sal*I fragment, giving rise to strain SOY133. Transformants were induced to sporulate in liquid sporulation media and asci were dissected into tetrads. Genomic DNAs prepared from the heterozygous diploid (SOY133), wild type parent (W303), and representative spores from a single tetrad were used as template in PCR using primers oSRP102-13 (5′-CTGAGCTCTTTAGAATTAGTT-3′; corresponding to nt -446 to nt -426 of the SRP102 sequence) and oSRP102-10 (5′-GATCATATAACTGCTGGAAC-3′; corresponding to nt 993 to nt 974 of the SRP102 sequence). PCR products from these reactions were separated using agarose gel electrophoresis and stained with ethidium bromide. When DNAs

from the wild type parent and the His^- spores were used as template in the PCR, the expected ~1.42 Kb fragment was seen. Use of the DNA isolated from the His^+ spores gave rise to a single expected ~2.65 Kb fragment. Only when DNA prepared from the heterozygous diploid was used as template in the reaction were both the 1.42 Kb and the 2.65 Kb fragments seen.

Plasmid and Strain Construction

In order to construct a plasmid containing *SRP102* under control of the *GAL1/10* promoter, we used PCR in order to produce a fragment corresponding to the *SRP102* coding sequences and subcloned this fragment into pTS210 (Tim Stearns, Department of Biology, Stanford University, Palo Alto, CA). The PCR used pSO451 as template and oligonucleotides oSRP102-2 (see above for sequence) and oSRP102-14 (5'-CGGATCC ATG CTT AGT AAT ACA CTT ATT-3'; corresponding to a *Bam*HI site and nt +1 to nt +21) as primers, followed by restriction digest of the expected 821 nt fragment with *Bam*HI and *Xba*I, in order to generate the fragment containing the *SRP102* coding sequence. This fragment was purified by agarose gel electrophoresis and ligated into pTS210 that had been digested with *Bam*HI and *Xba*I, generating pSO460. This plasmid was transformed into SOY133 and the resulting Ura^+ prototrophs were induced to sporulate. Asci were dissected into tetrads and allowed to germinate at room temperature on YEP plates containing 2% galactose and 2% sucrose as carbon sources. Colonies that were both Ura^+ and His^+ were chosen for further study. The fact that His^+, Ura^+ colonies arose that grew with wild type rates supports our assignment of the initiation codon, as Srp102p expressed from pSO460 starts at this codon. Additionally, these His^+, Ura^+ colonies were incapable of growing for more than a few generations on plates containing 2% glucose as the sole carbon

source, indicating that we had indeed placed *SRP102* under conditional control.

In order to generate the strains we used in our fractionation and immunofluorescence studies we placed plasmids containing Srp102p (pSO454, no epitope tag), or Srp102p-HA (pSO459) or Srp102p-myc (pSO457) into SOY133 and induced the diploid transformants to sporulate. Spores giving rise to colonies that were both His^+ (*SRP102::HIS3*) and Trp^+ (containing a plasmid) and that grew at wild type rates were chosen for further study and these strains were designated as indicated in Table I. We constructed pSO457 in the following manner; a PCR product from a reaction using oligos oSRP102-13 (see above for sequence) and oSRP102-12 (5'-GAACCCATGGCAGTTTTTCATCTATCCA-3'; corresponding to nt 732 to nt 715) as primers was digested with *Eco*RI and *Nco*I and ligated into pCS118 (kind gift of Caroline Shamu, UCSF) that had been digested with *Eco*RI and *Nco*I. pCS118 contains a 400 bp insert harboring the myc tag, stop codons in all three reading frames, and an actin transcriptional terminator on an *Nco*I–*Sph*I fragment inserted into YEplac112 (Geitz and Sugino, 1988). Thus pSO457 contains the SRP102 coding sequence fused at the C-terminus to the myc tag, followed by an actin terminator, all in the YEplac112 (TRP1, 2μ) backbone. A similar strategy was used to construct pSO459. pSF19 (kind gift of Peter Sorger, MIT, Boston, MA) containing the HA epitope, stop codons, and the actin terminator on an *Nco*I–*Xba*I fragment in pRS314 was digested with *Asp*718 and *Nco*I. A PCR product from a reaction using oSRP102-11 (5'-GGGGTACCGGTCCCGGTACGACTGG-3'; corresponding to nt -487 to nt -471) and oSRP102-12 (see above for sequence) was digested with *Asp*718 and

*Nco*I and ligated into the *Asp*718/*Nco*I digested pSF19 to give pSO459. This plasmid contains SRP102-HA in the pRS314 backbone (TRP1, CEN/ARS).

Site directed mutagenesis

Site directed mutagenesis was performed by the method of Kunkel (Kunkel, 1985; Kunkel et al., 1987). Single stranded uracil rich DNA used for template was prepared from the phagemid pSO459 (containing SRP102-HA). Plasmids that were recovered from a mutagenesis reaction and subsequently confirmed to have incorporated the desired mutation, are designated with the wild type amino acid in single letter code, position of the amino acid changed, and the name of the new amino acid in single letter code (e.g. S49A signifies that a serine at position 49 has been changed to an alanine). Every mutation was confirmed by sequencing both strands of the plasmid recovered. The following is a compilation of each of the mutations obtained and the corresponding oligonucleotide that was used to produce that mutation. Wild type sequences are in normal type and the codon changed is in bold. Nucleotide(s) that are non-complementary to the rescued strand of pSO459 are shown underlined.

S49A	oSRP102-25	5′-CGT TTT TCC **AG<u>C</u>** ATT TTG AGG-3′
K51I	oSRP102-16	5′-G CAA GCT CGT **<u>AA</u>T** TCC AGA ATT TTG-3′
T52N	oSRP102-17	5′-CGT AAG CAA GCT **<u>ATT</u>** TTT TCC AGA-3′
T66A	oSRP102-22	5′-GA AAC AAC **AG<u>C</u>** TGG TCT TAC-3′
G90L	oSRP102-18	5′-CTT GAC ATG <u>CAA</u> TGG GAA GTC-3′
H91L	oSRP102-20	5′-CAA CTT GAC <u>CAA</u> GCC TGG GAA GT-3′

N154I	oSRP102-19	5′-C GCT TTT **AAT** GCA TGC AAT TAA G-3′
E157Q	oSRP102-15	5′-GT GAA CAA **TTG** GCT TTT ATT GC-3′
S220A	oSRP102-23	5′-GC AAC TAC **AGC** TGC TTC C-3′
K51A, T52A	oSRP102-21	5′-CGT AAG CAA GCT **AGC AGC** TCC AGA ATT TTG-3′
K51I, H91L	oSRP102-20+oSRP102-16	see above
N154A, E157A	oSRP102-24	5′-GC AGT GAA CAA **AGC** GCT TTT **AGC** GCA TGC AAT TAAG-3′
ΔS49	oSRP102-26	5′-CT CGT TTT TCC **AGC AGC AGC** ACC TGC AATG-3′

Cell fractionation

Cell fractionation was performed essentially as described in Ogg et al. (1992) with the following modifications. Zymolyase-100T (ICN Biomedicals, Costa Mesa, CA) instead of lyticase was used at 5μg/ OD_{600} to convert cells into spheroplasts. Only PMSF and leupeptin were included as protease inhibitors.

Immunofluorescence

Immunofluorescence was performed essentially as described (Pringle et al., 1989). Anti-HA, and anti-myc antibodies were used at dilutions of 1:200 to 1:2000. Anti-Kar2p antibodies were used at a dilution of 1:10,000. Bound primary antibodies were decorated with either fluorescein isothyocyanate (FITC)-conjugated donkey anti-mouse IgG, or tetramethyl rhodamine isothiocyanate (TRITC)-conjugated donkey ant-rabbit IgG (Jackson

Immunoresearch, West Grove, PA) diluted 1:50. Slides were mounted in 90% glycerol containing 1 mg/ml p-phenylenediamine, pH 9.0 and containing 1 mg/ml 4', 6-diamino-2-phenylindole (DAPI). Cells were examined at X1000 magnification on a Zeiss Axioskop microscope. Images were recorded on Kodak TMAX 400 black-and-white film with a Zeiss MC 80 camera and controller.

Immunoprecipitations

Denaturing immunoprecipitaitons were performed as decribed (Ogg, et al., 1992). Non-denaturing immunoprecipitations were performed from detergent solubilized membranes in the following manner. Cells were grown to 0.5 OD_{600}/ml in synthetic complete medium lacking amino acids used for the maintaince of a plasmid containing SRP102-HA. Typically 30 total OD_{600} were harvested at a time. After pelleting in a clinical centrifuge and washing with 50mM NaCl, 20mM NaN_3, cells were resuspended in buffer A (Tris-SO_4 pH 9.4, 10mM DTT) at 10 OD_{600}/ml and incubated at room temperature for 20 min. Conversion of the cells to spheroplasts was then acheived by harvesting the cells in a clinical centrifuge, and resusupending them in spheroplast media (50mM Tris-Cl pH 7.5, 1.2M Sorbitol, 5mM $MgCl_2$, 5mM DTT, 10mM NaN_3) at 20 OD_{600}/ml. We used 5 μg/OD_{600} Zymolyase 100-T (ICN Biomedicals, Costa Mesa, CA) to digest the cell walls during a 30 min incubation at 30°C. Efficiency of spherplasting was monitored by phase contrast microscopy. Spheroplasts were recovered by centrifugation through a cushion (twice the volume of the spheroplasting cells) of spherplast media containing 1.9M sorbitol but no DTT at 7,800 X g for 5 min (7,000 rpm in a Beckman JS-13 rotor). All subsequent steps were performed at 4° C. Spherplasts were resuspended in lysis buffer, LB (200mM Sorbitol, 25mM

NaPi pH 7.5, 150mM NaCl, 5mM MgCl2, 1mM PMSF, 0.5 μg/ml of leupeptin, 1mM EDTA) at 100 OD_{600}/ml. Cells were lysed by addition of 3/4 volme of Zirconium beads (BioSpec Products, Bartlesville, OK) and vortexing gently (setting 3 on a scale of 1 to 10) for 4 rounds of lysis. Each round consisted of 15 s of vortexing followed by a 15 s cooling period in an ice-water bath. Lysate was removed from the beads which were washed once with ice cold LB. The lysate and bead wash were combined and the unbroken cells and nuclei were removed by centrifugation at 370 X g (1,200 rpm in a JS-13) for 4 min. This step was critical, longer centrifugation resulted in loss of most of the ER as judged by the pelleting of an ER marker, Srp101p. The low speed supernatant, containing crude membranes was transferred to TLA100.1 polycarbonate tubes and membranes were pelleted by centrifugation at 43,630 X g for 12 min (35,000 rpm) in the Beckman TLA100.1 rotor in a Beckman TL100 tabletop ultracentrifuge. The membrane pellet was washed (30 OD_{600}/ml) with LB. This was acheived by first resuspending the pellet in a minimal volume of LB (20-40 μl), followed by dilution to the appropriate volume with LB. Again the membranes were pelleted by centrifugation in the TL100 as above. The final membrane pellet was resuspended in LB + 10% glycerol (GLB) to 50 OD_{600}/ml using the same technique as described above to ensure even membrane resuspension. Membranes were solubilized by addition of 1/10th volume of 10% Triton X-100 (Calbiochem, La Jolla, CA) and incubation at 4° C for 20 min. Following incubation, the detergent solubilized membranes were cleared by centrifugation at 100,000 X g in the TL 100 (60,000 rpm in the TLA100.1) for 25 min. The resulting lysate was frozen in liquid nitrogen and stored at -80° C.

Immunoprecipitation were performed by diluting 2 OD_{600} units (40 μl) of the above lysate into 560 μl of GLBT (GLB containing 1% Triton X-100).

Non-specific binding of proteins in the lystate to Sepharose was removed by addition of 30 µl of a 50% slurry of Sepharose CL-4B (Pharmacia, Uppsala, Sweden), and rotation for 30 min at 4° C. Sepharose beads were removed by centrifugation in a Beckman microfuge and transfer of the lysate to a new tube. Antibody-Sepharose bead compexes (10 µl; corresponding to 3 µl of the 12CA5 ascites fluid) were added and the tube was mixed by rotation at 4° C for 15 min. We found that with the 12CA5 antibody, longer incubation times of the antibody-bead complex resulted in lower recovery of Srp101p in the immunoprecipitation. The 12CA5 antibody used in the native immunoprecipitations was covalently attached to a Sepharose matrix by using the Affinica antibody coupling kit (Schleicher and Schuell, Keene, NH) and the manufacturers instructions. Following extensive washing the antibody bead complex was stored as a 50% slurry in PBS containing 10mM NaN_3.

RESULTS

Disruption and Cloning of *SRP102*

Database searches revealed an open reading frame encoding a putative GTPase of unknown function on *S. cerevisiae* chromosome XI (YKL154w) with significant structural similarity to mammalian SRβ (Miller, et al., 1995). Data presented below confirm that this gene indeed encodes the yeast homolog of mammalian SRβ and plays an essential role in the SRP-dependent protein targeting pathway to the ER membrane. Henceforth, we refer to this gene encoding the β-subunit of the SRP receptor as *SRP102*, consistent with the designation of gene encoding the α-subunit of the SRP

receptor as *SRP101* (Ogg, et al., 1992). By convention, we shall refer to the corresponding gene products as Srp102p and Srp101p, respectively.

As the first step towards a functional characterization of *SRP102* , we examined the phenotype of a gene deletion. To this end, we replaced the central portion of *SRP102* with the selectable marker gene *HIS3* (see Methods and Fig. 1A). In brief, sequences flanking *SRP102* were cloned in tandem such that they were separated by a unique restriction site into which the *HIS3* gene was then inserted. Using this DNA insert, the genomic copy of *SRP102* was disrupted in the diploid histidine auxotroph strain W303. His^+ colonies bearing the *SRP102* gene disruption were isolated, yielding strain SOY133.

Southern blot analysis of genomic DNA of SOY133 cells confirmed that the *HIS3* gene was inserted into the genomic *SRP102* locus (Figure 1B). In *Eco*RI-digested DNA isolated from the wildtype strain, a fragment of the predicted size (2966 bp) was detected with a radioactive probe corresponding to the *SRP102* gene (Fig. 1B, lane 1, marked with an open arrow). The insertion of *HIS3* into one of the two genomic copies of *SRP102* resulted in an additional band migrating at about 4200 bp (Fig. 1B, lane 2, closed arrow), consistent with the insertion of the 1621 bp *HIS3* gene and the removal of 395 bp of the *SRP102* gene.

Tetrad analysis, following sporulation of SOY133 cells, resulted in four viable spores two of which grew at nearly wild type rates while the other two grew with a much reduced rate (Fig. 1C). In each of 7 tetrads analyzed, the growth defect, the His^+ phenotype, and the *srp102::HIS3* gene disruption (as monitored by PCR analysis; see Methods) segregated 2:2 from the *SRP102*

Figure 1.

Gene disruption of *SRP102*. (A) Cartoon of the genomic region around *SRP102*. Scale is in kilobases. Insertion of the *HIS3* gene used for the disruption is shown as well as the *Eco*R I sites used to estimate fragment size in the Southern blot. **(B)** Southern blot analysis showing genomic DNA from the parent diploid (lane 1) or transformants (lane 2) containing the *srp102::HIS3* disruption. DNA was digested with *Eco*R I. Fragments corresponding to the wild type gene are marked with an open arrowhead, those corresponding to the disrupted gene are marked with a closed arrowhead. **(C)** Tetrads from the strain SOY133 (*SRP102/srp102::HIS3*) dissected onto YEPD medium and incubated at 24°C for 10 days.

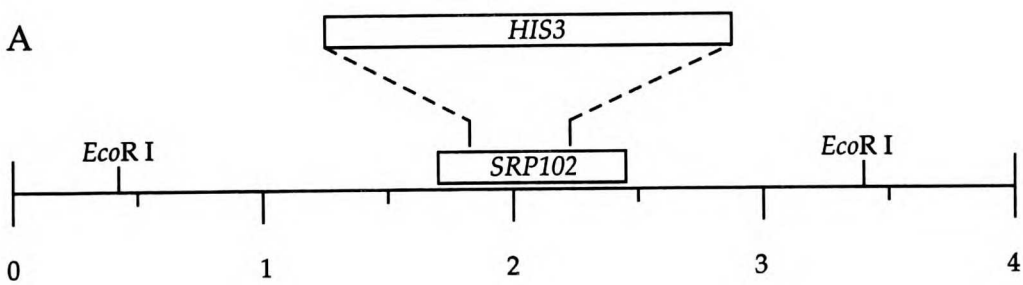

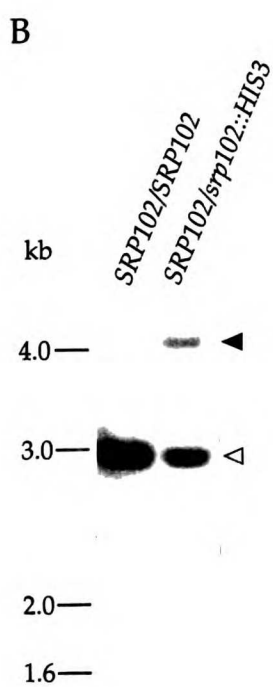

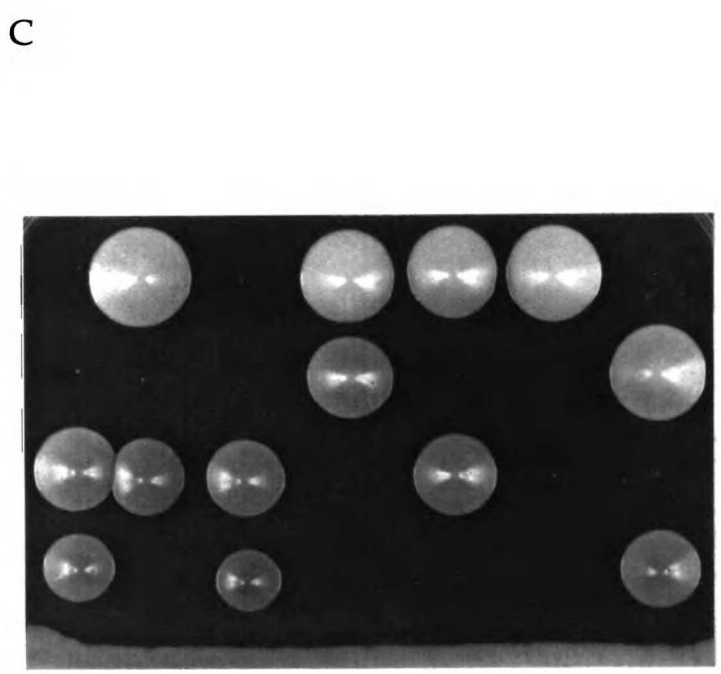

wildtype allele. Thus, we conclude that the loss of *SRP102* was directly responsible for the growth defect.

To allow further experimental manipulation, we used a PCR-generated probe to isolate a plasmid carrying the functional *SRP102* gene (see Methods). The 2966 bp *Eco*RI fragment containing the entire open reading frame and flanking sequences (Fig. 1A) was subcloned into a yeast shuttle vector pRS316 (*URA3*) yielding plasmid pSO452. To show that the information contained in this sequence was sufficient to complement the *srp102::HIS3* gene disruption, plasmid pSO452 was transformed into strain SOY133 (*SRP102/srp102::HIS3*). After sporulation, asci were dissected, and the colonies resulting from germination of each of the four spores were analyzed. All cells derived from the spores of 12 analyzed tetrads which contained the *srp102::HIS3* gene disruption (as detected by the His^+ phenotype) and which grew at wildtype rates also contained plasmid pSO452 (as detected by the Ura^+ phenotype). This confirms that pSO452 is required for cells to grow at wildtype rates and thus contains all the information necessary for the functional expression of *SRP102* .

The slow growth phenotype of cells bearing the *srp102::HIS3* gene disruption closely resembles that of cells in which *SRP101* or any of the seven known genes encoding SRP subunits are disrupted (Hann and Walter, 1991; Brown, et al., 1994; Ogg, et al., 1992). Furthermore, *srp102::HIS3* mutant cells—like yeast cells depleted of any SRP component or Srp101p—are rho^- and thus require a fermentable carbon source for growth (Hann and Walter, 1991; Brown, et al., 1994; Ogg, et al., 1992). Finally, yeast cells in which both *SRP101* and *SRP102*, or *SRP54* and *SRP102* are disrupted have a growth defect indistinguishable from cells bearing any single gene disruption (not shown),

suggesting that these genes operate in the same pathway. Taken together with the significant sequence similarities between Srp102p and mammalian SRβ, these results suggest that Srp102p is an essential component of the SRP-dependent protein targeting pathway in *S. cerevisiae*.

***SRP102* is important for translocation of proteins into the ER.**

To show directly that Srp102p plays a role in the SRP-dependent protein translocation pathway, we asked if protein translocation defects can be detected upon Srp102p inactivation. To this end, we used a temperature sensitive allele of *SRP102 srp102(K51I)* that was isolated by site directed mutagenesis (see below). Haploid cells (strain SOY246) containing the chromosomal *srp102::HIS3* gene disruption and bearing plasmid pSO462 that encodes the *srp102(K51I)* mutant allele were shifted from the permissive (24 °C) to the restrictive temperature (37 °C). The growth curve indicates that within two hours after the temperature shift, the strain carrying the *srp102(K51I)* allele decreases its growth rate by about seven-fold (Fig. 2A). This difference in doubling time (2.5 hours versus 17.5 hours, respectively) closely resembles the difference between the wildtype and the isogenic *srp102::HIS3* deletion strain, indicating that Srp102(K51I)p is inactivated upon temperature shift.

To monitor the effect of Srp102p inactivation on protein translocation, we pulse-labeled SOY246 cells with [^{35}S]-methionine at different time points after shift to the restrictive temperature. Lysates from labeled cells were analyzed by immunoprecipitation with antibodies raised against proteins that are known to be translocated across the ER membrane. Using antibodies specific for Kar2p, an ER lumenal protein, the accumulation of the

Figure 2

Srp102p is important for secretion. (A) Growth curves comparing the growth of a wild type strain (SOY223, *srp102::HIS3*, pSO459; open squares) to a strain containing the *srp102(K51I)* ts allele of *SRP102* (SOY246, *srp102::HIS3*, pSO462; closed circles). At time zero (arrow) a culture in mid logarithmic growth of each of the strains was shifted from 24 °C to 37 °C. Cell growth was monitored by change in the OD_{600} of the culture. **(B)** Immunoprecipitation, cells grown as in A were labeled with Tran(^{35}S)label for 7 min and harvested at the times indicated after a shift from 24 °C to 37 °C and processed for immunoprecipitation. Lysates at each of the time points indicated were immunoprecipitated with anti-Kar2p and subjected to SDS-PAGE followed by fluorography. Position of both mature and precursor forms of Kar2p are indicated. **(C)** Western blot, 0.5 OD_{600} cell equivalents (normalized to equivalent cpm) of the lysate prepared in B were subjected to SDS-PAGE, and subsequent transfer to nitrocellulose. Srp102p-HA, or Srp102(K51I)p-HA was detected with the anti-HA monoclonal antibody and visualized by enhanced chemiluminescence.

A

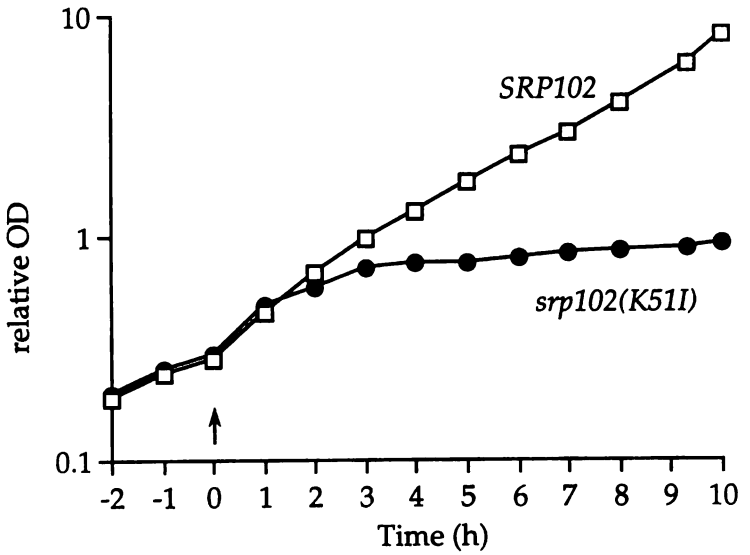

B

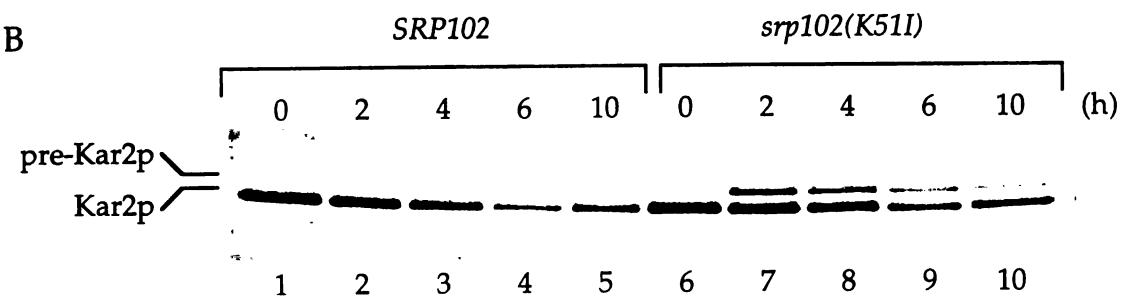

C

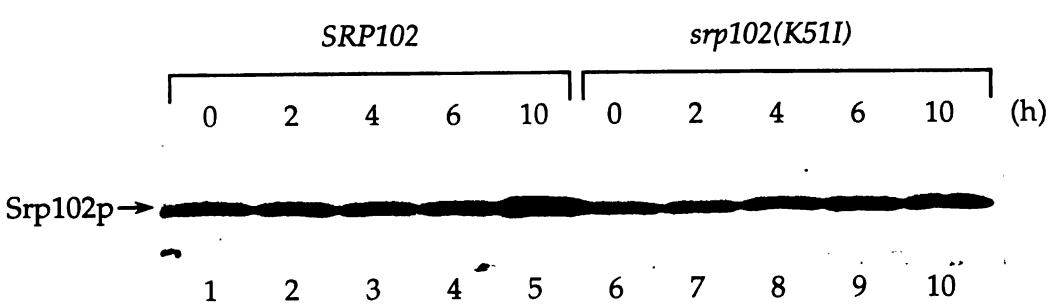

untranslocated precursor form, preKar2p, was detected (Figure 2B, lanes 7 - 10). The slower mobility of preKar2p in SDS-PAGE results from the presence of its signal sequence, which is normally cleaved upon entry into the ER. Significant amounts of Kar2p are apparent at the earliest time point taken after placing the cells at the restrictive temperature (2 hour time point in Fig. 2B, lane 7). In similar experiments, we have detected a similar fraction of preKar2p accumulation as early as 30 minutes after the temperature shift. As expected, no preKar2p was detected in the control strain carrying the wildtype allele of *SRP102* (Fig. 2B, lanes 1 - 5). Note that at later time points after the temperature shift, the translocation defect of Kar2p is diminished (Fig. 2B, lanes 8 - 10). This "adaptation" of cells in response to the loss of the SRP-dependent targeting pathway was previously observed after shut-off of the synthesis of SRP components and Srp101p (Ogg, et al., 1992). Adaptation is a physiological change in the cells that either improves the efficiency of the alternative targeting pathway or helps degrade cytosolic precursor molecules more efficiently.

The severity of translocation defects varies widely for different proteins in strains from which Srp101p and/ or SRP components are depleted (Hann and Walter, 1991; Ogg, et al., 1992). We obtained similar results when radiolabeled extracts of temperature shifted SOY246 cells were analyzed for translocation defects of two additional proteins, dipeptidyl aminopeptidase B (DPAP-B), a vacuolar membrane protein, and carboxypeptidase Y (CPY), a soluble vacuolar protein (not shown). The membrane integration of DPAP-B, like Kar2p, was significantly affected as Srp102p was rendered non-functional upon temperature shift, whereas the translocation of CPY was completely unaffected. These results closely mimic those obtained upon depletion of

other gene products that function in the SRP-dependent protein targeting pathway and lend further support to the notion that Srp102p functions as an essential subunit of the SRP receptor in the same pathway.

We monitored the fate of the mutant Srp102(K51I)p by Western blotting to determine of the loss of Srp102p activity is due to the degradation of the protein at the restrictive temperature. To this end, we took advantage of an HA-epitope tag (see below) that was added to the C-terminal end of Srp102p during construction of the mutant allele. Western blot analysis of lysates made from wildtype control and SOY246 cells during a time course after the temperature shift shows that the steady state level of Srp102(K51I)p does not change significantly during the duration of the 10 hour time course. This result suggests that the temperature sensitivity of protein translocation in SOY246 cells is not due to destabilization and subsequent degradation of Srp102(K51I)p at the restrictive temperature.

As an independent means to deplete cells of Srp102p, we placed *SRP102* under the control of the GAL1/GAL10 promoter to regulate its expression. Srp102p was depleted by switching cells from galactose (where *SRP102* is expressed) to glucose (where *SRP102* is repressed) containing media. We monitored growth and protein translocation as described above. As Srp102p was depleted, cells showed a five-fold decrease in their growth rate, and precursors of Kar2p and DPAP-B, but not CPY, accumulated to similar degrees as described above and shown previously in analogous experiments for the depletion of the other known components that function in the SRP-dependent protein targeting pathway (not shown).

Srp102p is localized to the endoplasmic reticulum

To characterize the cellular disposition of Srp102p, we constructed two alleles in which the wildtype *SRP102* gene is appended with sequences encoding epitopes which can be recognized by the well characterized monoclonal antibodies recognizing either a 12 amino acid sequence derived from influenza virus hemagglutinin ("HA epitope") (Field et al., 1988) or an 11 amino acid sequence derived from the mammalian c-myc protein ("myc epitope") (Evan et al., 1985). Both epitope tagged versions, Srp102p-HA and Srp102p-myc are fully functional as judged by their ability to complement the growth defect of cells in which *SRP102* is disrupted (not shown). In control Western blots (Figure 3), probed with the 12CA5 antibody (α-HA), a single band of approximately 30 kDa is recognized in lanes containing lysates made from cells expressing Srp102p-HA (lane 1) but not lysates made from cells containing either the wild type allele (lane 3) or from cells expressing Srp102p-myc (lane 2). An identical set of lanes was probed with the 9E10 antibody (α-myc) and only the lane containing the lysate derived from the strain expressing Srp102-myc shows immunoreactivity (Figure 3, compare lane 5 with lanes 4 and 6).

If Srp102p is indeed the yeast homolog of mammalian SRβ, it should be an integral membrane protein of the yeast ER. To test this prediction, we fractionated lysates prepared from cells expressing Srp102p-HA by differential centrifugation. After low speed centrifugation, Srp102p-HA present in the total extract (Figure 4, lane 1) partitioned about equally between the pellet (Fig. 4, lane 3) and the supernatant fractions (Fig. 4, lane 2). Presence of Srp102p in the low speed pellet is presumably due to incomplete cell lysis. Further

Figure 3

Characterization of epitope tagged SRP102p and antibodies against the epitope. Western blot showing that anti-HA recognizes only a single band in lysates made from cells containing Srp102p-HA as the only copy of Srp102p (compare lane 1 with lanes 2 and 3) and anti-myc recognizes a single band in lysates made from cells containing Srp102p-myc as the only copy of Srp102p (compare lane 5 with lanes 4 and 6). Each lane contains 0.5 OD_{600} cell equivalents of protein as judged by Ponceau S staining. Lanes 1 and 4 contain lysate from SOY223 (*srp102::HIS3*, pSO459), lanes 2 and 5 from SOY219 (*srp102::HIS3*, pSO457), and lanes 3 and 6 from SOY201 (*srp102::HIS3*, pSO454). The left panel was probed with the anti-HA monoclonal antibody 12CA5, and the right panel was probed with the 9E10 anti-myc monoclonal antibody.

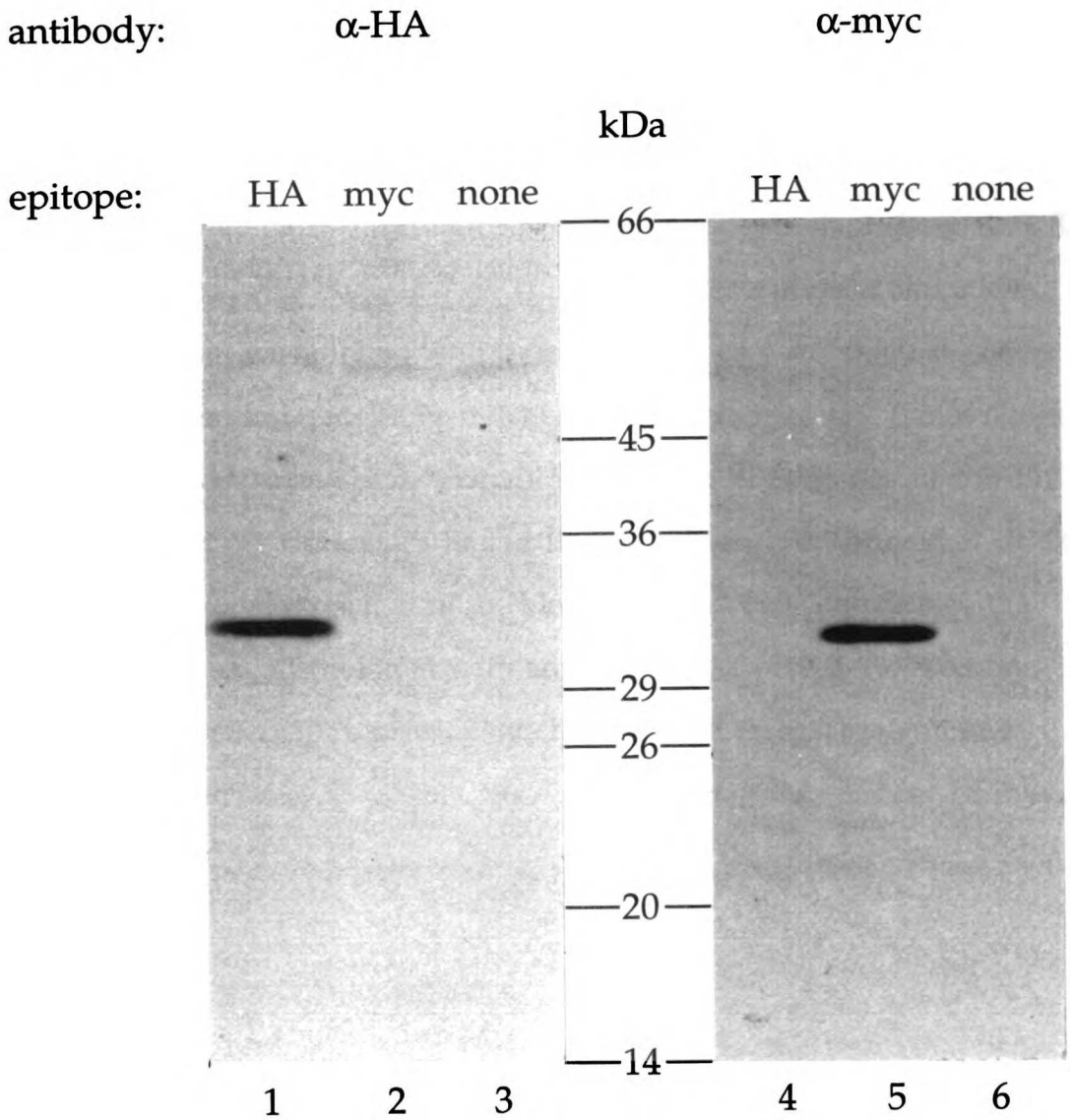

Figure 4

Subcellular localization of Srp102p. Extracts from SOY223 (*srp102::HIS3*, pSO459) were fractionated as detailed in Materials and Methods. Equivalent amounts (0.5 OD_{600}) of each fraction were analyzed by Western blot using anti-HA monoclonal antibodies, affinity purified anti-Srp101p antibodies, or anti-Sec61p antibodies. Lane 1, cell lysate; lane 2, low-speed supernatant; lane 3, low-speed pellet; lanes 4 through 13 contain the supernatant (lanes 4, 6, 8, 10, and 12) or the pellet (lanes 5, 7, 9, 11, and 13) after a portion of the low speed supernatant was diluted with lysis buffer (lanes 4 and 5, mock) or adjusted to a final concentrations of 600 mM potassium acetate (lanes 6 and 7, KOAc), 1.6M urea (lanes 8 and 9, Urea), 0.5% Triton X-100 (lanes 10 and 11, TX-100), or 0.1 M Na_2CO_3 (lanes 12 and 13, pH 11.5) and centrifuged at 100,000 X g. Only the relevant portion of the blot is shown. For comparison, the same fractions were also blotted with anti-Srp101p, a peripheral membrane protein, and anti-Sec61p, a previously characterized integral membrane protein of the ER.

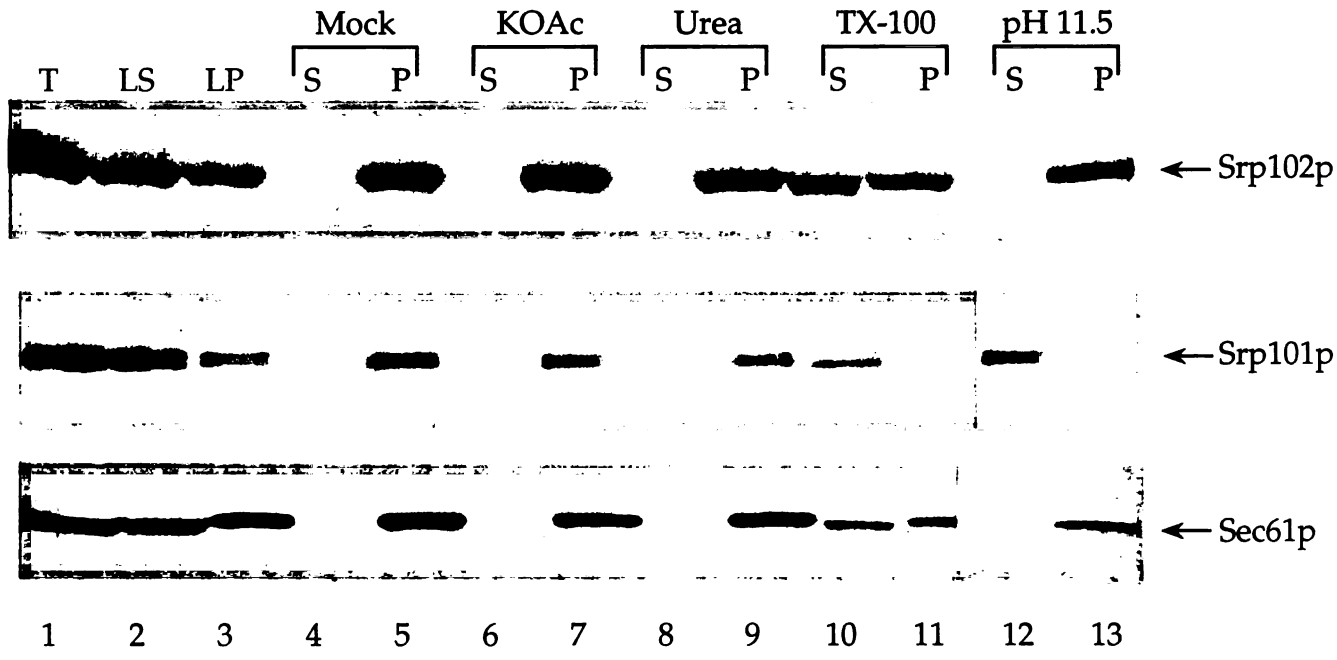

fractionation of the low speed supernatant at 100,000 x g_{av} resulted in complete sedimentation of Srp102p (Fig. 4, lanes 4 and 5), suggesting thatSrp102p is associated with a particulate fraction, possibly containing membrane vesicles. The association of Srp102p with this fraction was further characterized by treatment of the low speed supernatant with reagents known to perturb protein-protein or protein-membrane interactions, prior to centrifugation at 100,000 x g_{av}. Treatment with 500 mM potassium acetate (Fig. 4, lanes 6 and 7), 1.6 M urea (Fig. 4, lanes 8 and 9), or sodium carbonate at pH 11.5 (Fig. 4, lanes 12 and 13) did not solubilize Srp102p which, under all conditions, was recovered in the membrane fraction. In contrast, treatment of the low speed supernatant with 0.5% Triton X-100 resulted in solubilization of roughly 50% of Srp102-HA, which was recovered in the high speed supernatant fraction (Fig. 4, compare lanes 10 and 11). As controls for these experiments, we also probed the Western blot with antibodies to Sec61p, a *bona fide* yeast ER integral membrane protein, and Srp101p, thought to be peripherally associated with the ER membrane (Ogg, et al., 1992). Srp102p-HA co-fractionated under all conditions with Sec61p. In particular, both Srp102p and Sec61p were recovered in the pellet fraction after alkali treatment, whereas Srp101p was completely extracted and recovered in the supernatant fraction (Fig. 4, compare lanes 12 and 13). Thus, we conclude that Srp102p-HA, and by extension Srp102p, is an integral membrane protein. This is consistent with the predictions from its amino acid sequence that shows a stretch of 19 hydrophobic amino acids forming a putative transmembrane domain near its amino-terminus (Miller, et al., 1995).

To assess the intracellular localization of Srp102p in more detail, we visualized the distribution of the epitope-tagged forms of the protein by

Figure 5

Immunofluorescent localization of Srp102p to the ER. Cells containing either pSO454 (Srp102p lacking an epitope tag, SOY201, panels A through F, and M, N, O), pSO459 (Srp102p-HA, SOY223, panels G, H, I) or pSO457 (Srp102p-myc, SOY219, panels J, K, L) were fixed with formaldehyde and probed with anti-HA (panels A, B, C, G, H, I), anti-myc antibodies (panels D, E, F, J, K, L), or anti-Kar2p (panels M, N, O) followed by secondary decoration with FITC-conjugated donkey anti-mouse IgG or TRITC-conjugated donkey anti-rabbit IgG. The bar is 20 microns. The images in panels H and K are exposed for equivalent amounts of time (15s), and the images in B and E are exposed for twice the length of time as those images shown in H and K. Phase contrast images are shown in panels A, B, G, J, and M; fluorescein fluorescence is shown in panels B, E, H, and K; rhodamine fluorescence is shown in panel N, and DAPI staining of the nuclei is shown in panels C, F, I, L, and O.

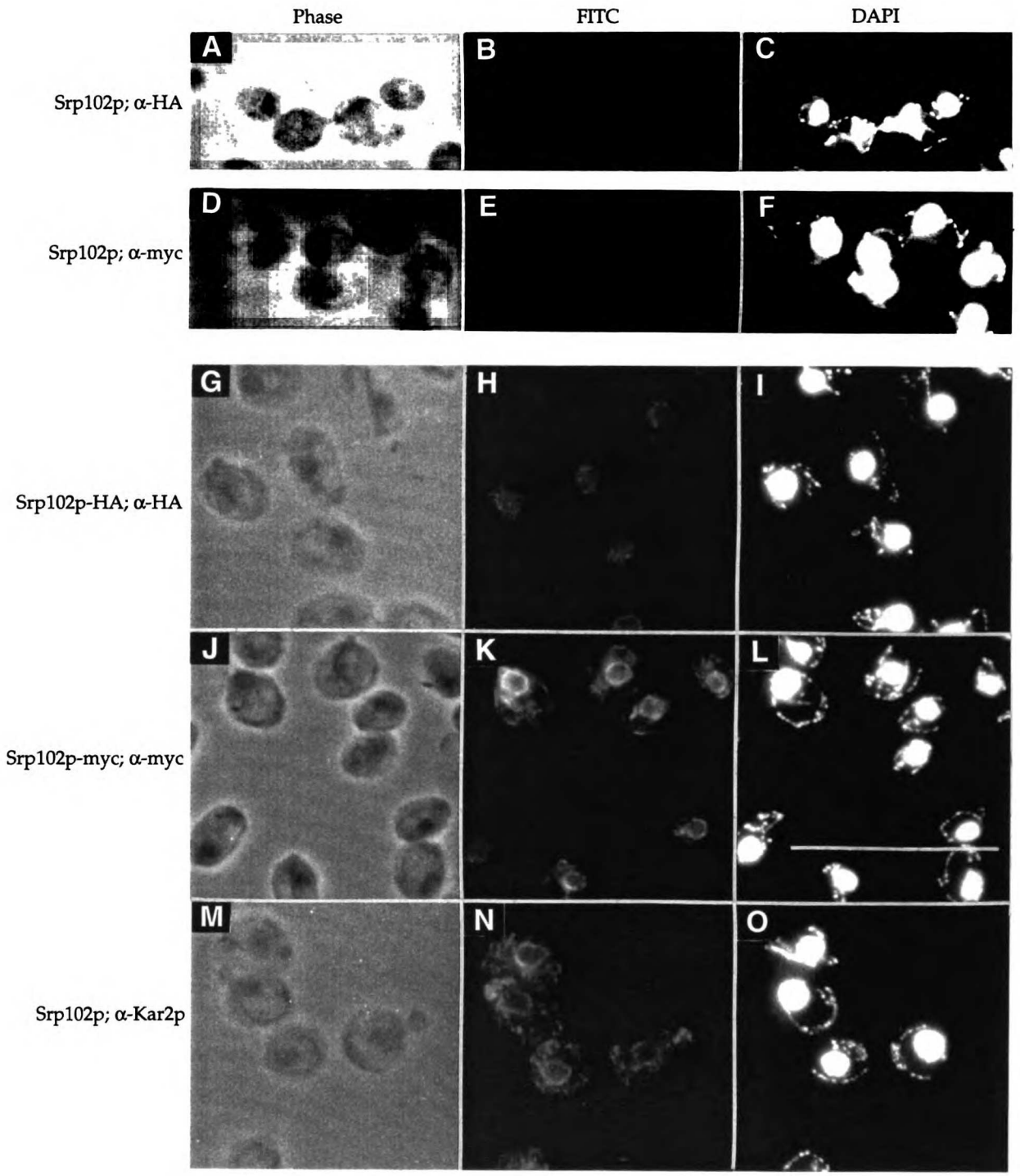

indirect immunofluorescent microscopy. Cells expressing Srp102p-HA at roughly wild type levels from a CEN/ARS plasmid (Fig. 5, panels G - I) or overexpressing Srp102p-myc on a 2μ plasmid (Fig. 5 panels, J - L) were analyzed. Following formaldehyde fixation, cell remnants were incubated with the appropriate primary and FITC-conjugated secondary antibodies (Fig. 5, panels B, E, H, and K); nuclei and mitochondria were visualized with the DNA binding dye DAPI (Fig. 5, panels C, F, I, and L). Anti-HA antibodies detected the characteristic yeast ER staining pattern, consisting of a distinct perinuclear ring, with fine strands of staining passing through the cytoplasm connecting the perinuclear ER to ER cisternae underlying the plasma membrane. This pattern was indistinguishable from that obtained in control samples stained with anti-Kar2p antibodies (Fig. 5, panel N). Overproduction of Srp102p-myc from the 2μ plasmid resulted in a more intense, but qualitatively identical pattern. In this case, however, staining was variable; some cells in every field stained very brightly, while others stained less brightly or not at all. We attribute this to variation in the copy number of the 2μ plasmid in the population. Wildtype cells not expressing either epitope-tagged version of Srp102p showed negligible staining (Fig. 5, panels B and E). Taken together, the results from the fractionation experiments and the results from the immunofluorescence microscopy authenticate our conjecture that Srp102p is an integral ER membrane protein.

Srp101p and Srp102p form a stable complex in the ER.

Mammalian SRα and SRβ are subunits of a heterodimeric complex (Tajima, et al., 1986). To test whether the yeast homologues Srp101p and Srp102p are likewise associated, we immunoprecipitated Srp102p-HA with anti-HA antibodies from extracts prepared by detergent solubilization of yeast

microsomal membranes under nondenaturing conditions. Anti-HA antibodies were coupled to protein A-Sepharose beads to allow the isolation of immunecomplexes. Immunecomplexes were subsequently solubilized in SDS sample buffer and subjected to SDS-PAGE followed by Western blot analysis. The blots were probed with affinity-purified polyclonal antibody directed against Srp101p. The results show Srp101p was recovered in the eluate fraction from the protein A-Sepharose beads when cells expressed Srp102p-HA (Fig. 6, lane 4), but was found exclusively in the supernatant fraction when cells expressed untagged Srp102p (Fig. 6, lanes 1 and 2) or when a peptide containing the HA epitope was added to compete for binding of the anti-HA antibody to Srp102p-HA (Fig. 6, lanes 5 and 6). These biochemical data strongly suggest that Srp101p and Srp102p directly interact to form a complex.

In vivo evidence for an interaction between Srp101p and Srp102p was obtained by genetic means. To this end, we used cells expressing the temperature sensitive *srp102(K51I)* allele. As temperature sensitive mutations can often be suppressed by the overproduction of interacting proteins, we asked directly whether overexpression of Srp101p could suppress the growth defect induced at the restrictive temperature. We transformed cells expressing Srp102(K51I)p either with pSO400 containing Srp101p under control of the *GAL1/10* promoter, or pSO211, a plasmid that contains Srp101p under the control of its own promoter. Each of these strains grew at wildtype rates at the permissive temperature utilizing either dextrose or galactose as the carbon source (Fig. 7, plates A and B). As expected, at the restrictive temperature neither plasmid suppressed the growth defect when cells were grown on glucose-containing medium (Fig. 7, plate C). In contrast, pSO400,

Figure 6

Srp101p and Srp102p form a complex in detergent solubilized membranes. Crude cellular membranes were prepared from SOY201 (*srp102::HIS3*, pSO454) or SOY223 (*srp102::HIS3*, pSO459) as described in the materials and methods. Detergent solubilized membranes were immunoprecipitated with anti-HA either in the absence (lanes 1 through 4) or the presence (lanes 5 and 6) of excess HA peptide (NH_2-YPYDVPDYA-COOH). Immunoprecipitated proteins were eluted from protein A Sepharose beads, subjected to SDS-PAGE and analyzed by Western blot using affinity purified anti-Srp101p antibodies. Immunoprecipitations were performed from solubilized membranes from SOY201 (lanes 1 and 2, no tag), SOY223 (lanes 3 through 6, Srp102p-HA). Eluates from each of the immunoprecipitations are in lanes 2, 4, and 6; supernatants are in lanes 1, 3, and 5. Lane 7 contains 2 OD_{600} cell equivalents of solubilized membranes from SOY223 as a marker for the amount of Srp101p that is in each of the immunoprecipitations.

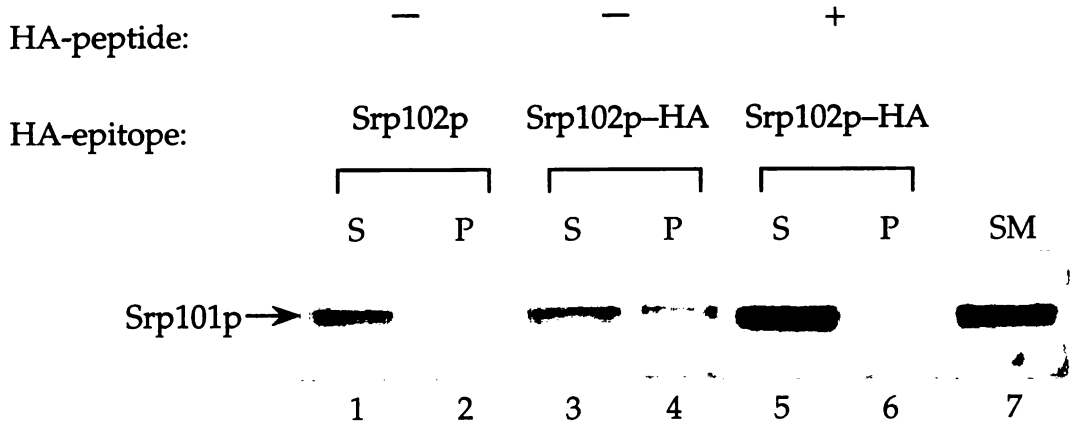

Figure 7

Overexpression of Srp101p can suppress the temperature sensitive growth defect of*SRP102-K51I*. SOY246 cells transformed with either pSO400 (*SRP101* under control of the GAL promoter) or pSO211 (*SRP101* under control of its own promoter) were plated onto synthetic plates lacking tryptophan and uracil and containing 2% galactose or 2% glucose as the sole carbon source. **(A)** plate containing 2% glucose incubated at 24 °C for three days. **(B)** plate containing 2% galactose incubated at 24 °C for three days. **(C)** plate containing 2% glucose incubated at 37 °C for three days. **(D)** plate containing 2% galactose incubated at 37 °C for three days.

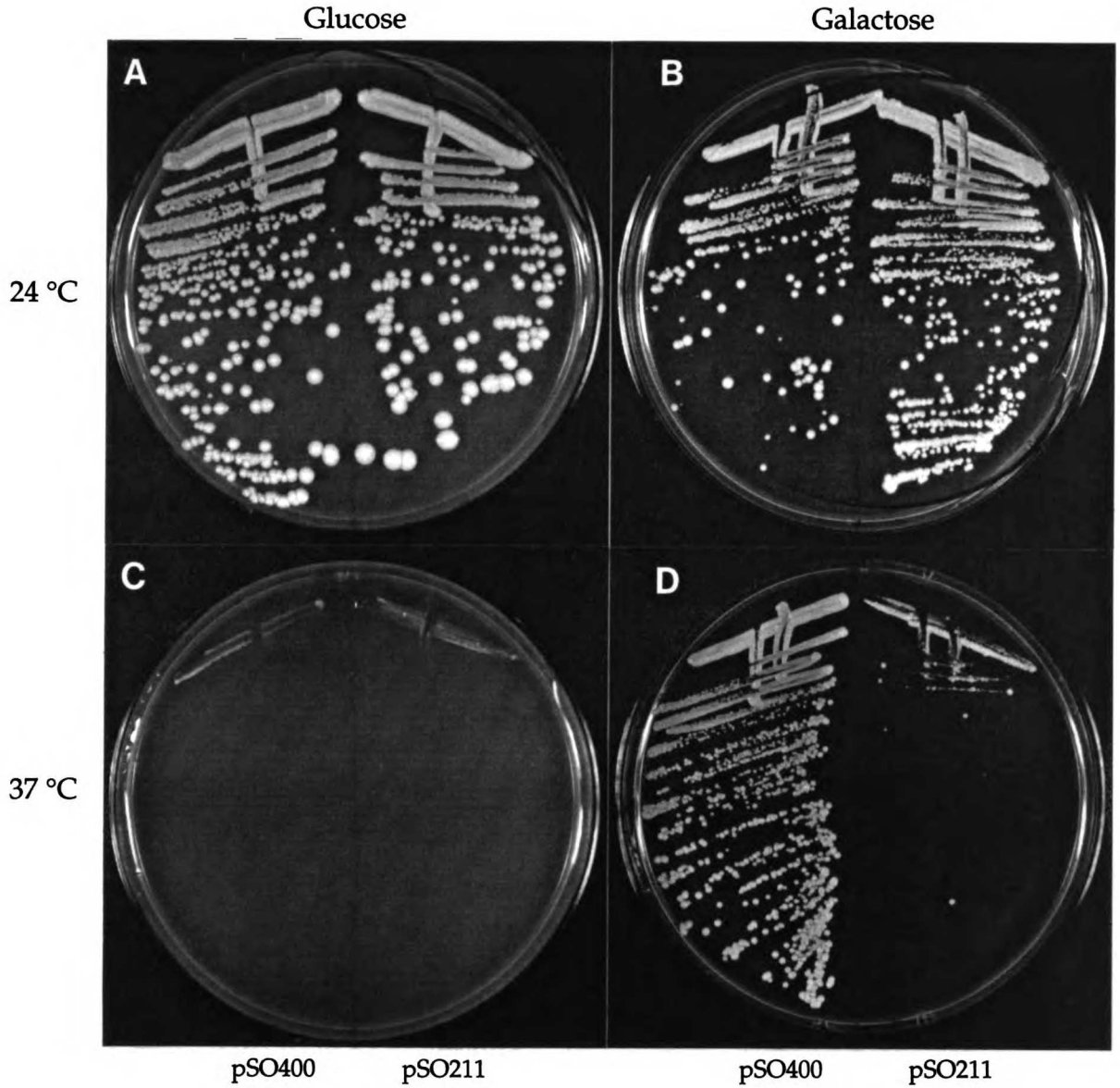

but not pSO211, suppressed the growth defect when cells were grown on galactose-containing medium (Fig. 7, plate D). Under the galactose induced conditions, Srp101p was about 50-fold overexpressed as estimated by immunoblot (Ogg, et al., 1992). Significanly, pSO400 failed to suppress the growth defect of cells containing a complete deletion of *SRP102* rather than the *SRP102(K51I)* allele (not shown).

Srp102p is required for the association of Srp101p with membranes.

Biochemical fractionation experiments have suggested that mammalian SRβ anchors the SRP receptor in the ER membrane and that SRα's association with the membrane is mediated through interactions with SRβ. This model predicts that in the absence of SRβ, SRα should not be stably associated with the ER membrane. Because yeast cells are viable in the absence of Srp102p, this prediction can be tested directly. To this end, we compared the membrane association Srp101p in wildtype and in isogenic SOY162 cells in which *SRP102* is disrupted. Cell extracts were fractionated by differential centrifugation followed by Western blot analysis with antibodies against Srp101p. In extracts prepared from SOY162 cells, Srp101p was quantitativley recovered in the supernatant fraction from the high speed (100,000 x g_{av}) centrifugation step (Fig. 8, compare lanes 4 and 5). In contrast and as expected, Srp101p was exclusively recovered in the microsomal pellet fraction, when extracts from wildtype control cells were analyzed.

To gain insight into the defect resulting in the temperature sensitivity of strains harboring the *srp102(K51I)* mutation, we asked whether either Srp101p and the mutant Srp102(K51I)p are properly membrane associated. To this end, we fractionated extracts prepared from the mutant cells.

Figure 8

Srp101p is mislocalized in the *SRP102* gene disruption. Lysates from *SRP102* (W303α, top panel) or *srp102::HIS3* (SOY162, bottom panel) were subjected to fractionation as detailed in materials and methods. Cell fractions were analyzed by Western blot using affinity purified anti-Srp101p. Each lane contains 0.5 OD_{600} cell equivalents of the fraction: lane 1, total cell lysate; lane 2, low-speed supernatant; lane 3, low-speed pellet; lane 4, high-speed supernatant; lane 5, high-speed pellet. Srp101p detected in strain SOY162 appears as a fuzzier band than that which is detected in W303α, we attribute this to increased susceptibility to proteolysis during the fractionation of Srp101p due to the lack of Srp102p with which it can complex.

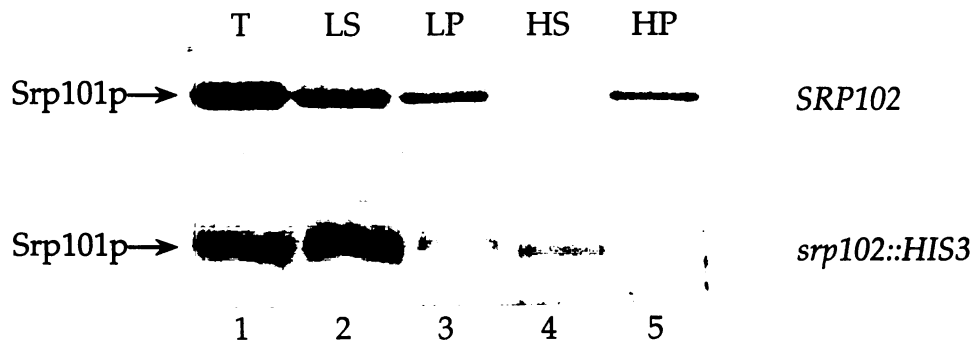

Figure 9

The SR complex is compromised in cells bearing *srp102(K51I).* Cells bearing wildtype Srp102p-HA (SOY223), or Srp102(K51I)p-HA (SOY246) were subjected to fractionation as detailed in materials and methods. Equivalent amounts of each fraction were subjected to SDS-PAGE followed by Western blot analysis. Srp101p was detected with affinity purified anti-Srp101p antibodies, while Srp102p was detected using the anti-HA monocloal anitibody. Each panel contains the fractions loaded in the same manner. Lane 1, "T", total cell lysate; lane 2, "LS", low-speed supernatant; lane 3, "LP", low-speed pellet; lane 4, "HS", high-speed supernatant; lane 5, "HP", high-speed pellet; lane 6, "DE", detergent extract; lane 7, "DP", detergent pellet. **A**, fractions from SOY223 (Srp102p) cells grown at 24 °C. **B**, fractions from SOY223 (Srp102p) cells after shift to 37 °C for three hours. **C**, fractions from SOY246 (Srp102(K51I)p) grown at 24 °C. **D**, fractions from SOY246 (Srp102(K51I)p) after shift to 37 °C for three hours.

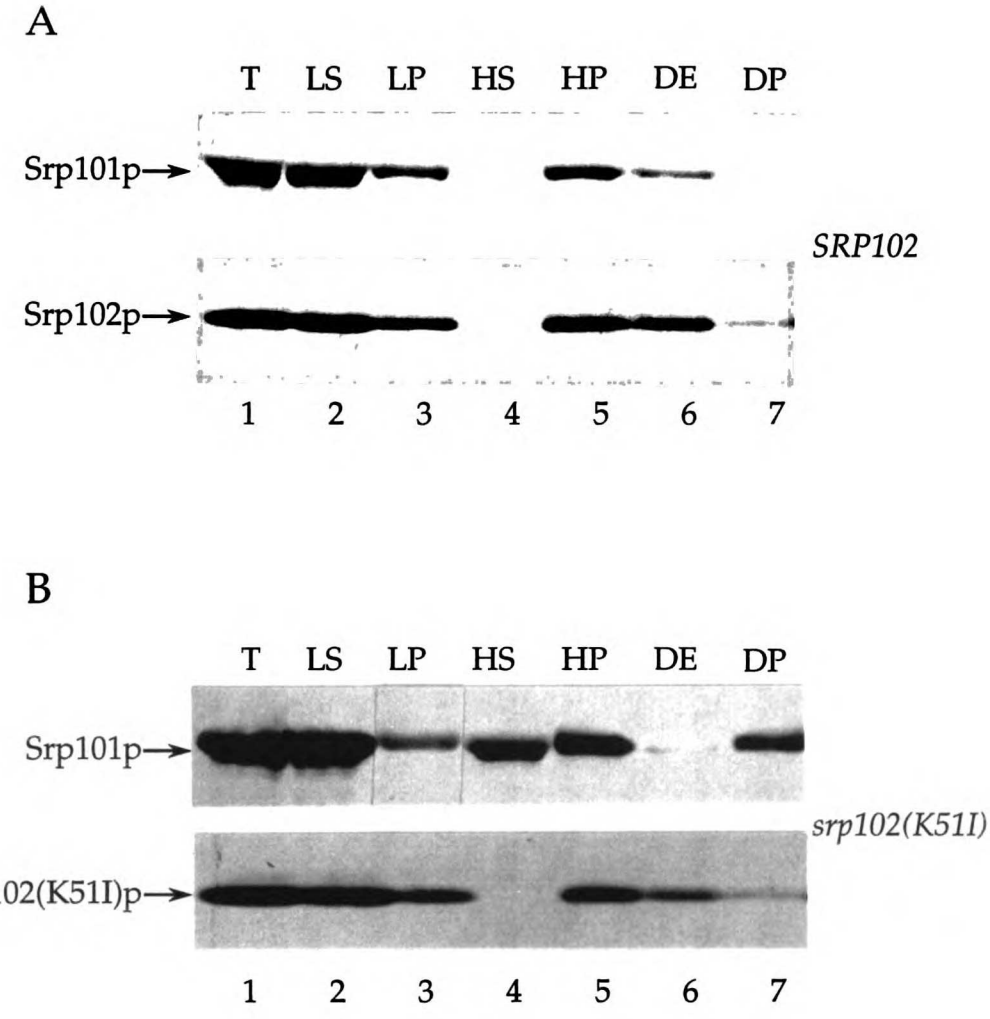

Interestingly, we found that Srp101p's membrane association is significantly perturbed in extracts prepared from cells expressing Srp102(K51I)p-HA (Fig. 9A and 9B). Only about half of the Srp101p found in the low speed supernatant is recovered in a high speed pellet fraction in the mutant cells (Fig. 9B, compare lanes 4 and 5), whereas Srp101p is almost quantitatively recovered in the high speed pellet fraction when extracts prepared from control cells are fractionated (Fig. 9A, compare lanes 4 and 5). Moreover, Srp101p found in the high speed membrane fraction isolated from the mutant cells is insoluble in 1% Triton X-100 (Fig 9B, lanes 6 and 7), whereas Srp101p is soluble under these conditions in the control extracts (Fig 9A, lanes 6 and 7). These results suggest that this mutation in Srp102p (K51I) alters the way in which Srp101p and Srp102p interact. From these studies we conclude that the interaction between Srp101p and Srp102p is perturbed in cells that express mutant Srp102(K51I)p. Similar results were obtained when cells were preincubated for three hours at the nonpermissive temperature before they were harvested. This suggests that the defects exhibited by the *srp102(K51I)* mutation may be exacerbated in vitro such that differences in extracts of between cells grown at the permissive and non-permissive temperature are not apparent.

Mutations in the putative GTP binding site of Srp102p.

To address whether the predicted GTP binding site of Srp102p is important for its function, we began a mutational analysis. We chose to construct different site-directed mutations in amino acid residues that comprise the GTP binding site and that are highly conserved between Srp102p and other well characterized GTPases, such as *ras* and ARF (Bobak et al., 1989; Ruta et al., 1986). Our choice of most of the mutations was based on reported

Table II

Phenotypes of each of the mutations in vivo, and some of the predicted molecular effects of the mutations. Each of the mutations is listed along with the phenotype when the mutation is the only copy of Srp102p in the cell. Some mutations were chosen on the basis of their predicted molecular phenotypes in other GTPases. These are shown and the reference for each is given.

Table II **Phenotypes of *SRP102* mutations in vivo, and some of the predicted molecular effects of the mutations.**

Allele	location of mutation in GTP binding site	Phenotype	effect of corresponding mutation in ras or EF-Tu, when known
S49A	G-1	None	Reduction in GTPase activity (Barbacid, 1987)
K51I	G-1	ts	Reduced affinity for both GDP & GTP (Pai et al., 1990)
T52N	G-1	ts	
T66A	G-2	None	Prevent GTP dependent interaction with GAP (Sigal et al., 1986)
G90L	G-3	None	
H91L	G-3	None	Reduction in GTPase activity (Jonak et al., 1994)
N154I	G-4	None	GDP/GTP exchange impaired in ras (Sigal et al., 1986)
E157Q	G-4	None	Reduced GTP affinity (Weijland et al., 1994)
S220A	G-5	None	Bypass requirement for GNRP (Camonis & Jacquet, 1988)
P46A, Q47A, N48A, ΔS49	G-1	None	
K51A, T52A	G-1	None	
N154A,E157A	G-4	None	
K51I, H91L	G-1, G-2	null	

effects of corresponding mutations in other GTPases. Table II lists nine single amino acid changes and four multiple amino acid changes that were introduced into Srp102p, primarily into regions comprising the GTP binding site. These regions are known from X-ray crystallographic analyses of ras, $G_{\alpha s}$ and EF-Tu to form loops on the surface of the GTPase fold that contact the bound nucleotide directly (Pai et al., 1989; Pai et al., 1990; Jurnak, 1985; Lambright et al., 1994).

After confirming each mutation by sequencing the relevant portion of Srp102p, we transformed dipoid SOY133 (*SRP102/srp102::HIS3*) cells with a plasmid containing the mutant form of Srp102p. To assess the phenotype of each mutation, the diploid cells were sporulated, and the resulting haploid strains bearing the *SRP102* gene deletion and the mutant form of *SRP102* on the plasmid were characterized. Table II lists the growth phenotype of each mutation, as well as the phenotype of the corresponding mutation in other GTPases, if known. Very much to our surprise, in 10 out of 13 cases cells carrying the mutant allele as the only copy of *SRP102* grew with wildtype rates. In contrast, two mutations in loop 1, which is predicted to straddle the β-γ-phosphate bond of the bound GTP, are temperature sensitive for growth. This includes the K51I mutation that was characterized by the experiments described above and the T52N mutation in the adjacent residue. Interestingly, combination of the K51I mutations with the silent H91L mutation results in a synthetic, severe defect that is indistinguishable from a complete *SRP102* gene disruption (Table II). Taken together, these results indicate that a surprisingly high number of individual amino acids can be changed in the GTP binding site of Srp102p without impairing its function.

Discussion

The recent explosion of information resulting from the yeast genome sequencing project allowed us to identify a putative yeast homolog of the mammalian SRP receptor β subunit (Miller, et al., 1995). We undertook a molecular genetic approach to elucidate the role of this protein *in vivo* in the yeast *Saccharomyces cerevisiae*. We have shown that this protein is the yeast homolog of mammalian SRβ. Many lines of evidence lead to this conclusion. First, the conservation of structural similarity. Both primary sequence elements and subunit interactions are highly conserved (Fig. 6). Second, disruption of the gene (*SRP102*) leads to an identical phenotype as that seen in cells in which any of the known SRP genes, or the SRP receptor α subunit gene are deleted (Fig. 1, Hann and Walter, 1991; Ogg, et al., 1992; Brown, et al., 1994). Similarly, a yeast strain in which both subunits of the SRP receptor have been deleted have identical growth defects to strains containing each single gene deletion separately. Third, we have demonstrated the importance of Srp102p for proper SRP dependent translocation of proteins into the ER (Fig. 2). Lastly, both by subcellular fractionation and immunofluorescence, we have localized Srp102p to the ER (Fig. 4 and Fig. 5). Therefore we conclude that *SRP102* is the yeast homolog of the mammalian SRP receptor β subunit, and that in yeast the gene product functions in the SRP dependent translocation of proteins across the ER membrane.

Structure of the yeast SR

Recently, the mammalian SRβ has been shown to be an integral membrane protein of the ER that mediates the attachment of the α subunit, a peripheral membrane protein, to the ER membrane (Miller, et al., 1995). In

yeast, it appears that this structure is reproduced. We have shown that Srp102p and Srp101p form a complex that is stable in detergent solubilized membranes (Fig. 6). Additionally, Srp102p is required for the association of Srp101p with a microsome containing fraction. A complete gene disruption of Srp102p causes Srp101p to behave as a cytosolic protein (Fig. 8), while a more subtle mutation in Srp102p, one that causes cells to become temperature sensitive for growth, results in a defective interaction between Srp101p and Srp102p (Fig. 9). In vivo evidence of interaction between Srp101p and Srp102p was obtained by showing that the overexpression of Srp101p could suppress the growth defect of the ts allelle of Srp102p (Fig. 7). We have only preliminarily explored the possibility that this complex contains other components. Negative results using two distinctly tagged *SRP102* genes in coimmunoprecipitation studies suggests that Srp102p does not interact with itself. Coimmunoprecipitation studies from cells containing ^{35}S labeled proteins suggests that, in addition to Srp101p and Srp102p, there are other components of this complex. We asked directly whether Sec61p was a stable component of this complex by Western blot analysis. Although we can detect Sec61p in the detergent extract, and the supernatant from the immunoprecipitation, none of the protein is present in the eluate from the immunoprecipitation containing the coimmunoprecipitated species. Because of the GTPase motifs present in Srp102p, we speculate that it may interact with other proteins dependent on its nucleotide bound state. Therefore our coimmunoprecipitation studies may not have identified proteins that are associated with this complex in regulated manner.

A complex involving proteins in addition to Srp101p and Srp102p, either transiently, or permanenetly is not surprising, however, given that

during the purification of the mammalian SR, other proteins are copurified (Tajima, et al., 1986). Mp30, one such component, has long been known to be associated with the SR, but as yet remains molecularly uncharacterized. In addition, models of translocation predict that the SR must interact with SRP, and may also interact with downstream components of the translocon, and/or the SRP-targeted ribosome. These interactions are likely to be regulated, and it is the means of this regulation which now poses the interesting questions to answer in future studies of *SRP102*. The easiest mode of regulation to imagine is one involving the GTPase cycle of Srp102p itself, either alone, or coupled to the GTPase cycles of Srp101p an/or Srp54p.

Does Srp102p act as a molecular switch?

Surprisingly, many of the site directed mutations we made in the GTPase consensus motifs were silent when placed *in vivo* (see Table II). Because the GTPase consensus motifs are very highly conserved, and the mammalian SRP receptor β subunit has been shown to bind GTP in vitro (Miller, et al., 1995), we expect that the yeast homolog also acts as a GTPase. The lack of a growth defect when many of these mutated forms of Srp102p are placed in the cell may be due to several possibilities. Although we do not favor this hypothesis, we must entertain the idea that the residues we have mutated, and therefore the GTPase function, is not important for the function of Srp102p. Two things argue against this possibility, first of all, two of the mutations we made did have an impact on the function of Srp102p (see table II). Second, and more importantly, the H91L mutation is silent when it is the only mutation in *SRP102*, yet it acts to exacerbate the phenotype of the K51I allele when placed in combination with this mutation. This suggests that even though it is silent when alone, it is altering the GTPase function of

Srp102p slightly and our assay (growth) is not sensitive enough to distinguish between wildtype function of Srp102p and Srp102(H91L)p. These results suggest that the observed defects result from impaired GTPase function. We conclude, therefore, that Srp102p's GTPase function is flexible, and the mutations we have chosen do not sufficiently alter this activity to affect growth. Becausee of the this unexpected behavior, predicting the phenotype of mutations in Srp102p based on the phenotype of mutations in Sar1p, a closely related member of the GTPase superfamily, is of little informative value. We have undertaken an approach utilizing random mutagenesis of *SRP102*, and subsequent selection of mutations displaying a phenotype in vivo.

REFERENCES

Barbacid, M. A. (1987). ras genes. Ann. Rev. Biochem. *56*, 779-827

Bernstein, H. D., Poritz, M. A., Strub, K., Hoben, P. J., Brenner, S. and Walter, P. (1989). Model for signal sequence recognition from amino-acid sequence of 54k subunit of signal recognition particle. Nature *340*, 482-486.

Bobak, D. A., Nightingale, M. S., Murtagh, J. J., Price, S. R., Moss, J. and Vaughan, M. (1989). Molecular cloning, characterization, and expression of human ADP-ribosylation factors: two guanine nucleotide-dependent activators of cholera toxin. Proc. Natl. Acad. Sci. USA *86*, 6101-6105.

Bourne, H. R., Sanders, D. A. and McCormick, F. (1991). The GTPase superfamily: conserved structure and molecular mechanism. Nature *349*, 117-127.

Brown, J. D., Hann, B. C., Medzihradszky, K. F., Niwa, M., Burlingame, A. L. and Walter, P. (1994). Subunits of the *Saccharomyces cerevisiae* signal recognition particle required for its functional expression. EMBO J. *13*, 4390-4400.

Camonis J. H. and Jacquet, M. (1988). A new RAS mutation that suppresses the *CDC25* gene requirement for growth of *Saccharomyces cerevisiae*. Mol. Cell. Biol. *8*, 2980-2983.

Christianson, T. W., Sikorski, R. S., Dante, M., Shero, J. H. and Hieter, P. (1992). Multifunctional yeast high-copy-number shuttle vectors. Gene *110*, 119-122.

Connolly, T. and Gilmore, R. (1986). Formation of a Functional Ribosome-Membrane Junction During Translocation Requires the Participation of a GTP-binding Protein. J. Cell Biol. *103*, 2253-2261.

Crowley, K. S., Liao, S., Worrell, V. E., Reinhart, G. D. and Johnson, A. E. (1994). Secretory proteins move through the ER membrane via an aqueous, gated pore. Cell *78*, 461-471.

Evan, G. I., Lewis, G. K., Ramsay, G. and Bishop, J. M. (1985). Isolation of monoclonal antibodies specific for human c-*myc* proto-oncogene product. Mol. Cell. Biol. *5*, 3610-3616.

Field, J., Nikawa, J., Broek, D., MacDonald, B., Rodgers, L., Wilson, I. A., Lerner, R. A. and Wigler, M. (1988). Purification of a RAS-responsive adenylyl cyclase complex from *Saccharomyces cerevisiae* by use of an epitope addition method. Mol. Cell. Biol. *8*, 2159-2165.

Geitz, R. D. and Sugino, A. (1988). New yeast-*Escherichia coli* shuttle vectors constructed with in vitro mutagenized yeast genes lacking six-base pair restriction sites. Gene *74*, 527-534.

Gilmore, R. and Blobel, G. (1983). Transient involvement of signal recognition particle and its receptor in the microsomal membrane prior to protein translocation. Cell *35*, 677-685.

Gilmore, R., Blobel, G. and Walter, P. (1982a). Protein translocation across the endoplasmic reticulum. I. Detection in the microsomal membrane of a receptor for the signal recognition particle. J. Cell Biol. *95*, 463-469.

Gilmore, R., Walter, P. and Blobel, G. (1982b). Protein translocation across the endoplasmic reticulum. II. Isolation and characterization of the signal recognition particle receptor. J. Cell Biol. *95*, 470-477.

Görlich, D. and Rapoport, T. A. (1993). Protein translocation into proteoliposomes reconstituted from purified components of the endoplasmic reticulum membrane. Cell *75*, 615-630.

Hann, B. C. and Walter, P. (1991). The Signal Recognition Particle in *S. cerevisiae*. Cell *67*, 131-144.

Ito, H., Fukuda, Y., Murata, K. and Kimura, A. (1983). Transformation of intact yeast cells treated with alkali cations. J. Bact. *153*, 163-168.

Jonak, J., Anborgh, P. H. and Parmeggiani, A. (1994). Histidine-118 of elongation factor Tu: its role in aminoacyl-tRNA binding and regulation of the GTPase activity. Febs Letters *343*, 94-98.

Jurnak, F. (1985). Structure of the GDP domain of EF-Tu and location of the amino acids homologous to *ras* oncogene proteins. Science *230*, 32-36.

Krieg, U. C., Walter, P. and Johnson, A. E. (1986). Photocrosslinking of the signal sequence of nascent preprolactin to the 54-kilodalton polypeptide of the signal recognition particle. Proc. Natl. Acad. Sci. USA *83*, 8604-8608.

Kunkel, T. A. (1985). Rapid and efficient site-specific mutagenesis without phenotypic selection. Proc. Natl. Acad. Sci. USA *82*, 488-492.

Kunkel, T. A., Roberts, J. D. and Zakour, R. A. (1987). Rapid and efficient site-specific mutagenesis without phenotypic selection. Meth. Enz. *154*, 367-382.

Kurzchalia, T. V., Wiedmann, M., Girshovich, A. S., Bochkareva, E. S., Bielka, H. and Rapoport, T. A. (1986). The signal sequence of nascent preprolactin interacts with the 54K polypeptide of the signal recognition particle. Nature *320*, 634-636.

Lambright, D. G., Noel, J. P., Hamm, H. E. and Sigler, P. B. (1994). Structural determinants for activation of the alpha-subunit of a heterotrimeric G protein. Nature *369*, 621-628.

Meyer, D. I., Louvard, D. and Dobberstein, B. (1982). Characterization of molecules involved in protein translocation using a specific antibody. J. Cell Biol. *92*, 579-583.

Miller, J. D., Tajima, S., Lauffer, L. and Walter, P. (1995). The β-subunit of the signal recognition particle receptor is a transmembrane GTPase that anchors the α-subunit, a peripheral membrane GTPase, to the endoplasmic reticulum membrane. J. Cell Biol. *128*, 273-282.

Miller, J. D., Wilhelm, H., Gierasch, L., Gilmore, R. and Walter, P. (1993). GTP binding and hydrolysis by the signal recognition particle during initiation of protein translocation. Nature *366*, 351-354.

Ogg, S., Poritz, M. and Walter, P. (1992). The signal recognition particle receptor is important for growth and protein secretion in *Saccharomyces cerevisiae*. Mol. Biol. Cell *3*, 895-911.

Pai, E. F., Kabsch, W., Krengel, U., Holmes, K. C., John, J. and Wittinghofer, A. (1989). Structure of the guanine-nucleotide-binding domain of the Ha-*ras* oncogene product p21 in the triphosphate conformation. Nature *341*, 209-214.

Pai, E. F., Krengel, U., Petsko, G. A., Goody, R. S., Kabsch, W. and Wittinghofer, A. (1990). Refined crystal structure of the triphosphate conformation of H-ras p21 at 1.35 A resolution: implications for the mechanism of GTP hydrolysis. EMBO J. *9*, 2351-2359.

Pringle, J. R., Preston, R. A., Adams, A. E. M., Stearns, T., Drubin, D. G., Haarer, B. K. and Jones, E. W. (1989). Fluorescence microscopy methods for yeast. Meth. Cell Biol. *31*, 358-435.

Römisch, K., Webb, J., Herz, J., Prehn, S., Frank, R., Vingron, M. and Dobberstein, B. (1989). Homology of the 54K Protein of signal recognition particle, docking protein, and two *E. coli* proteins with putative GTP-binding domains. Nature *340*, 478-482.

Rose, M. D., Misra, L. M. and Vogel, J. P. (1989). *KAR2*, a karyogamy gene, is the yeast homolog of the mammalian BiP/GRP78 gene. Cell *57*, 1211-1221.

Rose, M. D., Novick, P., Thomas, J. H., Botstein, D. and Fink, G. R. (1987). A *Saccharomyces cerevisiae* genomic plasmid bank based on a centromere-containing shuttle vector. Gene *60*, 237-243.

Ruta, M., Wolford, R., Dhar, R., Defeo-Jones, D., Ellis, R. W. and Scolnick, E. M. (1986). Nucleotide sequence of the two rat cellular *ras*H genes. Mol. Cell. Biol. *6*, 1706-1710.

Sherman, F. and Lawrence, C. 1974. *Saccharomyces*. Handbook of Genetics King, R.C., Eds. Plenum Press, New York. 359-393.

Sigal, I. S., Gibbs, J.B., D'Alonzo, J.S. Temeles, G. L., Wolanski, B. S. Socher, S. H., and Scolnick EM. (1986). Mutant ras-encoded proteins with altered

nucleotide binding exert dominant biological effects. Proc. Natl. Acad. Sci. USA. *83*,952-956.

Sikorski, R. S. and Heiter, P. (1989). A System of Shuttle Vectors and Yeast Host Strains Designed for Efficient Manipulation of DNA in *Saccharomyces cerevisiae*. Genetics *122*, 19-27.

Simon, S. M. and Blobel, G. (1992). Signal peptides open protein-conducting channels in *E. coli*. Cell *69*, 677-684.

Tajima, S., Lauffer, L., Rath, V. L. and Walter, P. (1986). The signal recognition particle receptor is a complex that contains two distinct polypeptide chains. J. Cell Biol. *103*, 1167-1178.

Walter, P. and Blobel, G. (1980). Purification of membrane-associated protein complex required for protein translocation across the endoplasmic reticulum. Proc. Natl. Acad. Sci. USA *77*, 7112-7116.

Walter, P. and Blobel, G. (1982). Signal recognition particle contains a 7S RNA essential for protein translocation across the endoplasmic reticulum. Nature *299*, 691-698.

Walter, P., Gilmore, R. and Blobel, G. (1984). Protein translocation across the endoplasmic reticulum. Cell *38*, 5-8.

Walter, P. and Johnson, A. E. (1994). Signal Sequence Recognition and Protein Targeting to the Endoplasmic Reticulum Membrane. Ann. Rev. Cell Biol. *10*, 87-119.

Weijland, A., Parlato, G. and Parmeggiani, A. (1994). Elongation factor Tu D138N, a mutant with modified substrate specificity, as a tool to study energy consumption in protein biosynthesis. Biochemistry *33*, 10711-10717.

Chapter 4

Signal Recognition Particle Samples Nascent Chains for the Presence of Signal Sequences by Interacting with Ribosomes at a Discrete Step during Translation Elongation

ABSTRACT

The signal recognition particle (SRP) binds to ribosomes that synthesize nascent chains bearing signal sequences and catalyzes their targeting to the endoplasmic reticulum membrane. In *S. cerevisiae*, a ts mutation in the *SEC65* gene, encoding an SRP subunit, results in lowered levels of SRP. Growth and protein translocation defects induced by this mutation can be suppressed specifically by sublethal doses of cycloheximide but not anisomycin, each inhibitors of different steps of translation elongation. Cycloheximide also suppresses protein translocation defects caused by depletion of a different SRP subunit. We propose that reduced elongation rates in the presence of cycloheximide allow otherwise insufficient SRP to interact efficiently with ribosomes. These results are consistent with a sampling model in which SRP cycles on and off translating ribosomes at specific steps during the elongation cycle to inspect all nascent chains for the presence of signal sequences.

INTRODUCTION

The signal recognition particle (SRP) is a cytosolic ribonucleoprotein that selects ribosomes synthesizing membrane and secretory proteins and targets these ribosome-nascent chain complexes to the endoplasmic reticulum (ER) membrane (for review see Walter and Johnson, 1994). Selection involves the binding of SRP to signal sequences as they emerge as part of the nascent chain from the ribosome. As a consequence of this interaction, SRP binds more tightly to the ribosome/nascent chain complex, and the elongation of the nascent protein chain pauses ("elongation arrest"), suggesting that SRP interacts directly with the ribosome (Wolin and Walter, 1989) Upon targeting of the SRP/ribosome/nascent chain complex to the ER membrane, the interaction of the SRP with the SRP receptor, an ER membrane protein, displaces SRP in a GTP-dependent reaction from both the signal sequence and the ribosome (Connolly et al., 1991; Miller et al., 1993). Released from SRP, the ribosome engages with the protein translocation apparatus in the ER membrane, translation resumes and, concomitant with its synthesis, the nascent protein chain is translocated across or, in the case of an integral membrane protein, integrated into the ER membrane. Thus, SRP can be viewed as an adapter between the protein translation machinery in the cytosol and protein translocation machinery in the ER membrane that ensures that selection and targeting of ribosomes synthesizing signal sequence-bearing nascent chains occurs in a co-translational manner.

Much of this model describing SRP function was derived from biochemical studies of mammalian SRP. Recently, structurally similar SRP and SRP receptor homologs from the yeast *Saccharomyces cerevisiae* have

been identified and shown to function in protein translocation *in vivo* (Brown et al., 1994; Hann et al., 1989; Ogg et al., 1992; Stirling and Hewitt, 1992). Deletion of the genes encoding any SRP or SRP receptor component leads to identical phenotypes: slow cell growth and inefficient protein translocation across the ER membrane. In the absence of SRP, the efficiency with which proteins are translocated across the ER differs between individual proteins: the translocation of some proteins is severely impaired, while some others are not affected at all (Hann and Walter, 1991). Because of this observation and because yeast cells can grow, albeit slowly, in the absence of SRP, there must be an alternative, SRP-independent route by which proteins can be translocated across the ER membrane in cells lacking SRP. In vitro studies have shown that protein translocation across ER-derived membranes can occur post-translationally (Hansen et al., 1986; Rothblatt and Meyer, 1986; Waters and Blobel, 1986), and hence it is plausible that in yeast, SRP-dependent co-translational and SRP-independent post-translational pathways coexist that are, at least in part, functionally redundant.

SRP homologs have been identified in all cells analyzed to date, including bacteria, archae and eucaryotes. In *E. coli*, the SRP consists of a single protein subunit, Ffh, that is homologous to the eucaryotic Srp54 protein, the SRP subunit that binds to signal sequences, and a small RNA, 4.5 S RNA, that shares a structurally similar domain with eucaryotic SRP RNA. There is increasing evidence that these structurally related bacterial RNPs function like their eucaryotic counterparts in signal sequence recognition and protein targeting (Wolin, 1994). As in *S. cerevisiae*, an SRP-independent targeting pathway can operate in *E. coli*; but in contrast to yeast, this pathway cannot sustain life in the absence of the SRP.

The evolutionary conservation of SRP suggests that its function must be important. One explanation is that the co-translational nature of the signal recognition event by SRP guarantees that nascent chains are targeted to the appropriate membrane early during their synthesis, i.e. before too much of the protein has been synthesized. This may assure targeting of short nascent chains that can be efficiently translocated before they–after further elongation–may have had the opportunity to misfold or aggregate into a translocation-incompetent state in the cytosol. Here we present evidence that the function of SRP early in the synthesis of a protein is assured through a mechanism where the ribosome plays a direct role in the signal recognition event. In particular, we show that the interaction of SRP with the ribosome is obligatory for SRP function in vivo. Furthermore, our data suggest that the SRP/ribosome interaction is restricted to a defined state in the elongation cycle of the ribosome. Taken together, our results point at a much more intimate and exquisitely regulated interaction between SRP and ribosomes than previously appreciated.

RESULTS

SEC65 encodes the yeast homologue of mammalian SRP19, an essential component of SRP (Stirling and Hewitt, 1992). The gene was identified genetically and cloned by complementation of the recessive *sec65-1* mutation which renders yeast cells ts for growth (Stirling et al., 1992). We mapped the mutation responsible for the ts phenotype to a C to T transition that results in a change of proline-152 (C<u>C</u>A) to leucine (C<u>T</u>A) (see Experimental Procedures). As previously shown, this mutation causes Sec65p to be unstable

at the nonpermissive temperature, causing SRP in these cells to be partially disrupted (Hann et al., 1992). Surprisingly, yeast cells bearing the *sec65-1* mutation not only growth arrest, but die when incubated at the nonpermissive temperature. In contrast, cells bearing a complete disruption of *SEC65* are viable, although—like cells in which genes encoding other SRP components are disrupted— they have growth and protein translocation defects. Thus, it seems a paradox that *sec65-1* cells are conditionally lethal, yet cells bearing the *SEC65* gene disruption are viable.

To test whether the ts phenotype of *sec65-1* cells is related to SRP function or is due to some indirect interference of mutant Sec65p with some essential cellular process, we constructed strain SOY288 (see Table 1) bearing both a disruption of the gene encoding SRP RNA (*scr1Δ*) and the *sec65-1* mutation (see Experimental Procedures). Growth analyses showed that SOY288 cells were not ts: cells grew at the rate characteristic for SRP-depleted cells at both 24° C and 37° C, the permissive and nonpermissive temperatures for *sec65-1* (Figure 1). Transformation with a plasmid bearing the wildtype *SCR1* gene complemented the growth defects and restored the ts phenotype. We infer from these data that the ts phenotype of the *sec65-1* mutation is manifested only in cells that contain SRP; i.e., cells that lack SRP are immune to the detrimental effects of the *sec65-1* mutation at the nonpermissive temperature. This result suggests that the temperature-induced disruption of the mutant SRP directly causes cell death.

A possible explanation for the paradox described above is that yeast cells are sensitive to the kinetics with which SRP is lost: as SRP levels drop suddenly when *sec65-1* cells are shifted to the nonpermissive temperature, cells might not have enough time to switch over to an SRP-independent

Figure 1

Intact SRP is required for *sec65-1* cells to manifest the ts defect. Cells with the indicated relevant genotype (SOY288 (*scr1::HIS3, sec65-1*) and BHY132 (*scr1::HIS3, SEC65*)) were streaked onto YEPD plates and incubated at the indicated temperatures (left and middle plates). Both strains were transformed with pSCR1, a plasmid containing the wild type *SCR1* sequence, streaked onto a YEPD plate and incubated at 37 °C (right plate).

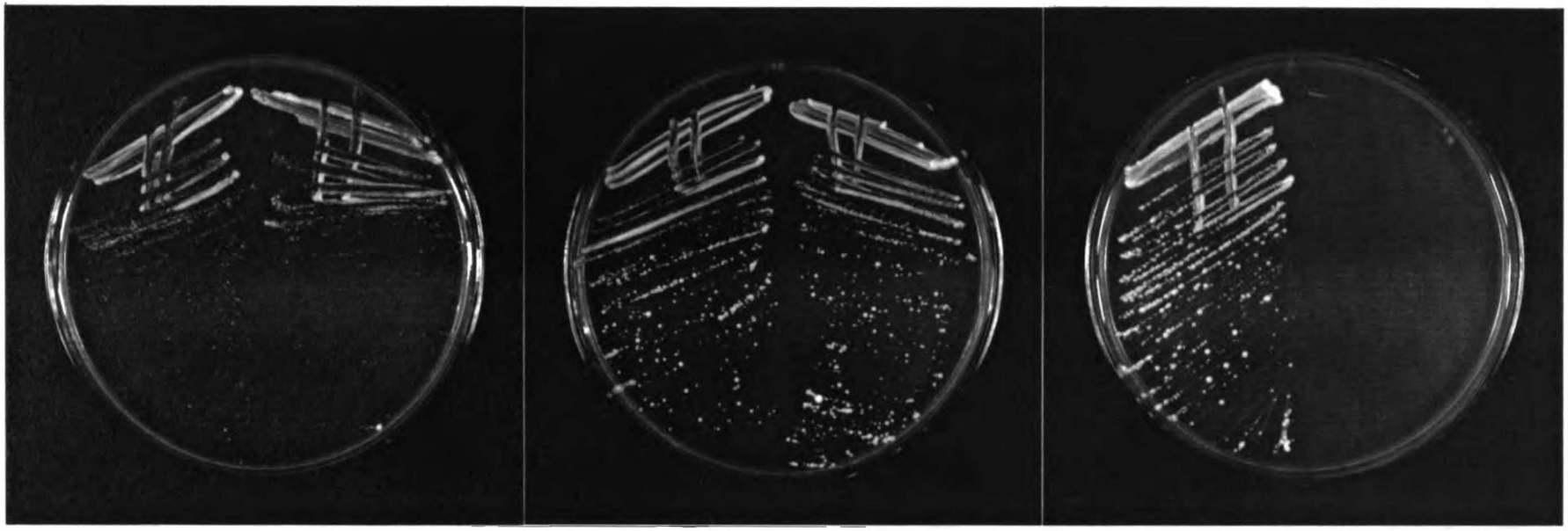

mode of protein targeting. This failure to adapt would result in cell death. This model suggests that it might be possible to suppress the ts phenotype of the *sec65-1* mutation if i) SRP-independent targeting were enhanced, ii) SRP levels at the nonpermissive temperature were stabilized or iii) an insufficient SRP concentration present in *sec65-1* cells at the nonpermissive temperature could be made to suffice.

To explore these possibilities, we pursued the observation—first made by David Feldheim and Randy Schekman—that sublethal concentrations of cycloheximide, an inhibitor of translation elongation, can suppress the ts growth defect of *sec65-1* cells. To demonstrate suppression, a lawn of *sec65-1* cells was plated on YEPD plates and filter disks soaked either in water (Fig. 2A, "-CHX") or in a cycloheximide solution (Fig. 2A, "+CHX") were placed in the center of the plates. When plates were incubated at 37° C, a distinct ring of cell growth was observed surrounding the filter disk that contained cycloheximide (Fig. 2A, bottom right), whereas no cells grew on the plate containing the disk soaked in water (Fig. 2A, bottom left). The diameter of this ring was dependent on the amount of cycloheximide added to the filter disk: higher amounts produced a ring with a larger diameter, whereas lower amounts produced a ring with a smaller diameter (not shown). The most plausible interpretation of these results is that, during the incubation time, cycloheximide diffuses from the disk and forms a radially symmetric concentration gradient. Within a narrow concentration range, cycloheximide suppresses the growth defect of *sec65-1* cells at the nonpermissive temperature resulting in a ring of cell growth. To quantitate this result, we measured the growth rate of *sec65-1* cells in liquid culture at different cycloheximide concentrations at 24 °C and 37 °C (Fig. 2B). In agreement with the plate assay, addition of low concentrations of cycloheximide resulted in

Figure 2

Cycloheximide, but not anisomycin, suppresses the ts defect of *sec65-1* cells. **(A)** Cells (RSY457, *sec65-1*) were plated on YEPD plates. Filter disks containing 6 nmoles of cycloheximide (in water), were placed in the center of each plate ("+CHX"). Filter disks containing only water serve as the control ("-CHX"). Plates were incubated at the indicated temperatures for three days. **(B, C)** Cells were grown in liquid YEPD medium containing the indicated amount of cycloheximide at 24 °C (open squares) or 37 °C (closed circles). Growth rates were determined by measuring the OD_{600} of the cultures. Each data point represents the average of two experiments. Panel B shows the growth rates for strain RSY457 (*sec65-1, CYH2*), and panel C for strain SOY158 (*sec65-1, cyh2*). **(D)** RSY457 (*sec65-1*) cells were grown in the presence of anisomycin at 24 °C (open squares) or 37 °C (closed circles).

A

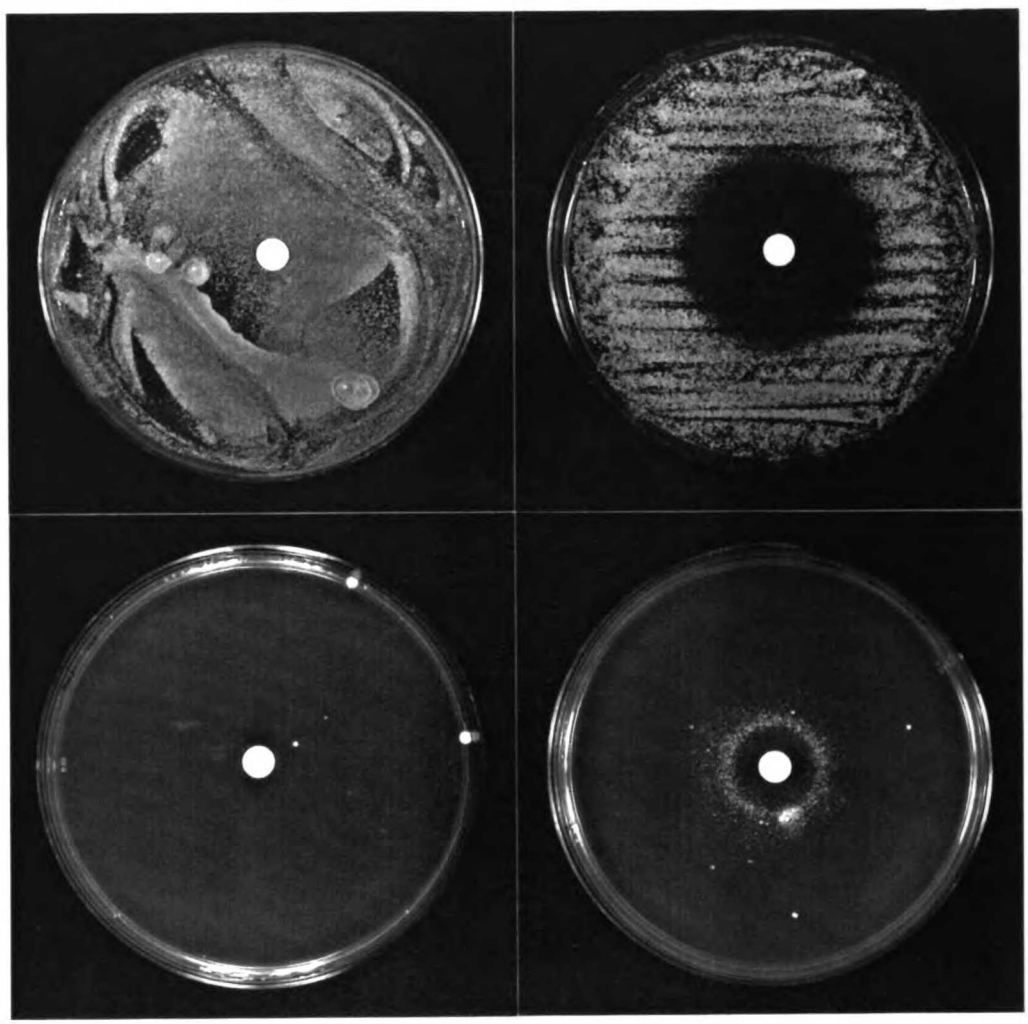

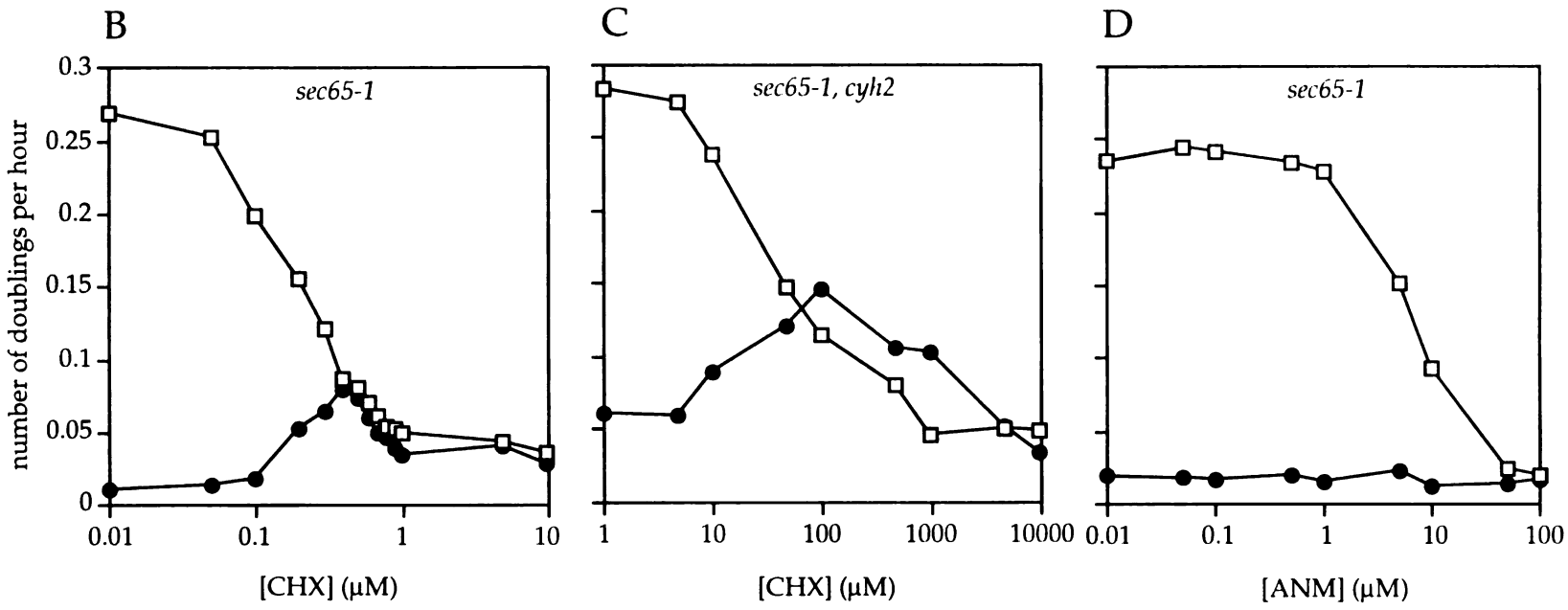

Figure 3

Cycloheximide suppresses the protein translocation defect of *sec65-1* cells. RSY457 (*sec65-1*) cells growing at the indicated temperatures in the presence (lanes 2 and 4) or absence (lanes 1 and 3) of 0.4 μM cycloheximide were pulse labeled with [^{35}S]-methionine for 7 min. Cell extracts were immunoprecipitated with antibodies against either Kar2p or DPAP-B. The precursor and mature forms of each of the immunoprecipitated proteins are indicated. Immunoprecipitated proteins were visualized by autoradiography following SDS-PAGE .

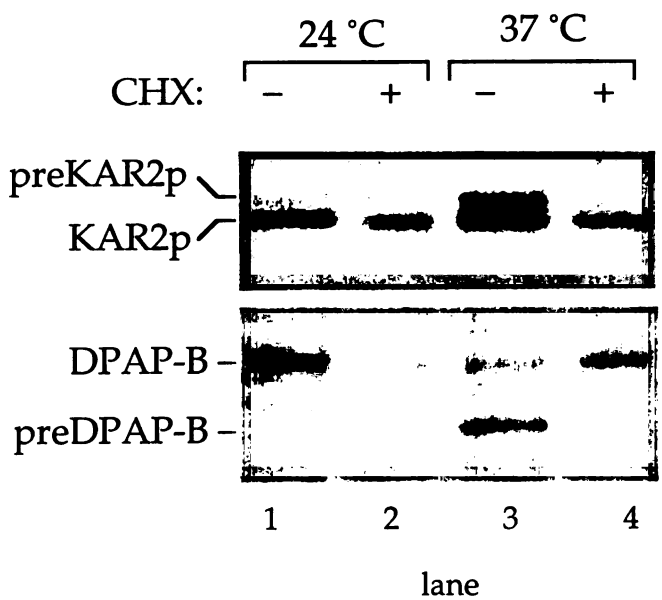

cell growth at the nonpermissive temperature. The growth rate was maximal at 0.4 μM cycloheximide and, at this concentration, was identical at the permissive and nonpermissive temperature. Cycloheximide concentrations in excess of 0.4 μM inhibited the growth rate equally at either temperature, presumably because the rate of translation became limiting for cell growth. *Sec65-1* cells show marked protein translocation defects upon shift to the nonpermissive temperature (Stirling and Hewitt, 1992; Stirling et al., 1992). To ask whether cycloheximide suppresses the protein translocation defects in addition to the growth defect, we pulse-labeled *sec65-1* cells with [^{35}S]-methionine, either at 24 °C or 37 °C, and in the presence or absence of 0.4 μM cycloheximide. Using antibodies that recognize Kar2p or DPAP-B, two proteins that use the SRP-dependent protein targeting pathway to the ER membrane, we performed immunoprecipitation reactions from extracts of the radiolabeled cells. Accumulated precursor forms of both Kar2p and DPAP-B were significantly increased when *sec65-1* cells were shifted to the nonpermissive temperature (Fig. 3, compare lane 3 to lane 1). Translocation defects in Kar2p are indicated by the accumulation of a slower migrating band, preKar2p, containing an uncleaved signal sequence, whereas translocation defects of DPAP-B results in the accumulation of a faster migrating band, preDPAP-B, lacking N-linked glycosylation. The addition of 0.4 μM cycloheximide completely abolished precursor accumulation of both Kar2p and DPAP-B at the nonpermissive temperature. Thus, both cell growth and protein translocation defects manifested in *sec65-1* cells at the nonpermissive temperature are suppressed by cycloheximide .

Cycloheximide is a well characterized inhibitor of eucaryotic protein translation elongation (Gale et al., 1981). We therefore sought to ascertain that

suppression resulted from direct effects of cycloheximide on protein synthesis, rather than from pleiotropic effects of the drug on an unrelated target. To this end, we isolated mutations in ribosomal protein L29, encoded by *CYH2*, which render cells resistant to higher levels of cycloheximide (Stöcklein and Piepersberg, 1980). Such mutants arise spontaneously and can be readily selected by growing cells on plates containing cycloheximide. This allowed us to isolate *cyh2* mutant cells in the same strain background bearing the *sec65-1* mutation. Cycloheximide resistant colonies were isolated from strain RSY457 (*sec65-1*). One of these colonies was designated as strain SOY158 and chosen for further study. To confirm that the cycloheximide-resistance of these cells was due to a mutation in *CYH2*, cells from strain SOY158 were crossed to strain 5114-2 bearing the *cyh2* mutation. The resulting diploid strain was resistant to cycloheximide and, after sporulation, the cycloheximide resistance phenotype segregated 4:0 in 20 tetrads analyzed, indicating that the cycloheximide resistance phenotype was due to a mutation in *CYH2*. Like the parent strain, SOY158 cells were ts for growth. Growth of RSY457 (*sec65-1, CYH2*) cells at the permissive temperature was inhibited by 50% at 0.2 μM cycloheximide, whereas growth of SOY158 (*sec65-1, cyh2*) cells was inhibited by 50% at 50 μM cycloheximide (compare Fig 2B and 2C). We therefore conclude that SOY158 cells bear both the *sec65-1* and the *cyh2* mutations.

To test whether cycloheximide would suppress the temperature-sensitive growth defect of SOY158 cells, we grew the cells in liquid culture at either the permissive or nonpermissive temperature in the presence of increasing concentrations of cycloheximide. As shown in Figure 2C, cycloheximide suppressed their growth defect at the nonpermissive

[redacted]

temperature; however, suppression required 250-fold higher levels of cycloheximide (100 μM) than that required to suppress the growth defect of *sec65-1* cells (Fig. 2B). This difference correlated directly with the resistance of SOY158 cells to 250-fold higher level of cycloheximide when grown at the permissive temperature.

These results strongly suggest that the effects of cycloheximide on translating ribosomes are directly responsible for the suppression of the defects caused by the *sec65-1* mutation. Furthermore, the defects caused by the *sec65-1* mutation must result from a loss of SRP, because they are only manifested in cells that initially harbor intact SRP. We can explain these results with the following model: In the presence of limiting concentrations of cycloheximide , nascent polypeptide chains emerge more slowly from the ribosome. This results in a longer time window during which the signal peptide of a nascent polypeptide chain can be recognized by SRP co-translationally. Given this model, the cycloheximide-induced reduction of the elongation rate would allow a smaller, and otherwise insufficient amount of SRP, to perform its normal function.

We examined the fate of Sec65p in *sec65-1* cells to ask directly whether a small amount of Sec65p still remained after incubation at the nonpermissive temperature. To this end, we probed Western blots of lysates identical to those used for Figure 3 with antibodies specific for Sec65p. When shifted to 37 °C, Sec65p levels fall to roughly 10% of those seen in cells grown at 24 °C in the absence of cycloheximide (Fig. 4A, compare lane 3 with lane 1). Growth in the presence of cycloheximide at 37 °C further reduced the level of Sec65p to roughly 5% of that seen in cells grown in the absence of cycloheximide (Fig. 4A, compare lanes 4 and 6, with lane 1. Lane 6 contains 10

Figure 4

Cycloheximide does not stabilize Sec65p or increase the efficiency of protein translocation into the ER. (A) Lysates made from cells grown as in Figure 3 were subjected to Western blot analysis. Lanes 1 - 4 contain 0.5 OD_{600} cell equivalents of lysate. Lanes 5 and 6 are duplicates of lanes 3 and 4, except that 5.0 OD_{600} cell equivalents of lysate were loaded. The position of Sec65p is indicated with an arrow. **(B)** RSY457 (*sec65-1*) cells were shifted from 24 °C to 37 °C for 30 min prior to pulse labeling for 1 min with [^{35}S]-methionine. Concomitant with the addition of nonradiolabeled methionine in a 1000 fold molar excess, cycloheximide was added to cells as indicated. Cells were incubated for 0 or 32 minutes, and then processed for immunoprecipitation using anti-Kar2p. Kar2p and preKar2p were separated by SDS-PAGE followed by quantitation on a Phosphorimager.

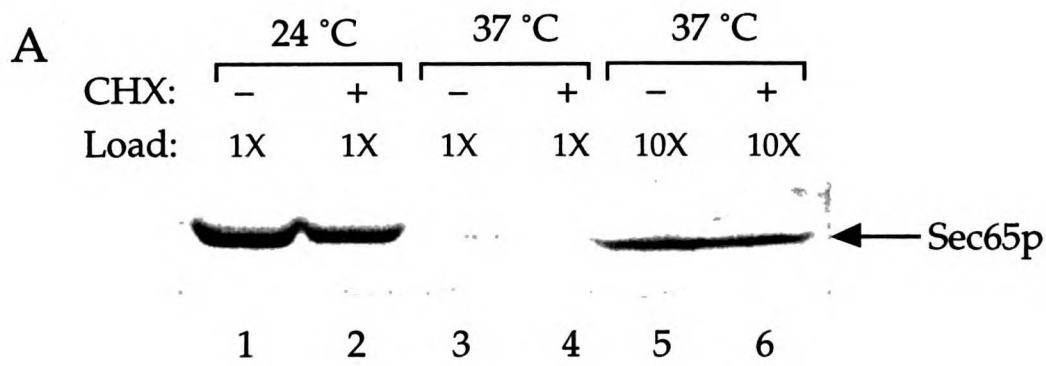
A
24 °C
37 °C
37 °C
CHX:
–
+
–
+
–
+
Load:
1X
1X
1X
1X
10X
10X
Sec65p
1
2
3
4
5
6

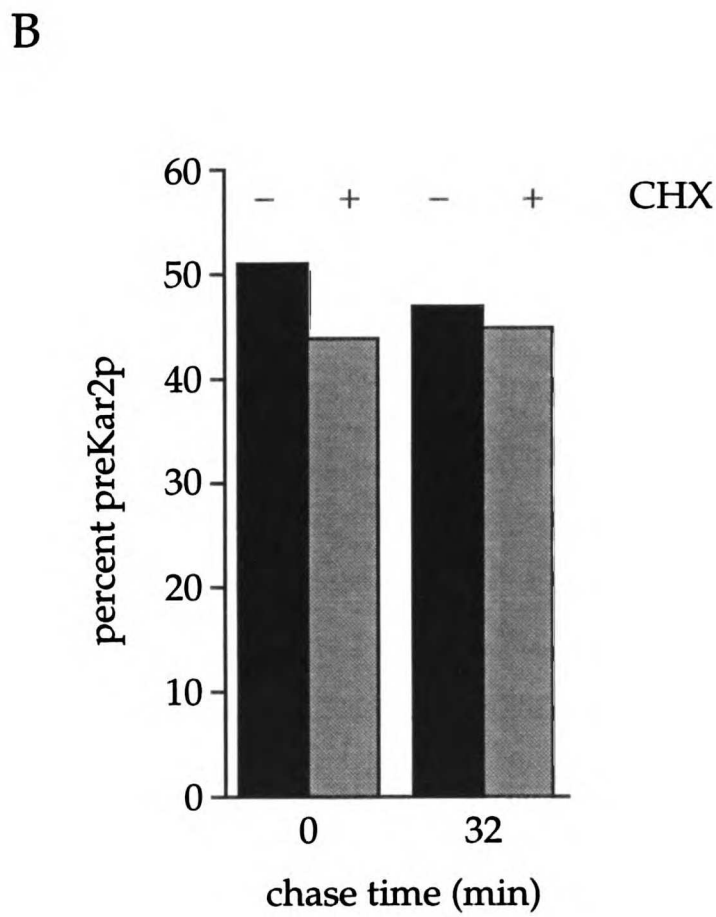
B
60
50
40
30
20
10
0
– + – + CHX
percent preKar2p
0
32
chase time (min)

times the amount of cell extract as lane 4). This reduced level of Sec65p in cycloheximide-treated cells grown at 37 °C was the same whether the cells were tested at 30 minutes, or 1.5 hour after a shift to 37 °C (not shown). These results show that a small amount of Sec65p remains in cells, even after prolonged incubation at the nonpermissive temperature, and thus are consistent with the model presented above. The data also rule out the alternative possibility that Sec65p is somehow stabilized by cycloheximide at the nonpermissive temperature.

According to another possible mechanism of suppression, cycloheximide treatment might cause detrimental precursor proteins to be degraded or would induce an SRP-independent, post-translational translocation pathway. To test these possibilities, we accumulated radiolabeled precursor proteins by shifting *sec65-1* cells to 37 °C followed by pulse-labeling with [^{35}S]-methionine. After the addition of a large excess of unlabeled methionine, the incubation was continued at 37 °C either in the presence or absence of cycloheximide, and the fate of labeled preKar2p was monitored. Aliquots of the cell culture were removed at the intervals indicated in Figure 4B and immunoprecipited with antibodies to Kar2p. As demonstrated by the results shown in Figure 4B, preKar2p was stable throughout the duration of a 32 minute chase period regardless of the presence or absence of cycloheximide. Because the time needed for cycloheximide to exert its effect is no longer than 10 minutes (conditions under which the experiment in Figure 3 was performed), we know that the temperature-induced protein translocation defect can be suppressed by cycloheximide during the first third of the chase period shown in Figure 4B. Thus, we can conclude that the suppression of the translocation defect shown

[redacted]

Figure 5

Protein translocation defects caused by SRP-depletion is suppressed by cycloheximide. BHY104 cells containing *SRP54* under the control of the *GAL10* promoter were shifted from galactose to glucose to repress the expression of Srp54p. At the indicated time points after repression of Srp54p samples were incubated in the presence (bottom panels in A and B) or absence (top panels in A and B) of cycloheximide for 5 min. Cells were pulse labeled with Trans-[^{35}S]-label for 15 min, followed by a 2 min chase period to complete processing of all Kar2p chains. Kar2p and preKar2p were visualized as in Fig. 3. Higher levels of Kar2p at later time points are due to the induction of the heat shock response upon accumulation of cytoplasmic precursors (Arnold and Wittrup, 1994). **(A)** Portions of the radiolabeled extracts were subjected to Western blot analysis with anti-Srp54p antibodies. Each lane contains 0.5 OD_{600} cell equivalents of lysate and contained equivalent amounts of protein as judged by Ponceau S staining. **(B)** Immunoprecipitations were performed using anti-Kar2p antibodies. **(C)** Quantification of the data in (B) was performed on a Phosphorimager. Squares: – CHX; circles: + CHX. **(D)** In a similar, but separate experiment, cycloheximide (squares) and anisomycin (circles) were titrated after cells were grown for 11 h in glucose medium to deplete Srp54p . After incubation of the cells for 5 min with the indicated amount of each drug, cells were processed as above, and the ratio of preKar2p to Kar2p was determined. The concentration range of each drug was chosen based on the data in Fig. 2. 40% preKar2p accumulated in the absence of drug compared to only 25% at the corresponding time point in Panel C. This is due to variation between separate experiments.

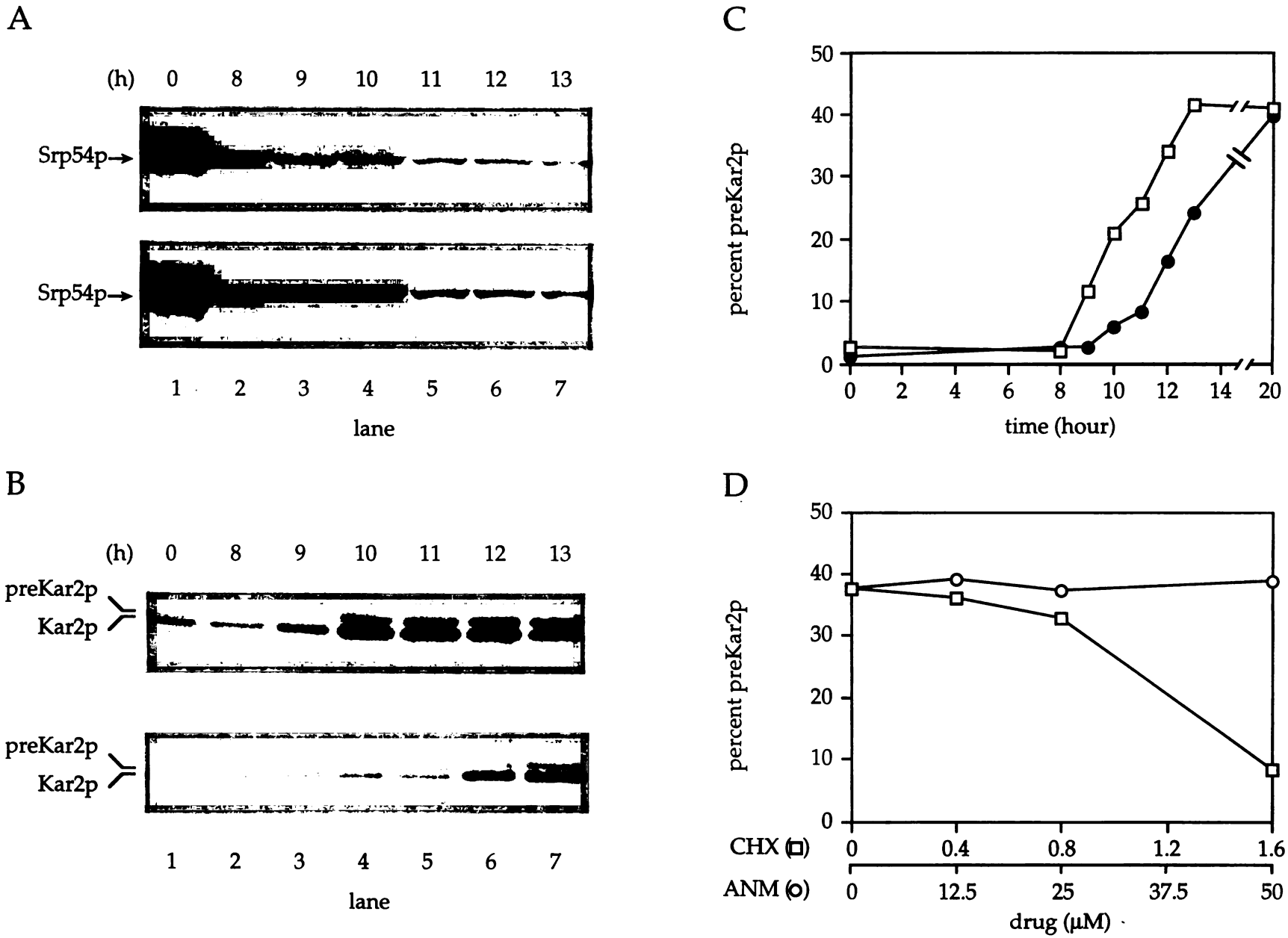
A
(h) 0 8 9 10 11 12 13
Srp54p
Srp54p
1 2 3 4 5 6 7
lane
B
(h) 0 8 9 10 11 12 13
preKar2p
Kar2p
preKar2p
Kar2p
1 2 3 4 5 6 7
lane
C
percent preKar2p
time (hour)
D
percent preKar2p
CHX (□)
ANM (○)
drug (μM)

in Figure 3 was not simply due to precursor degradation, nor was it caused by the precursors being translocated in a post-translational manner.

To test the validity of our model, we used an independent approach—not involving the sec65-1 mutation—to reduce the amount of functional SRP in cells and then monitored the effects of cycloheximide on the efficiency of protein translocation. Strain BHY104 contains *SRP54* under the control of the *GAL1* promoter, and SRP can be depleted from these cells by switching the carbon source from galactose- to glucose-containing media (Fig. 5A). As shown previously, precursors of normally translocated proteins accumulate as the concentration of SRP becomes limiting in these cells (Hann and Walter, 1991). Thus, monitoring the efficiency of protein translocation at different times after repression of Srp54p synthesis—i.e., in cells containing decreasing concentrations of SRP—allowed us to test directly whether a reduction of the elongation rate by cycloheximide would allow a limiting concentration of SRP to work more efficiently. To perform this experiment, aliquots were taken from a culture of BHY104 cells at different times after repression of *SRP54* and incubated both in the presence and absence of cycloheximide for 5 minutes. [^{35}S]-methionine was then added to pulse-label newly synthesized proteins. We examined the accumulation of preKar2p in cells labeled in the absence or presence of cycloheximide after immunoprecipitation.

Pulse-labeling in the absence of cycloheximide gave the expected results (Fig. 5B, top panel, and Fig. 5C, squares). PreKar2p started to accumulate at 9 hours after *SRP54* expression was repressed and reached a plateau at 13 hours at about 40% of the total immunoprecipitated Kar2p species. In contrast, in the presence of cycloheximide, the accumulation of preKar2p was

significantly delayed (Fig. 5B, bottom panel, and 5C, circles), indicating that cycloheximide allowed the limiting concentration of SRP in these cells to work more efficiently. As shown in the Western blot analysis in Figure 5A, the delay of preKar2p accumulation was not due to differences in Srp54p levels in the untreated and cycloheximide-treated samples. While the preKar2p accumulation in the presence of cycloheximide was significantly reduced at the 9 to 13 hour time points, it eventually reached the same plateau as in the absence of cycloheximide . This result is expected, because cells must switch from an SRP-dependent mode of protein translocation to an SRP-independent mode when SRP is depleted. From the data shown in Figure 5C, we surmise that between 9 and 11 hours after repression of Srp54p synthesis, the levels of functional SRP become limiting but are still high enough to afford efficient protein translocation, if the rate of protein elongation is reduced by cycloheximide. At the later time points, however, an increasing fraction of Kar2p becomes targeted through the SRP-independent pathway and, because the level of functional SRP becomes too low, efficient co-translational SRP-dependent protein translocation can no longer be reinstated even if the elongation rate is reduced by the addition of cycloheximide. Consistent with this interpretation, the growth and protein translocation defects in strains deleted for *SRP54* or *SEC65* cannot be abrogated by the addition of cycloheximide (not shown).

To determine the concentration of cycloheximide that would give the greatest difference of precursor accumulation, we performed a titration experiment with cells taken from a fixed time point (11 hours after shift to glucose) in the SRP-depletion experiment. The results show that increasing amounts of cycloheximide progressively improved translocation efficiency

(Fig. 5D, squares), indicating that the more protein elongation is slowed, the more efficiently protein translocation occurs in the presence of a fixed concentration of SRP. The optimum cycloheximide concentration was found to be 1.6 μM. The difference between this concentration and the one required to suppress the growth defect of *sec65-1* cells (0.4 μM) may be due to differences in the strain background between RSY457 (*sec65-1*) and BHY104 (pGALSRP54) cells. Alternatively, the optimal concentration of cycloheximide that allows efficient Kar2p translocation in a 5 min pulse (conditions in Fig. 5) may not allow sustained growth of yeast in liquid culture (conditions in Fig. 2).

According to our model, the nascent protein chain has to emerge from the ribosome more slowly to allow a reduced concentration of SRP to target the nascent chains co-translationally. If this is the case, then inhibiting protein synthesis initiation should not suppress the *sec65-1* induced growth defects, because—while reducing the flux of newly synthesized protein—this would not reduce the rate with which they emerge from the ribosome. To reduce translation initiation, we expressed dominant, constituitively active alleles of *GCN2* in either *sec65-1* or wildtype cells. Gcn2p is a protein kinase that inactivates initiation factor eIF-2α by phosphorylation, and cells expressing dominant alleles of *GCN2* grow at reduced rates because of limiting concentrations of active eIF-2α. The severity of the growth defect correlates with the degree to which the mutations in *GCN2* activate its kinase activity (Dever et al., 1992). We expressed the wild type and three constitutively active alleles of *GCN2* (in increasing strengths: *GCN2^{C}-516, GCN2^{C}-518, GCN2^{C}-515*) in either *sec65-1* or wildtype cells. Figure 6A depicts plates on which either *sec65-1* or wild type cells were grown at 24 °C or 37 °C.

The particular allele of *GCN2* that was present in the cells in each quadrant of the plates is indicated below. To quantitate the severity of the growth defect produced by the different $GCN2^C$ alleles, we measured the growth rates of cells in liquid culture under the conditions shown in Figure 6A.

None of the *GCN2* alleles suppressed the *sec65-1* growth defect at the nonpermissive temperature (Fig. 6A), even though the growth of *sec65-1* cells expressing the $GCN2^C$-*515* allele was more than 4-fold reduced compared to cells bearing the wildtype *GCN2*. This is a similar fold reduction in growth rate to that caused by the presence of 0.4 μM cycloheximide (compare Figure 6B with Figure 2B) which caused suppression. Thus, a reduction of the overall protein synthesis rate is not sufficient to suppress the *sec65-1* growth defect, rather a reduction in the rate of protein elongation is required.

To determine whether defects in cells containing limiting amounts of SRP can be suppressed by slowing translation elongation at any point in the elongation cycle, we tested an additional drug, anisomycin, which inhibits the transpeptidylation reaction (Gale et al., 1981). Surprisingly, in contrast to cycloheximide, anisomycin was unable to suppress the growth defect of *sec65-1* cells at 37 °C (Fig 2, panel D, closed circles). Similarly, anisomycin was unable to suppress the translocation defect at early times after Srp54p depletion (Fig. 5D, circles). Anisomycin was able, however, to enter yeast cells efficiently and inhibit growth of *sec65-1* cells at the permissive temperature (Fig 2, panel D, squares).

These results raised the possibility that the different effects of cycloheximide, anisomycin and the $GCN2^c$ mutation could, in principle, result from differential effects of these three inhibitors on the translation of

Figure 6

Inhibition of translation initiation does not suppress the growth defect of *sec65-1* cells. (A) RSY457 or W303-1A cells (either *sec65-1* or *SEC65*) were transformed with plasmids containing the indicated dominant allele of *GCN2*. These cells were grown on media selecting for the plasmid at either 24 °C or 37 °C. The cartoon illustrates which quadrant of each plate contains cells harboring the indicated allele of *GCN2*. **(B)** The growth rates of the strains used in (A) were determined. The average of two separate experiments is shown.

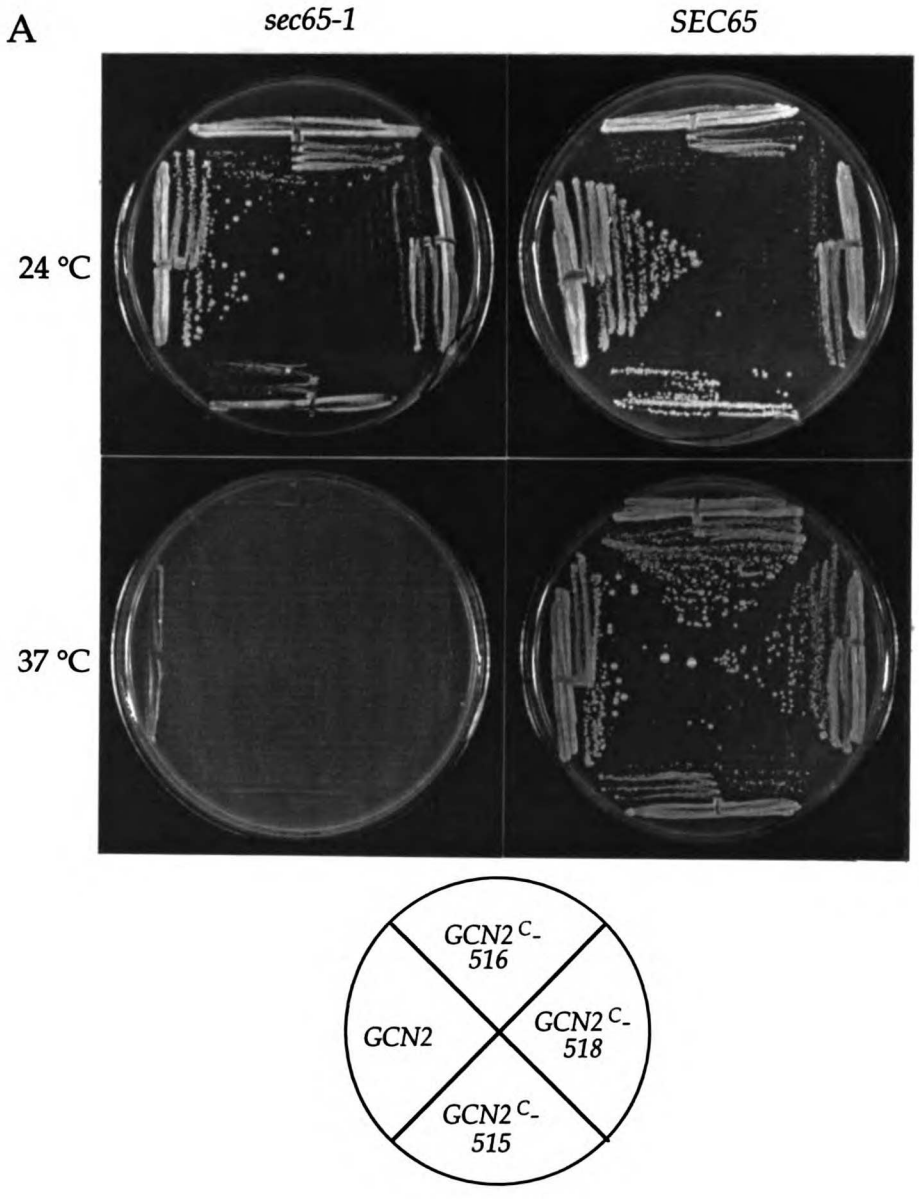
A
sec65-1
SEC65
24 °C
37 °C
GCN2 C-516
GCN2 C-518
GCN2
GCN2 C-515

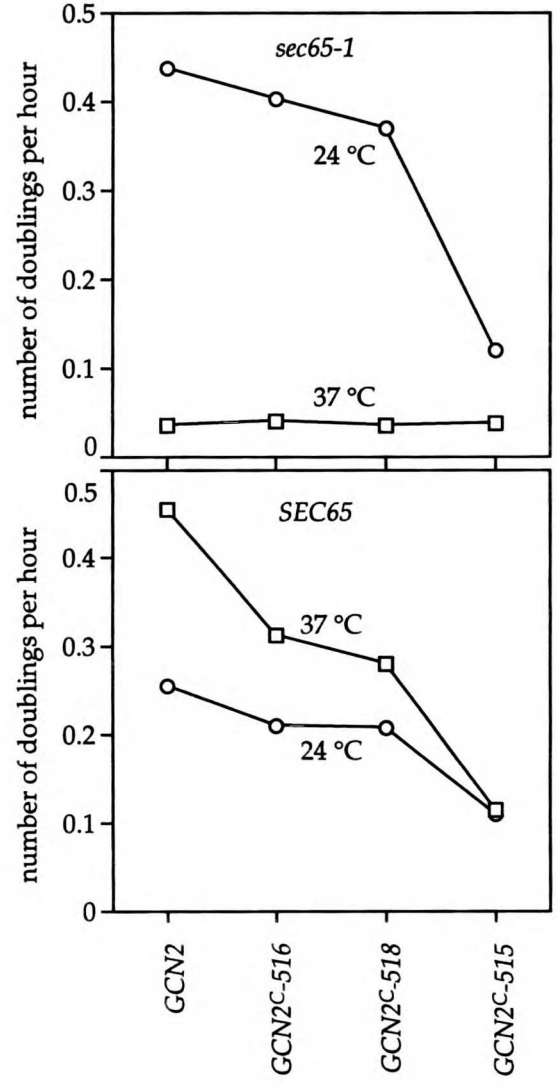
B
sec65-1
24 °C
37 °C
SEC65
37 °C
24 °C
number of doublings per hour
0.5
0.4
0.3
0.2
0.1
0
GCN2
GCN2C-516
GCN2C-518
GCN2C-515

individual mRNAs. Translation of a subset of proteins could, for example, be irreversibly blocked in one case but not another, and the different effects leading to the suppression of the translocation defect under conditions of limiting SRP might then result from the different spectrum of proteins synthesized. To test for this possibility directly, we determined the effects of cycloheximide, anisomycin and the *GCN2^{c}-515* mutation on the overall pattern of protein synthesized. To this end, we monitored the rate of incorporation of [^{35}S]-methionine into protein in the absence or in the presence of the three inhibitors under conditions that were shown in Figures 2 and 6 to slow cell growth to approximately similar extents (Fig. 7A). Incorporation of [^{35}S]-methionine was linear over the course of the 3 min experiment, and its rate was decreased by about 25% in the presence of the inhibitors. We chose a late time point (130 s) from this labeling reaction to analyze the pattern of newly synthesized proteins in the presence of the three inhibitors. Total labeled cell protein was fractionated by SDS-PAGE, and the lanes were scanned along their lengths with a PhosphorImager (Fig. 7B). In each case, the upper trace represents the profile of proteins synthesized in the absence of inhibitor, while the lower trace represents the profile of proteins synthesized in the presence of inhibitor. These results show that all three inhibitors diminish uniformly the incorporation of [^{35}S]-methionine across the entire spectrum of the labeled protein species. From these data, we conclude that the observed differences between the inhibitors most likely result because they affect different steps of protein translation and not because they have differential effects on the translation of individual mRNAs.

Figure 7

Translation elongation and initiation inhibitors affect the same spectrum of proteins. **(A)** Incorporation of [^{35}S]-methionine at 24 °C is plotted as a function of time. *Sec65-1* cells were pulse-labeled in the absence (open squares) or presence (open circles) of either cycloheximide ("+CHX") or anisomycin ("+ANM"). At the indicated times after [^{35}S]-methionine addition, hot TCA-precipitable counts in aliquots containing equal OD_{600} cell equivalents were measured by scintillation counting. W303 cells containing a plasmid bearing wild-type *GCN2* (open squares), or the dominant allele *GCN2^{C}-515* (open circles) were treated identically ("*GCN2^{C}-515*"). **(B)** Aliquots (0.1 OD_{600} cell equivalents/lane) from lysates prepared at the 130 s time point from the labeling reaction shown in (A) were subjected to SDS-PAGE, followed by scanning of the lanes with a PhosphorImager (Molecular Dynamics, Sunnyvale, CA). The positions of molecular weight markers are indicated below each panel. In each panel the top trace is that obtained in the absence of inhibitor, while the bottom trace is obtained from cell lysate labeled in the presence of either cycloheximide ("+CHX"), anisomycin ("+ANM"), or the dominant negative allele of *GCN2* ("*GCN2^{C}-515*").

A

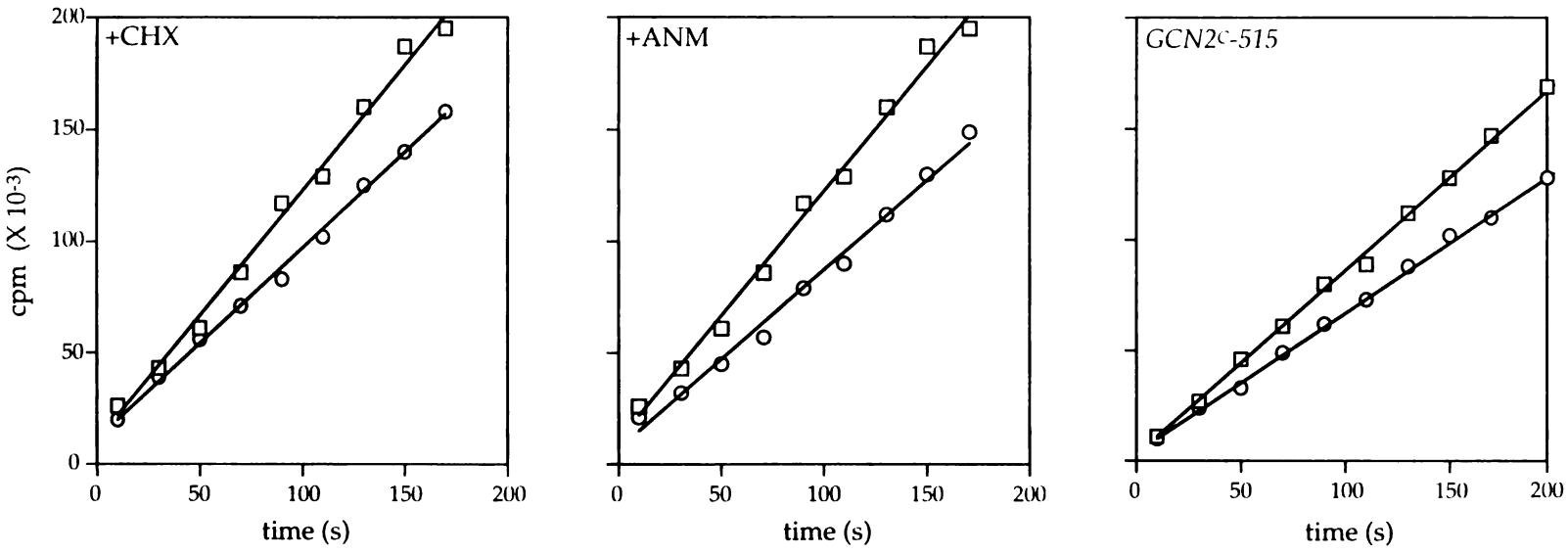

B

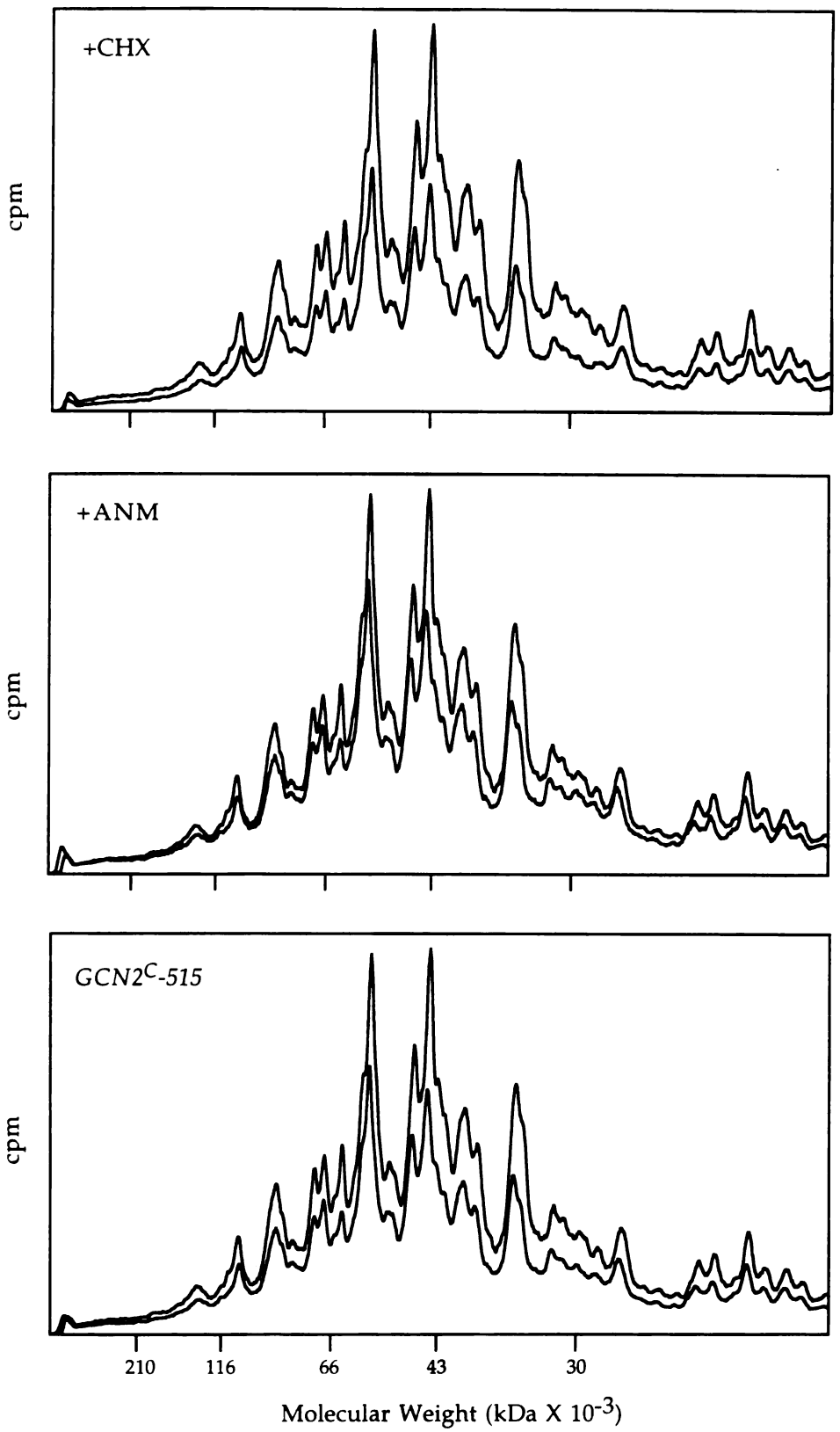
+CHX
cpm
+ANM
cpm
GCN2C-515
cpm
210
116
66
43
30
Molecular Weight (kDa X 10-3)

Figure 8

Model for SRP interaction in the translational cycle.

Translation is shown as a cycle of translational elongation preceded by initiation (blocked by *GCN2*^{C} alleles) and followed by termination. Translational elongation is simplified in this cartoon as consisting of three steps: aminoacyl-tRNA binding to the ribosomal A-site **(A)**, transpeptidylation **(B)**, and translocation of the peptidyl-tRNA from the A-site to the P-site **(C)**. SRP interacts with the ribosome-nascent chain complex after the anisomycin block but before the cycloheximide block. This model is adapted from the hybrid sites model of translational elongation as proposed by Moazed and Noller, 1989.

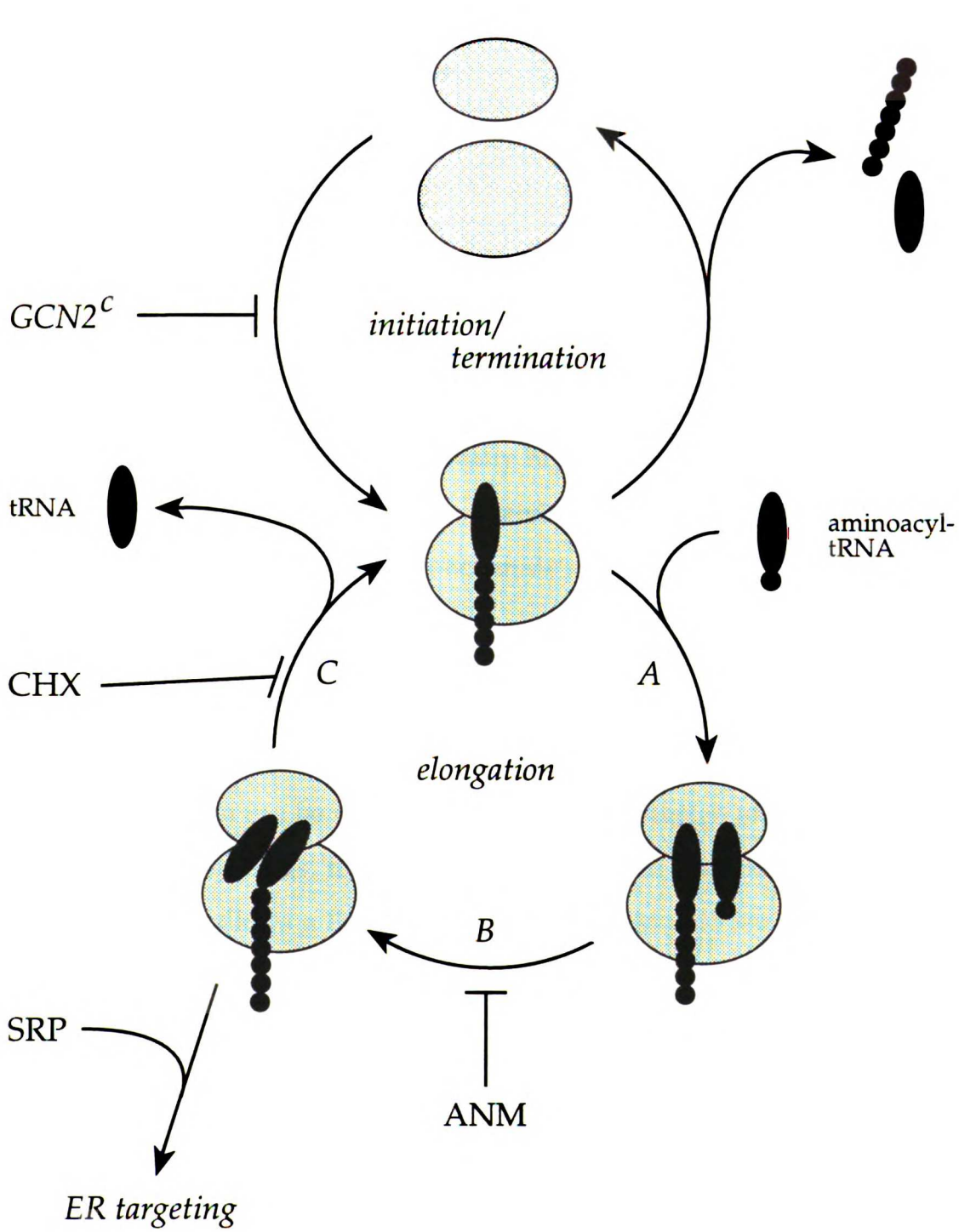
GCN2c
initiation/
termination
tRNA
aminoacyl-
tRNA
CHX
C
A
elongation
B
SRP
ANM
ER targeting

DISCUSSION

We have shown that growth and protein translocation defects induced in yeast cells containing limiting concentrations of SRP can be suppressed by slowing protein elongation with low concentrations of cycloheximide. Two independent means of lowering SRP levels were used: shifting *sec65-1* cells to the nonpermissive temperature and depleting Srp54p after transcriptional repression. Cycloheximide ameliorates growth and translocation defects in both cases, but not after prolonged Srp54p depletion or in cells bearing complete SRP gene disruptions, indicating that some residual SRP must be present in cells for cycloheximide to exert this effect. Furthermore, cycloheximide resistant cells harboring a mutation in ribosomal protein L29 (encoded by *CYH2*) require significantly higher concentrations of cycloheximide to affect suppression, thereby demonstrating that suppression is mediated directly through cycloheximide's effects on the ribosome.

These observations strongly support a model in which cycloheximide causes nascent polypeptide chains to emerge more slowly from the ribosome, creating a longer time window during which the signal peptide of a nascent polypeptide chain can be recognized by SRP and targeted to the ER membrane co-translationally. Thus, the cycloheximide-induced reduction of the elongation rate allows a limiting amount of SRP to perform its normal function.

Consistent with this model, we found that inhibition of translation initiation (experimentally induced by the introduction of the *GCN2^c* mutations, Fig. 6) does not cause suppression. Unexpectedly, another well characterized inhibitor of translation elongation, anisomycin, also failed to

cause suppression, indicating that slowing down the rate of protein elongation *per se* is not sufficient to suppress defects caused by low levels of SRP. Anisomycin blocks transpeptidylation, while cycloheximide blocks translocation, which is the eEF2-catalyzed movement of peptidyl-tRNA from the A-site to the P-site (Fig. 8C). These data suggest that SRP can interact productively with ribosomes and signal sequence-bearing nascent chains only at a specific step(s) in the elongation cycle, which is the step at which ribosomes accumulate in the presence of cycloheximide.

The notion of an intimate, elongation step-specific interaction of SRP and the ribosome suggests a mechanism that can explain how SRP selects signal sequence bearing ribosomes from the total ribosomal pool. Estimation of the concentration of SRP mammalian cells, yeast (Hann and Walter, unpublished) and *E. coli* (Jensen and Pedersen, 1994) suggest that there is one SRP for every ten to one hundred translating ribosomes. SRP has to scan every nascent chain for the presence of a signal sequence, yet—based on the estimated SRP levels—only a small fraction of the translating ribosomes can have an SRP associated at any one time. Based on the results presented here, SRP can interact with ribosomes only during a specific step in the translation cycle. This is consistent with a "sampling" mechanism in which SRP is constantly cycling on and off the ribosome, as opposed to a "scanning" mechanism in which SRP would remain ribosome associated. We propose that SRP binds to the translating ribosome when it has just completed the transpeptidylation reaction, but before it has undergone translocation of the peptidyl-tRNA from the A site to the P site. While bound, the SRP checks whether the emerging nascent protein contains a signal sequence. If this is the case, SRP targets the ribosome to the ER membrane; if no signal sequence is

found, SRP dissociates, and the ribosome continues through the elongation cycle. According to this mechanism, a substoichiometric concentration of SRP would suffice to monitor each ribosome for the presence of a signal sequence. Because SRP can recognize signal sequences on nascent chains of different lengths, we surmise that sampling need not occur during every elongation cycle (Siegel and Walter, 1988).

Concomitant with a tighter association of SRP to the ribosome, elongation pausing is observed upon binding of SRP to a signal sequence (Walter and Blobel, 1981). This suggests that SRP dissociation is obligatory for the ribosome to resume elongation. According to this model, it should be possible to isolate SRP mutants that inhibit protein synthesis because they bind inappropriately tightly to ribosomes.

The definition of the point of action of SRP during the translation elongation cycle is in agreement with results obtained in procaryotic cells. In *E. coli*, the SRP RNA homolog 4.5S RNA and the Srp54p homolog Ffh are essential for cell growth (Brown and Fournier, 1984; Phillips and Silhavy, 1992). Prior to results suggesting its SRP-like role in protein secretion, 4.5S RNA was proposed to be directly involved in translation (Brown, 1987; Brown and Fournier, 1984). In particular, suppressor mutations were isolated in components of the translation apparatus that allowed cells to grow even though they contained sublethal levels of 4.5S RNA. Suppressor mutations were found in elongation factor G (EF-G, the procaryotic homolog of eEF-2), in 23S ribosomal RNA in the region defining the EF-G binding site, and in tRNA synthetases, resulting in higher levels of some uncharged tRNAs (Brown, 1987; Brown, 1989). Intriguingly, these mutations are predicted to impair the translation cycle at the translocation step of peptidyl-tRNA from

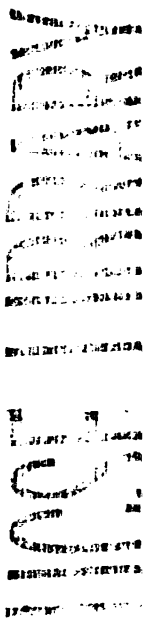

the A to the P site. EF-G mutants and mutations in the ribosomal EF-G binding site would impair translocation directly, whereas uncharged tRNAs might bind to the tRNA exit site ("E-site") on the ribosome, thereby backing-up the ribosome to prevent translocation. These mutations suppressed defects caused by lowering the concentration of 4.5S RNA, but no mutations could be isolated that would allow cells to live in its absence. Brown (1989) concluded that 4.5S RNA participates in an event required for ribosomal translocation.

The results presented here and the increasing evidence pointing at an SRP-like role for the Ffh/4.5S RNP, suggest a different interpretation for these data. We surmise that the lowered levels of 4.5S RNA resulted in lowered levels of functional SRP in E. coli, strictly analogous to the experimental scenarios described here in yeast. Mutations that slow the translocation step would therefore suppress the defects caused by reduced SRP levels, because of an increase in the time window in which SRP can productively recognize a signal sequence. Our data are in agreement with evidence suggesting that the *E. coli* Ffh/4.5S RNP indeed functions as a procaryotic SRP.

EXPERIMENTAL PROCEDURES

Strains, Plasmids, Antibodies and General Methods

Yeast strains used in this study are listed in Table 1. Anti-DPAP-B serum was kindly provided by Tom Stevens, University of Oregon; anti-Sec65p is described in Brown et al. (1994); anti-Srp54p is described in Hann and Walter (1991); anti-Kar2p was produced in our laboratory from protein overexpressed in *E. coli* from a clone kindly provided by Joe Vogel and Mark Rose (Princeton U.). SDS-PAGE was performed on 10-15% gradient gels, and Western blots were visualized by enhanced chemiluminescence ("ECL", Amersham Corporation, Arlington Heights, Ill) according to the instructions of the manufacturer. Plasmid pSCR1 was constructed by ligating the *SCR1* containing *Kpn* I to *Hind* III fragment from pSR6.21 into the *Kpn* I-*Hind* III sites of pRS316 (Felici, et al., 1989).

Strain SOY288, containing both the *sec65-1* and the *scr1-Δ2* mutations was constructed by mating strain RSY457 to strain BHY133. Sporulation of the resulting diploid followed by tetrad dissection allowed the identification of tetrads that contained colonies resulting from two of the four spores with the *SEC65, SCR1* genotype. These colonies were identified, because they were not ts and grew at wild type rates. We therefore reasoned that colonies resulting from the other two spores must contain both the *sec65-1* and *scr1-Δ2* mutations. Presence of *scr1-Δ2* was confirmed by the slow growth phenotype of the cells. Confirmation that these cells also contained the *sec65-1* mutation was achieved by transformation of the cells with a plasmid (pSCR1) bearing wild type *SCR1* resulting in the recovery of the ts phenotype as shown in Figure 1.

Table I **Yeast Strains**

Strain	Genotype	Source
RSY457	MATa *sec65-1, ura3-52, ade2-1, trp1-Δ1, leu2-3-112, his3*	Stirling et al. (1992)
W303-1A	MATa *ura3-1, ade2-1, trp1-1, leu2-3-112, his3-11 can1-100*	R. Rothstein, Columbia U.
CSY186	MATα *trp1, lys2, his3, ura3, ade2, sec65::HIS3*	Stirling and Hewitt (1992)
BHY104	MATα *trp1, lys2, his3, ura3, ade2, srp54-Δ1,* (pGALSRP54)	Hann and Walter (1991)
BHY133	MATα *trp1, lys2, his3, ura3, ade2, scr1::HIS3* [rho-]	Brown et al. (1994)
SOY158	MATa *sec65-1 cyh2, ura3-52, ade2-1, trp1-Δ1, leu2-3-112, his3*	This Study
SOY288	MATα *sec65-1 scr1-Δ2, his3, ura3, trp1*	This Study
5114-2	MATα *leu2-3-112, ura3-52, trp1-289, his7, hom3, can1, cyh2, gal1*	N. Hollingswort, SUNY, Stonybrook

Strain SOY158, containing both *sec65-1* and *cyh2* mutations was constructed in the following manner: RSY457 cells were plated onto YEPD plates containing 10 mg/ml of cycloheximide . From approximately 10^8 cells, we recovered 3 cycloheximide -resistant colonies. One of these colonies was designated SOY158. That the cycloheximide -resistant phenotype resulted from a mutation at the *CYH2* locus was confirmed by crossing strains SOY158 and 5114-2. The resulting diploid was able to grow on cycloheximide plates, indicating that whatever mutation had occurred did not complement the *cyh2* mutation of 5114-2. Colonies resulting from the sporulation and subsequent tetrad dissection (20 tetrads analyzed) of the diploid strain SOY158 x 5114-2 were all resistant to high concentrations of cycloheximide.

Sequencing of the sec65-1 allele

Plasmid pJDY32, was constructed by PCR using oligonucleotides complementary to bases -336 to -354 on the N-terminal end of the *SEC65* gene and +1051 to +1068 on the C-terminal side, and pCS52 as template DNA (Stirling and Hewitt, 1992). The PCR product was ligated into the *Sma* I site of pRS314 (Sikorski and Heiter, 1989). We recovered the *sec65-1* allele from RSY457 by gap repair (Orr-Weaver et al., 1988). Towards this end, pJDY32, containing the entire coding sequence of *SEC65*, as well as *TRP1*, *CEN* and *ARS* sequences, was digested with the restriction enzymes *Nhe*I and *Nde*I, which cut at two unique sites to remove a portion of the *SEC65* gene. The gap begins 63 nt upstream of the A of the initiating codon and continues through the last nucleotide of codon 207, removing a fragment that encodes 207 of the 273 amino acids of the *SEC65* gene. The resulting vector fragment was transformed into strain RSY457 (*sec65-1*). Eight Trp^+ colonies failed to grow at

37 °C, indicating that they were not able to complement the *sec65-1* temperature sensitive growth defect. Plasmids were isolated from two of these colonies, amplified in bacteria and shown to contain the entire *SEC65* gene. The plasmids were transformed into strain CSY186 (*sec65::HIS3*). Trp^+ transformants were tested for their ability to complement the growth defect of the deletion allele. Deletion of any of the components of the SRP pathway results in a 3- to 5-fold reduction in the growth rate of the cells containing the deletion. Two plasmids, pSO438-1 and pSO438-2, restored temperature sensitive growth to cells containing the *sec65* deletion (CSY186) but failed to complement the temperature sensitive growth of the original *sec65-1* mutation (RSY457). Thus, we concluded that the plasmids contain the mutation which causes the *sec65-1* temperature sensitive growth. Because the *sec65-1* allele had been repaired to a gapped plasmid, the mutation must occur within the boundaries of the gap. The DNA sequences of pSO438-1, pSO438-2, and pJDY32 were determined between these two restriction sites on both strands. Both pSO438-1 and pSO438-2 contained the same single base change when compared to the sequence of pJDY32. This difference was a C to T transition at position 795 of the coding strand. This occurs in the 2nd position of codon 152 and is predicted to change a Proline codon (C<u>C</u>A) in the wild type allele of *SEC65* to a Leucine codon (C<u>T</u>A) in the *sec65-1* mutant allele. Ethylmethanesulfonate, the mutagen used in the selection that yielded *sec65-1*, is known to produce this type of mutation.

Cell labeling and Immunoprecipitations

Radiolabeling and immunoprecipitations were performed as described in Ogg et al. 1992. The pulse chase experiment shown in Fig. 4 was performed by pulse labeling cells for 2 min at 30 °C with 60 μCi/OD_{600} Tran [^{35}S]-label (ICN Biomedicals, Costa Mesa, CA) followed by the addition of a 1000-fold molar excess of non-radiolabeled methionine, and cycloheximide at 0.4 μM to one of two aliquots. The tubes were incubated at 30 °C for the duration of the 32 minute chase period. Aliquots containing 5 OD_{600} cell equivalents were processed for immunoprecipitation at both the 0 and 32 minute time points. Following immunoprecipitation with anti-Kar2p antibodies, immunoprecipitated proteins were visualized and quantified by SDS-PAGE followed by analysis with a PhosphorImager (Molecular Dynamics, Sunnyvale, CA).

Quantitation of the rate of [^{35}S]-methionine incorporation was performed by labeling *sec65-1* cells for 200 s at 24 °C with 30 μCi/OD_{600} Tran [^{35}S]-label, in the presence of a 50-fold excess of non-radioactive methionine to prevent depletion of methionine during the experiment. Analysis of the media after removal of the cells confirmed that during the time course of this experiment, the external pool of [^{35}S]-methionine remained unchanged. A logarithmically growing culture of *sec65-1* cells was split into three portions, ANM (10 μM), and CHX (0.4 μM) were each added to a separate portion, while the third served as a control. These cultures were incubated at 24 °C for 10 min prior to initiating the labeling experiment. In addition, cells containing either wild-type *GCN2* or *GCN2^{C}-515* on a plasmid were subjected to the same analysis. At different time points, aliquots of cells were plunged into ice-cold 10% TCA and lysed immediately in the presence of 2/3 volumes of zirconium

beads (Biospec Products, Bartelseville, OK) using a benchtop vortex. The lysates were incubated at 100 °C for 10 min in 10% TCA to discharge any methionyl-tRNAs containing [^{35}S]-methionine. After TCA precipitation, proteins were solubilized in SDS sample buffer and subjected scintillation counting or SDS-PAGE analysis.

Growth of cells on cycloheximide and anisomycin

Sterile filter disks containing 6 nmoles of cycloheximide in distilled water were placed on YEPD plates. In liquid culture, YEPD was supplemented with the indicated concentration of cycloheximide or anisomycin . Cycloheximide was prepared as a 100 mM stock solution in distilled water and sterilized by passage through a 0.2 micron filter. Anisomycin was prepared in a similar manner as a 7.5 mM stock solution in 70% ethanol.

ACKNOWLEDGMENTS

We thank the members of the laboratory for critical reading of the manuscript, and Jeff Cox and Jeremy Brown for kindly providing the plasmids pSCR1, and pJDY32 respectively. We thank Tom Stevens, Joe Vogel, Mark Rose, and Nancy Hollingsworth for strains and antibodies. We also thank David Feldheim and Randy Schekman for communicating the initial observation on which this work is based. This work was supported by an HHMI predoctoral fellowship to S.C.O. and grants from the NIH to P.W.

REFERENCES

Arnold, C. E., and Wittrup, K. D. (1994). The stress response to loss of signal recognition particle function in *S. cerevisiae*. J. Biol. Chem. *269*, 30412-8.

Brown, J. D., Hann, B. C., Medzihradszky, K. F., Niwa, M., Burlingame, A. L., and Walter, P. (1994). Subunits of the *Saccharomyces cerevisiae* signal recognition particle required for its functional expression. EMBO J. *13*, 4390-4400.

Brown, S. (1987). Mutations in the gene for EF-G reduce the requirement for 4.5S RNA in the growth of *E. coli*. Cell *49*, 825-33.

Brown, S. (1989). Time of action of 4.5 S RNA in Escherichia coli translation. J. Mol. Biol. *209*, 79-90.

Brown, S., and Fournier, M. J. (1984). The 4.5S RNA Gene of *Escherichia coli* is Essential for Cell Growth. J. Mol. Biol. *178*, 533-550.

Connolly, T., Rapiejko, P. J., and Gilmore, R. (1991). Requirement of GTP Hydrolysis for Dissociation of the Signal Recognition Particle from Its Receptor. Science *252*, 1171-3.

Dever, T. E., Feng, L., Wek, R. C., Cigan, A. M., Donahue, T. F., and Hinnebusch, A. G. (1992). Phosphorylation of Initiation Factor 2α by protein kinase *GCN2* mediates gene-specific translational control of *GCN4* in yeast. Cell *68*, 585-596.

Gale, E. F., Cundliffe, E., Reynolds, P. E., Richmond, M. H., and Waring, M. J. (1981). The Molecular Basis of Antibiotic Action, 2nd Edition (London: J. Wiley & Sons).

Hann, B., Stirling, C., J., and Walter, P. (1992). *SEC65* gene product is a subunit of the yeast signal recognition particle required for its integrity. Nature *356*, 532-533.

Hann, B. C., Poritz, M. A., and Walter, P. (1989). Saccharomyces cerevisiae and Schizosaccharomyces pombe Contain a Homologue to the 54-kD Subunit of The Signal Recognition Particle That in *S. cerevisiae* Is Essential for Growth. J. Cell Biol. *109*, 3223-3230.

Hann, B. C., and Walter, P. (1991). The Signal Recognition Particle in *S. cerevisiae*. Cell *67*, 131-144.

Hansen, W., Garcia, P. D., and Walter, P. (1986). In vitro protein translocation across the yeast endoplasmic reticulum: ATP-dependent post-translational translocation of the prepro-α factor. Cell *45*, 397-406.

Jensen, C. G., and Pedersen, S. (1994). Concentrations of 4.5S RNA and Ffh protein in *Escherchia coli*: the stability of Ffh protein is dependent on the concentraion of 4.5S RNA. J. Bact. *176*, 7148-7154.

Miller, J. D., Wilhelm, H., Gierasch, L., Gilmore, R., and Walter, P. (1993). GTP binding and hydrolysis by the signal recognition particle during initiation of protein translocation. Nature *366*, 351-354.

Moazed, D., and Noller, H. F. (1989). Intermediate states in the movement of transfer RNA in the ribosome. Nature *342*, 142-148.

Ogg, S., Poritz, M., and Walter, P. (1992). The signal recognition particle receptor is important for growth and protein secretion in *Saccharomyces cerevisiae*. Mol. Biol. Cell *3*, 895-911.

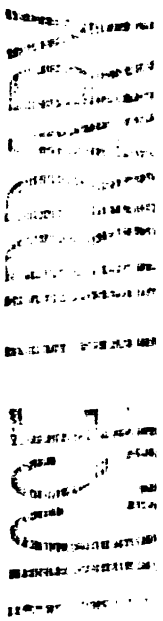

Orr-Weaver, T. L., Nicolas, A., and Szostak, J. W. (1988). Gene conversion adjacent to regions of double-strand break repair. Mol. Cell. Biol. *8*, 5292-5298.

Phillips, G. J., and Silhavy, T. J. (1992). The *E. coli ffh* gene is necessary for viability and efficient protein export. Nature *359*, 744-746.

Rothblatt, J. A., and Meyer, D. I. (1986). Secretion in yeast: Translocation and glycosylation of prepro-α factor in vitro can occur via ATP-dependent post-translational mechanism. EMBO J. *5*, 1031-1036.

Siegel, V., and Walter, P. (1988). The affinity of signal recognition particle for presecretory proteins is dependent on nascent chain length. EMBO J. *7*, 1769-1775.

Stirling, C. J., and Hewitt, E. W. (1992). The *Saccharomyces cerevisiae SEC65* gene encodes a component of the yeast signal recognition particle with homology to human SRP19. Nature *356*, 534-537.

Stirling, C. J., Rothblatt, J., Hosobuchi, M., Deshaies, R., and Schekman, R. (1992). Protein translocation mutants defective in the insertion of integral membrane proteins into the endoplasmic reticulum. Mol. Biol. Cell *3*, 129-142.

Stöcklein, W., and Piepersberg, W. (1980). Altered ribosomal protein L29 in a cycloheximide-resistant strain of *Saccharomyces cerevisiae*. Curr. Gen. *1*, 177-183.

Walter, P., and Johnson, A. E. (1994). Signal Sequence Recognition and Protein Targeting to the Endoplasmic Reticulum Membrane. Ann. Rev. Cell Biol.*10*, 87-119.

Waters, G., and Blobel, G. (1986). Secretory protein translocation in a yeast cell free system can occur post-translationally and requires ATP hydrolysis. J. Cell Biol. *102*, 1543-1550.

Wolin, S. L. (1994). From the elephant to *E. coli*: SRP-dependent protein targeting. Cell *77*, 787-790.

Wolin, S. L., and Walter, P. (1989). Signal recognition particle mediates a transient elongation arrest of preprolactin in reticulocyte lysate. J. Cell Biol. *109*, 2617-2622.

Chapter 5

Maternal Inheritance of Signal Recognition Particle Receptor Required for its Continued Function

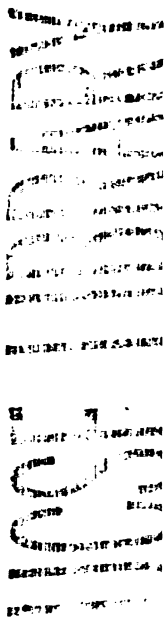

ABSTRACT

Yeast strains deleted for SR components display the characteristic reduced growth rate of SRP gene deletions in yeast. Transformation of a haploid strain with a plasmid containing the wildtype gene for which the strain was deleted, however, does not result in an increase in the growth defect. Transformation of the same plasmid into a diploid strain that is heterozygous for an SR gene deletion followed by meiosis of the strain and tetrad analysis results in a different answer–the growth rate of the haploid deletion that has also inherited the plasmid remains wildtype. Thus, the plasmid contains all the sequences necessary for functional complementation. In contrast, the reduced growth rate of a haploid SRP deletion strain can be directly compensated by transformation with a plasmid containing the wildtype SRP gene. We term this inability of the SR deletion strains to be complemented "[srf$^-$]" for loss of SRP receptor function, and show that it is inherited in a non-Mendelian fashion. Both subunits of the SR display this unusual phenotype. Unexpectedly, strains that are [srf$^-$] still express and correctly localize plasmid expressed SR protein, although this protein fails to increase the growth rate of the [srf$^-$] strain. Further, protein expressed from a plasmid is capable of forming a stable SR complex composed of both Srp101p and Srp102p. This complex is indistinguishable from the wildtype complex. Cells rarely switch from [srf$^-$] to [srf$^+$], we estimate the frequency to be less than 1 in 10^6. Interestingly, the transfer of cytosol from a [srf$^+$] strain to a [srf$^-$] strain in a setting that prevents nuclear (and presumably ER) fusion also fails to increase the growth rate of the [srf$^-$] cells.

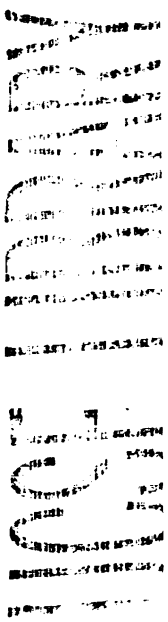

INTRODUCTION

A cell's ability to live is compromised if the cell is unable to define and continuously maintain its boundaries. So far, we have examined one means– the SRP dependent translocation pathway into the ER membrane– that the cell uses to maintain order. From mammalian in vitro studies, the signal recognition particle (SRP) and SRP receptor (SR) have been identified as required components for the targeting of nascent proteins to the membrane of the endoplasmic reticulum (ER) membrane (for review see Walter and Johnson, 1994). Briefly, SRP binds to those ribosomes synthesizing nascent proteins destined for entry into the secretory pathway. This binding prevents further translation of the nascent protein until SRP can target the ribosome-nascent chain complex to the ER membrane by virtue of an interaction between SRP and its membrane bound receptor, the SRP receptor. Once targeting has occurred, the ribosome/nascent chain complex dissociates from the SRP/SR complex and is recruited into a translocon (assembly of membrane components required to translocate the nascent protein into the lumen of the ER). After delivering the ribosome-nascent chain complex to the translocon, in a reaction that is dependent on GTP, the SRP/SR complex dissociates into its constituents, thereby restoring SRP and SR to their proper states to initiate another round of targeting.

This pathway is conserved in the yeast *Saccharomyces cerevisiae*, and subunits of the yeast SRP homologue as well as the SR homologue have recently been identified and cloned (see Chapters 2, 3, and Hann and Walter, 1991; Brown et al., 1994). Mammalian SR was originally purified by its affinity for SRP, and consists of an ER membrane protein containing two subunits

(SRα; 69 kDa, and SRβ; 30 kDa) (Tajima et al., 1986). A PCR-based approach allowed us to isolate *SRP101*, the gene encoding the yeast SRα homologue (Ogg et al., 1992), while information from the yeast genome sequencing project allowed us to identify and subsequently characterize *SRP102*, the gene encoding the yeast SRβ homologue (chapter three). Both subunits have been localized to the ER membrane, and have been shown to form a heterodimer in yeast (chapter 3). SRβ contains a 19 a.a. hydrophobic stretch predicted to span the membrane near its amino terminus, and is required for SRα's association with the membrane.

This chapter diverges from further characterization of the SRP pathway in *Saccharomyces cerevisiae*. In this Chapter, I describe a genetic phenomenon unique to the signal recognition particle receptor (SR). I pursued the observation that the compromised growth rate of a haploid strain deleted for SRα could not be augmented by transformation with a plasmid containing the wildtype SRα gene. I show here that this phenotype is specific for the SR, and is inherited in a non-Mendelian fashion. In addition, I demonstrate that the inability to complement is not due to a plasmid defect or a defect in the expression or localization of the SR subunits. We hypothesize that preexisting SR is required for the activation of newly made SR. That is, functional SR must be extant in the membrane for newly synthesized SR to become functional in the membrane. I believe that this phenomenon is providing information to us about the ability of a cell's ER membrane to be properly maintained in a spatial and temporal fashion.

MATERIALS AND METHODS

Strains, Plasmids, Antibodies and General Methods

Yeast strains used in this study are listed in Table 1. Genetic techniques were performed as described except where noted (Sherman and Lawrence, 1974). Recombinant DNA techniques were performed as described (Sambrook et al., 1989). SDS-PAGE was performed on 10-15% gradient gels, and Western blots were visualized by enhanced chemiluminescence ("ECL", Amersham Corporation, Arlington Heights, Ill) according to the instructions of the manufacturer. Plasmid rescue into *E. coli* was performed according to Guthrie and Fink (1991).

Growth rate Calculations

To calculate the growth rates of strains depicted in Figures 1 and 2, a fresh culture was started at time zero. This culture was inoculated with previously grown stationary phase cultures to an OD_{600} of less than 0.1 OD_{600} per milliliter. The OD_{600} was monitored as a function of time. To include only data from the exponential portion of the growth of each of the cultures, the OD was never allowed to exceed 0.7 OD_{600}. The data were plotted on a semi-log plot and the slope of the best fit least squares regression line through the data was taken as a measure of the growth rate of the culture.

Cell Fractionation and Immunoprecipitation

Subcellular fractionation and coimmunoprecipitation are performed as in Chapter 3.

Switch Estimate

Given that the wildtype doubling time is approximately 2 hours, and that the [srf⁻] cells grow 5 times slower than wildtype cells, a single mutant cell will take ~50 hours to become 50% of the population of the culture. If a single cell mutated to wild type growth rate out of the 10^6 initially inoculated into the culture, then calculating the amount of time needed for the progeny of this cell to populate 50% of the culture is a matter of solving the following two simultaneous equations ((2) and (3)). The doubling time of a culture is given by:

(1) $$\text{doubling time} = \frac{\ln 2 \ (\text{time difference})}{\ln\left(\frac{\#\text{ of cells at time 2}}{\#\text{ of cells at time 1}}\right)}$$

for each population of cells we can substitute the known factors into equation (1) to give

for the 1 newly mutant cell, with a wildtype growth rate:

(2) $$2 = \frac{\ln 2(\text{time difference})}{\ln\left(\frac{1/2 \text{ of the } \#\text{ of cells at time 2}}{1}\right)}$$

(3) for the 10^6 [srf⁻] cells $$10 = \frac{\ln 2(\text{time difference})}{\ln\left(\frac{1/2 \text{ of the } \#\text{ of cells at time 2}}{10^6}\right)}$$

Because the two populations exist in the same culture, we know that the lifetime (or time difference) of the culture will be equal, and we have set the "# of cells at time 2" to be equal. Solving equation (2) for the "time difference" gives us

(4) $$\text{time difference} = 2.885 \ln(1/2 \text{ of the } \#\text{ of cells at time2})$$

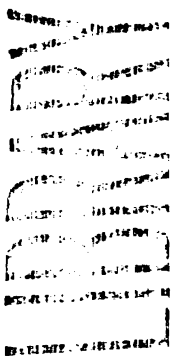

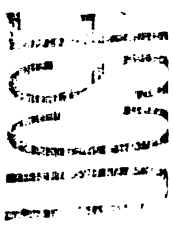

and substituting this expression for "time difference" into equation (3) gives

$$10 = \frac{\ln 2\left(2.885 \ln\left(1/2 \text{ of the \# of cells at time 2}\right)\right)}{\left(\frac{1/2 \text{ of the \# of cells at time 2}}{10^6}\right)} \quad (5)$$

We can now solve this equation for the expression "1/2 of the # of cells at time 2" which gives

$$1/2 \text{ of the \# of cells at time 2} = 3.16 \times 10^7 \text{ cells} \quad (6)$$

Substituting 3.16×10^7 back into (4) for "1/2 of the # of cells at time 2" allows us to solve for the amount of time that we need to grow the culture before plating out a portion to check the growth rate of individual cells.

$$\text{time difference} = 2.885 \ln(3.16 \times 10^7) \quad (7)$$

$$\text{time difference} = 49.8 \text{ hours} \quad (8)$$

Thus, if a mutation occurred just after diluting the cells into fresh media, it would take 49.8 hours of exponential growth in order to populate 50% of the culture with cells growing at the wildtype rate. While growing the cells for this experiment, fresh media was added to keep the OD_{600} below 1.0 OD_{600} per milliliter, and thus keep the cells growing exponentially.

Cytoduction

Isogenic [srf$^-$] strain SOY324 and [srf$^+$] strains SOY100 were transformed with a fragment from pMR868 (a kind gift of Dr. Mark Rose, Princeton University) to Leu$^+$ prototrophy, giving rise to [srf$^-$] strain SOY327, and [srf$^+$] strain SOY328, respectively. Additionally W303-1B was also transformed to Leu+ with this fragment, giving rise to strain SOY326. This fragment contains *LEU2* flanked by the 5′ and 3′ flanking sequences of *KAR3*, required

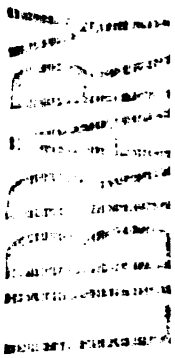

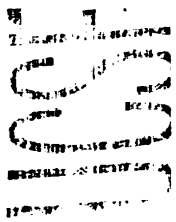

for karyogamy. Strains containing the *kar3::LEU2* gene disruption form diploids at a much reduced rate compared to the wildtype. Disruption of the *KAR3* gene in these strains was confirmed by the fact that matings between these strains produced no diploids. Strain SOY328 was further converted to [rho$^-$] by growth on ethidium bromide (Guthrie and Fink, 1991). Of the colonies that grew after mating, eight (of eight tested) were shown to be haploid based on their inability to sporulate, and their ability to mate with a partner containing a wildtype *KAR3* allele. Cytoductants were selected on casamino acid plates supplemented with tryptophan (operationally, these are Ade$^-$, Ura$^-$), and containing ethanol and glycerol as the carbon source. Growth on these plates required the cytosol from the [rho+] strain to have transferred to the [srf$^-$] (and therefore [rho$^-$]) strain, in order for the cell to grow on ethanol and glycerol, and it also required the nucleus (and plasmid) from the [srf$^-$] strain in order to grow in the absence of adenine and uracil.

RESULTS

In previous work (see Chapter 2) we demonstrated that a plasmid bearing the *SRP101* gene (pSO211) was functional in vivo, and that this plasmid contained all the necessary information to restore wildtype growth to cells that contained the *SRP101* gene deletion (Ogg, et al., 1992). To show this, we transformed pSO211 (*URA3*, *SRP101*) into diploid strain SOY34, heterozygous for the *SRP101* gene deletion. Following meiosis and tetrad analysis, we recovered haploid cells that contained both the deletion marker (*ADE2*) and the marker for the complementing plasmid (*URA3*). Colonies arising from these cells grew at the rate characteristic of wild type cells (the *SRP101* deletion phenotype is slow growth, see chapter 2, Fig. 5). Every spore which gave rise to a colony growing at wild type rates and containing the

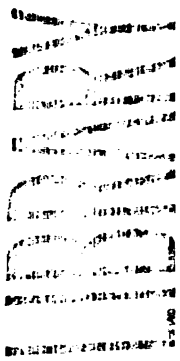

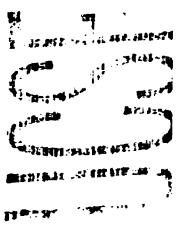

Figure 1

SRP pathway knockouts show differential effects upon reintroduction of a plasmid bearing the wildtype gene. (A) Growth rates of strains derived from each of the four spores of a single tetrad from strain SOY34 bearing pSO211. The top panel shows the growth rates of the four strains in which each spore has inherited pSO211. The growth rates of the same four strains after selection on 5-FOA for the loss of plasmid pSO211 is shown in the middle panel. The two spores which have inherited the *srp101::ADE2* gene disruption, now grow with a much reduced growth rate. Upon retransformation with pSO211, the growth rates of the four strains are shown in the bottom panel. The growth rates of the two gene disruption strains are only modestly increased. The growth rates are calculated from cultures grown at 30 °C in YEPD, and are shown in doublings per hour. **(B)** A similar analysis as in (A), for the *SRP54* gene. Again the top panel shows the growth rates of cultures derived from the four spores after dissection of WBY6 containing plasmid pSRP54SC. Selection for cells which have lost plasmid pSRP54SC on 5-FOA results in strains having the growth curves shown in the middle panel. We see again the slow growth characteristic in cells deleted for an SRP component in those strains which have received the gene deletion during meiosis. In contrast to (A), upon reintroduction of pSRP54SC, cultures deleted for *SRP54*, revert back to a near wildtype growth rates (lower panel). The modest reduction is due to the fact that the cells are rho^- after being SRP^-.

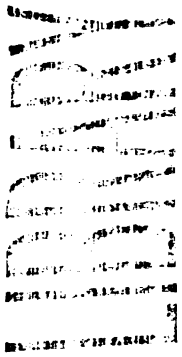

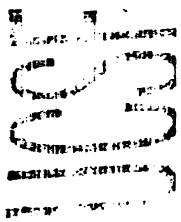

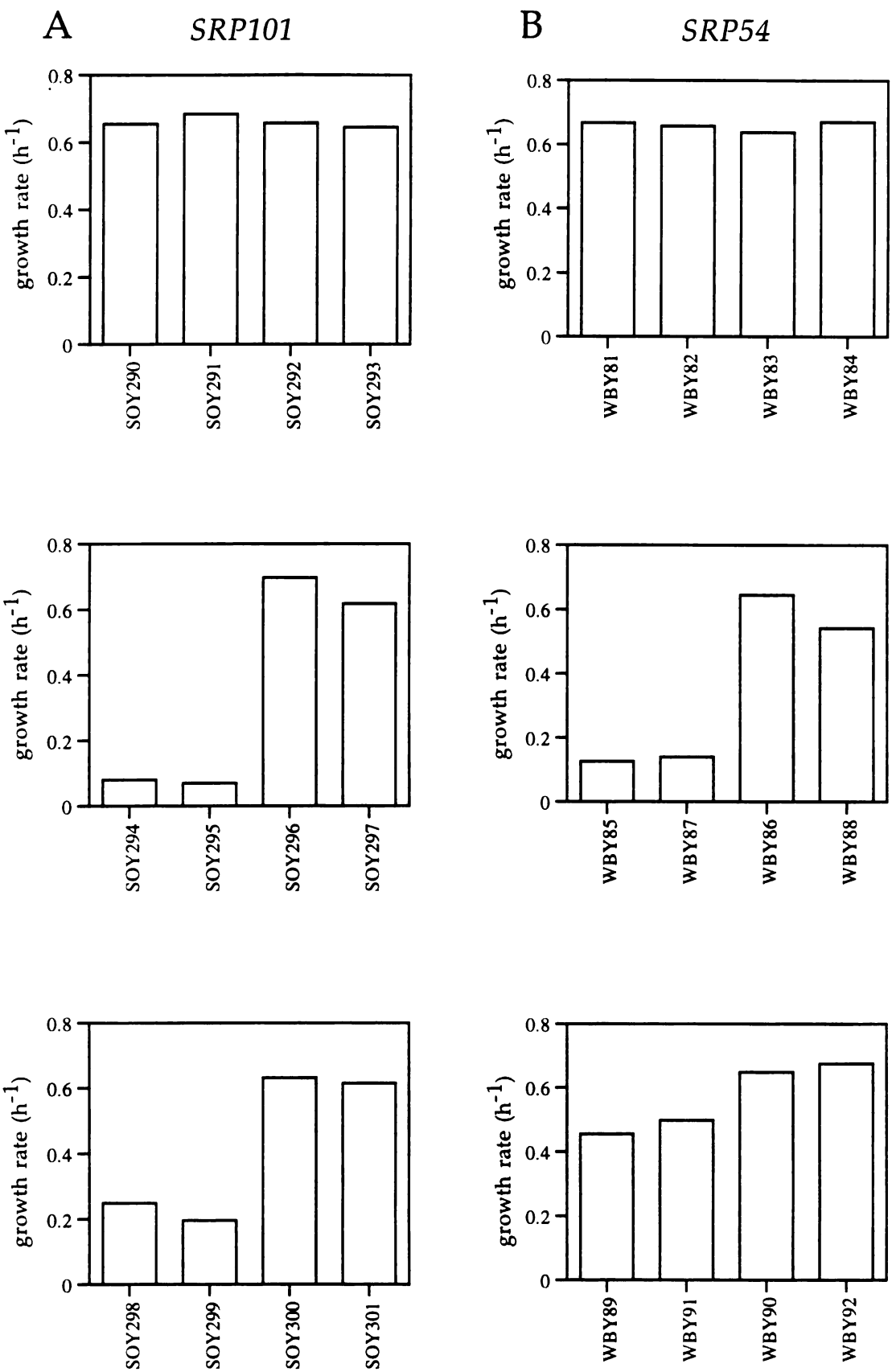
A
SRP101
B
SRP54
growth rate (h-1)
0.8
0.6
0.4
0.2
0
SOY290
SOY291
SOY292
SOY293
WBY81
WBY82
WBY83
WBY84
SOY294
SOY295
SOY296
SOY297
WBY85
WBY87
WBY86
WBY88
SOY298
SOY299
SOY300
SOY301
WBY89
WBY91
WBY90
WBY92

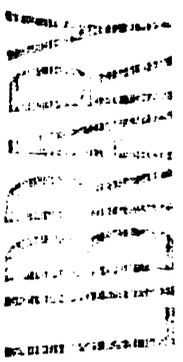

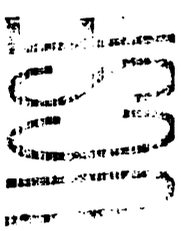

SRP101 gene deletion also contained the plasmid bearing the wildtype copy of *SRP101* (pSO211). From these data, we concluded that pSO211 contained all the necessary information for *SRP101* function in vivo. We were thus surprised, when the same plasmid pSO211, bearing the wildtype *SRP101* gene, was transformed into haploid strain SOY36 (containing the *SRP101* gene deletion), and transformants grew at the characteristic rate of the *SRP101* deletion strain (SOY36).

To document this phenomenon, and extend the result, we returned to strain SOY34 (*SRP101/srp101::ADE2*) containing plasmid pSO211. Tetrad analysis of the colonies arising after sporulation and tetrad dissection again gave similar results to those previously published (Ogg et al., 1992). Every spore that contained the marker for the *SRP101* gene disruption (*ADE2*), and growing at wildtype rates also contained the plasmid (pSO211). Figure 1A (top panel) shows the growth rates of each colony from a representative tetrad derived from such an analysis. Each of the four spores grew at roughly equivalent rates, similar to each of the haploid parent strains (W303-1A, and W303-1B, see (Ogg, et al., 1992)). Two of the four strains were Ade^+, indicating that these colonies arose from the spores that had inherited the *SRP101* gene deletion during meiosis. In addition, in this particular case, each of the four spores is also Ura^+, confirming that each of the spores had also received pSO211. We conclude therefore, that plasmid pSO211 is capable of expressing functional Srp101p and that the presence of this plasmid prevents the slow growth phenotype of cells bearing the *SRP101* gene deletion.

Each of the four strains in top panel of figure 1A was cured of pSO211 by growth on media containing 5-fluoroorotic acid (5-FOA). Only those cells that have lost pSO211 and are therefore Ura^- will propagate. This treatment

gives rise to the four strains shown in the middle panel of figure 1A. These strains are genotypically identical to those in figure 1A, except that they do not carry pSO211. Two of these strains continue to grow at wildtype rates, while the other two have dramatically reduced growth rates. As expected, the two strains that grow slowly after loss of pSO211 also contain the *SRP101* gene deletion (i.e., they are Ade$^+$). This result is consistent with the notion that Srp101p is important for normal cell growth. Removal of pSO211 has resulted in the cells' inability to maintain the growth rate observed for wildtype cells. We use this difference in growth rate as a measure of whether or not the strain contains functional SRP receptor. Because strains that contain gene deletions in both *SRP54* and *SRP102* grow at the same rate as strains containing either gene deletion alone, we conclude that the impaired growth rate of gene deletions in SR components is directly due to the loss of SR function.

Reintroduction of pSO211 into each of the four strains in the middle panel of figure 1A gave rise to the four strains used in the bottom panel of figure 1A. These four strains are genotypically identical to the four strains shown in the top panel of figure 1A. Surprisingly, the growth rate of the two strains bearing the *SRP101* gene deletion is only slightly enhanced by the presence of pSO211. In addition, we observed that the growth rates of haploid cells bearing the *SRP101* gene deletion and transformed with an *SRP101* containing plasmid varied considerably among individual isolates. In some isolates (see Figure 2 for the variability) the growth rate was unchanged upon reintroduction of the plasmid, in others, we saw an increase in growth rate to approximately 1/4 to 1/3 or even 1/2 of that seen in [srf$^+$] cells. From this result, we conclude that pSO211 cannot complement the gene

deletion when introduced into the haploid *SRP101* deletion bearing strain (SOY36). This completely unexpected result suggests that reintroduction of *SRP101* after the cells have expressed the *SRP101* phenotype (i.e., they obtain a slow growth rate) can only partially restore the growth rates of these cells to wildtype rates. We refer to this phenotype as [srf$^-$] for SRP receptor function. Cells containing the *SRP101* gene deletion and growing slowly are [srf$^-$] while cells that contain the *SRP101* gene deletion, but are growing with wildtype rates are [srf$^+$]. Because it is inherited in a non-Mendelian fashion (see below), we denote this phenotype in square brackets.

We were curious about this phenotype due to the fact that a similar analysis using the gene for one of the SRP subunits, *SRP54*, gave a different result. The impaired growth rate of a haploid strain bearing the *SRP54* gene deletion could be abrogated by reintroduction of a plasmid containing the wildtype *SRP54* gene (figure 1B). In an analogous manner to the analysis in figure 1A, strain WBY6, heterozygous for the *SRP54* gene deletion and containing plasmid pSRP54SC, was sporulated and the resulting tetrads were subjected to growth rate analysis. In cases where all four of the haploid spores inherited the pSRP54SC, all four resulting strains grew with wildtype rates (Figure 1B, top panel). Again, only one representative tetrad is shown for clarity. Once again, we used media containing 5-FOA to obtain plasmid free strains and in each case, strains that contained the *SRP54* deletion, converted to the slow growth rate typical of SRP gene deletions (Figure 1B, middle panel). Unlike our results in Figure 1A, reintroduction of pSRP54SC changed the slow growth rate of the *srp54Δ* cells into a growth rate that resembled wild type growth rate (Figure 1B, bottom panel). The growth rate returns to about 85% of the rate for wild type cells. One consequence of an SRP component

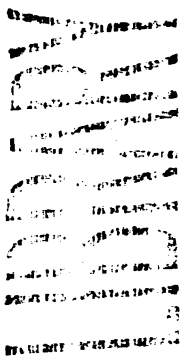

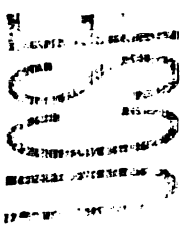

Table II

The [srf] phenotype is inherited in a non-Mendelian manner. After backcrossing the [srf$^-$] strain SOY324 to W303-1A, diploids were selected and forced to undergo meiosis. Tetrad analysis revealed four types of spores. Type I had inherited a wildtype *SRP102* gene and plasmid pSO459 (phenotypically Ade$^-$, Ura$^+$). Type II had also inherited the wildtype *SRP102* gene, but had not received plasmid pSO459 during meiosis (phenotypically Ade$^-$, Ura$^-$). Type III had inherited the *srp102::HIS3* gene disruption, and pSO459 (phenotypically Ade$^+$, Ura$^+$), while type IV had also inherited the gene disruption, but not the plasmid (phenotypically Ade$^+$, Ura$^-$). Importantly, in all cases where the disruption was inherited along with pSO459 (type IIII), the cells grew with near wildtype rates. In spores of type IV, however, growing in the absence of the plasmid, the growth rate was the characteristic *SRP101* null phenotype (slow). In this table, I have inferred growth rate from colony size. Upon inspection of the tetrad dissection plates, big colonies were scored as having a fast growth rate and small colonies as having a slow growth rate.

Table II **[srf] is inherited in a non-Mendelian manner**

Cross	Growth of Diploid	# of tetrads with the following growth characteristics (fast : slow)			Of spores that contain srp101::ADE2, which also contain the plasmid pSO459, and what are their growth characteristics	
SOY324 [srf$^-$] X W303-1A (N=30)	wt	4:0	10	(33%)	36	Ura$^+$ and grow quickly
		3:1	13	(43%)	0	Ura$^+$ and grow slowly
		2:2	7	(23%)	0	Ura$^-$ and grow quickly
					24	Ura$^-$ and grow slowly
SOY100 [srf$^+$] X W303-1A (N=18)	wt	4:0	7	(39%)	22	Ura$^+$ and grow quickly
		3:1	8	(44%)	0	Ura$^+$ and grow slowly
		2:2	3	(17%)	0	Ura$^-$ and grow quickly
					14	Ura$^-$ and grow slowly

deletion is that the cells become rho$^-$ and therefore grow slightly slower on media containing glucose as the carbon source than an otherwise isogenic but rho$^+$ strain (Ogg, et al., 1992; Hann and Walter, 1991). The rho$^-$ phenotype is due to loss of the ability of the cells to respire and, therefore, would not be expected to be complemented by the pSRP54SC.

To show that the [srf$^-$] phenotype is inherited in a non-Mendelian fashion, we crossed two genotypically identical strains (one [srf$^-$] and one [srf$^+$]) back to the wildtype parent strain (W303-1A). Each of the resulting diploid strains grew with a wildtype rate (indicated by a "wt" in Table II), verifying that the [srf$^-$] phenotype is recessive to the wildtype. Sporulation of these diploids, now heterozygous for the *SRP101* gene deletion and containing pSO211, resulted in similar segregation pattern of the gene deletion and growth rates, independent of whether the original haploid *SRP101* gene deletion, from which the diploid was derived, had come from a [srf$^-$] or [srf$^+$] strain. When all four spores of a single tetrad inherit the plasmid (pSO211), each spore grows with wildtype rates (Table II, both [srf$^-$] and [srf$^+$]). The plasmid is still required to promote wildtype growth, because spores that inherit the gene deletion without a complementing plasmid grow with the characteristic [srf$^-$] rate, and every spore that inherited the *SRP101* gene deletion and that grew with wildtype growth rate, also contained pSO211. These results suggest that although one of the two haploids contributing to the diploid was [srf$^-$] (i. e., was slow growing), there is no genetic memory of this phenotype. Once the cell is [srf$^+$], the phenotype can be complemented by the plasmid. Thus the [srf$^-$] phenotype is inherited in a non-Mendelian fashion.

Figure 2

SRβ shares the [srf⁻] phenotype with SRα. The growth rates of eight independent isolates carrying the *srp102::HIS3* gene disruption were measured before (white bars) and after transformation with either a vector (pRS314, striped bars) alone or a plasmid containing the wildtype *SRP102* gene (pSO459, black bars). For comparison, the growth rate of a wildtype strain is shown (stippled bar). Growth rates are calculated for cultures grown at 30 °C in minimal complete media (gene disruption alone, and wildtype control), or minimal media lacking uracil (selecting for either pRS314, or pSO459).

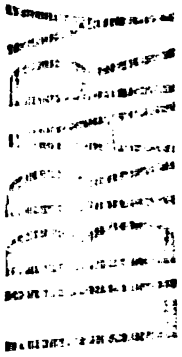

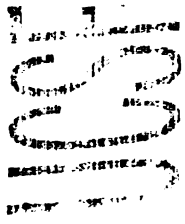

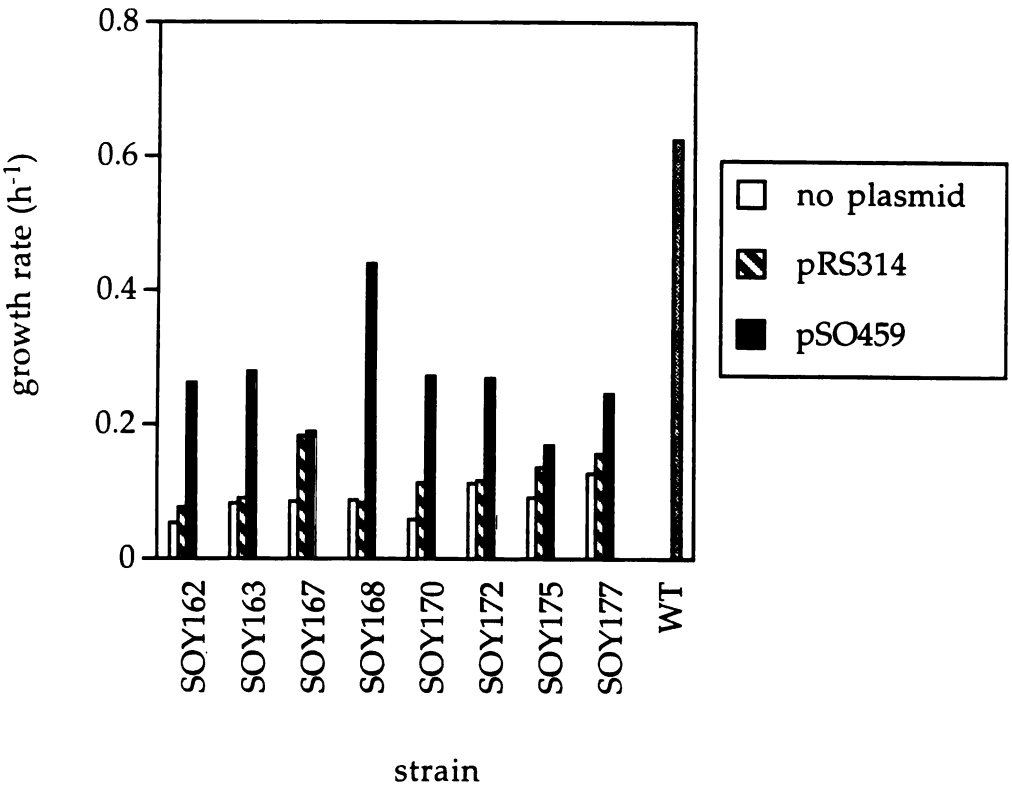
0.8
0.6
0.4
0.2
0
growth rate (h^{-1})
no plasmid
pRS314
pSO459
SOY162
SOY163
SOY167
SOY168
SOY170
SOY172
SOY175
SOY177
WT
strain

We next asked whether SRβ, the other subunit of the SRP receptor, encoded in yeast by the *SRP102* gene (see Chapter 3) would also exhibit the [srf⁻] phenotype. Instead of tetrad analysis as in figure 1, we started with eight haploid strains bearing the *SRP102* gene deletion (*srp102::HIS3*). These eight strains are derived from tetrad dissection following meiosis of strain SOY134, heterozygous for the SRP102 gene deletion. Each of the strains grows slowly (Figure 2, white bars). The growth rates of transformants of each of these strains with either pRS314 (*CEN, TRP1*) (Figure 2, striped bars) or pSO459 (*CEN, TRP1, SRP102*) (Figure 2, black bars) suggests that the [srf⁻] phenotype is shared by both known components of the SRP receptor. Although the growth rates are enhanced due to introduction of pSO459, in some cases, an equal enhancement is shown upon introduction of pRS314. In no case does reintroduction of *SRP102* cause cells to grow as well as wildtype cells (Figure 2, stippled bar). From these data, in conjunction with those presented in figure 1, we conclude that the [srf⁻] phenotype is uniquely due to loss of the SRP receptor subunit genes. Because loss of SRP or SRP receptor components results in equal translocation defects, yet the loss of SRP components can be restored upon reintroduction of the deleted gene, we also conclude that the [srf⁻] phenotype seen due to the loss of SRP receptor function is not solely the result of impaired translocation in these cells.

We wanted to be sure that what we were observing was not due to some trivial explanation such as damaged plasmids or impaired expression of the protein from the plasmid. To show that the plasmid could function, even though the growth defect in [srf⁻] strains could not be complemented, we isolated plasmids from several [srf⁻] strains. Our goal was the reintroduction of these plasmids into diploid strains heterozygous for one or the other SRP

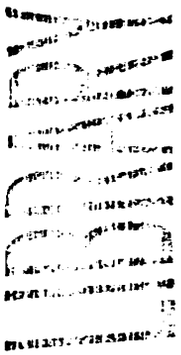

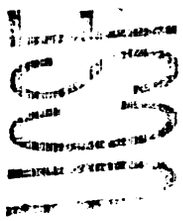

Table III

The plasmids in [srf–] strains are not defective. SR encoding plasmids were isolated from several [srf$^-$] or [srf$^+$] strains. Plasmids were rescued into *E. coli* and transformed from this stock into the heterozygous diploid disruption of the appropriate gene. In every case, and notably, when a plasmid was isolated from a [srf$^-$] strain, it could still functionally complement after rescue and transformation into the appropriate heterozygous diploid prior to meiosis.

Table III **SR encoding plasmids are not defective**

Plasmid encodes:	Plasmid isolated	from strain:	reintroduced into diploid strain:	plasmid can confer wildtype growth on spores receiving the deletion?
Srp101p (SRα)	pSO211	[srf+]	SOY34	+
Srp101p (SRα)	pSO211	[srf–]	SOY34	+
Srp101p (SRα)	pSO408	[srf–]	SOY34	+
Srp101p (SRα)	pSRP101(2μ)	[srf–]	SOY34	+
Srp101p (SRα)	pSO475	[srf–]	SOY34	+
Srp102p (SRβ)	pSO454	[srf+]	SOY134	+
Srp102p (SRβ)	pSO454	[srf–]	SOY134	+

receptor subunits. Tetrad analysis of the meiotic products from these diploids should then tell us whether the plasmids are capable of functional SRP receptor expression. Table III shows the results of several such experiments. From these results we conclude that the plasmid can be functional. In addition, these results rule out the possibility that pSO211 is unique in its inability to complement the SRP101 gene deletion, because we have isolated 4 different plasmids from the *srp101::ADE2* [srf$^-$] strains and one plasmid from a *srp102::HIS3* [srf$^-$] strain. As can be seen in Table III, any plasmid isolated from a [srf$^-$] strain could functionally complement the relevant gene deletion, if it was first transformed into the heterozygous diploid. In this manner, the complementing plasmid arrived in the haploid strain via meiosis rather than via direct transformation into the deletion strain. In every case, plasmids isolated from [srf$^-$] strains complemented with a similar frequency as those isolated from a [srf$^+$] strain. This suggests a simple model to explain the [srf$^-$] phenotype. Functional SR must be present to convert newly synthesized, but non-functional SR into functional SR (Figure 4).

Other simple explanations for the [srf$^-$] phenotype are that i.) reintroduction of the plasmid does not result in renewed expression of the SR protein, or ii.) new protein expressed from the reintroduced plasmid cannot be properly localized. We have previously used subcellular fractionation as a means to determine the cellular disposition of both Srp101p and Srp102p. In this case, we performed subcellular localization by differential fractionation on congenic pairs of strains deleted for the *SRP102* gene, one [srf$^+$] (SOY223), and the other [srf$^-$] (SOY319). The plasmid that is reintroduced contains *SRP102* with the well characterized "HA" epitope appended at its C-terminus to allow the expressed protein to be detected on a Western blot (see Chapter 3

Figure 3

SR is expressed, properly localized, and forms a complex in [srf⁻] strains. (A) Subcellular fractionation. Extracts from SOY223 [srf⁺] or SOY319 [srf⁻] were fractionated as detailed in Materials and Methods. Equivalent amounts (0.5 OD_{600}) of each fraction were analyzed by Western blot using anti-HA (against Srp102p-HA) monoclonal antibodies, or affinity purified anti-Srp101p antibodies. Lane 1, total cell lysate; lane 2, low-speed supernatant; lane 3, low-speed pellet; lanes 4 through 13 contain the supernatant (lanes 4, 6, 8, 10, and 12) or the pellet (lanes 5, 7, 9, 11, and 13) after a portion of the low speed supernatant was diluted with lysis buffer (lanes 4 and 5, mock) or adjusted to a final concentrations of 600 mM potassium acetate (lanes 6 and 7, KOAc), 1.6M urea (lanes 8 and 9, Urea), 0.5% Triton X-100 (lanes 10 and 11, TX-100), or 0.1 M Na_2CO_3 (lanes 12 and 13, pH 11.5) and centrifuged at 100,000 X g. Only the relevant portion of each blot is shown. The localization of both Srp101p and Srp102p was identical, independent of whether the fractionation was performed on a [srf⁻] or a [srf⁺] strain. **(B)** Coimmunoprecipitation. Crude microsomal membranes were prepared from SOY223 [srf⁺] (lanes 4-6) or SOY319 [srf⁻] (lanes 1-3) as described in the Materials and Methods. Detergent solubilized membranes were immunoprecipitated with anti-HA. Immunoprecipitated proteins were eluted from protein A sepharose beads, subjected to SDS-PAGE and analyzed by Western blot using affinity purified anti-Srp101p, or monoclonal anti-HA antibodies. Eluates from each of the immunoprecipitations are in lanes 3 and 6; supernatants are in lanes 2 and 5. Lanes 1 and 4 contain 2 OD_{600} cell equivalents of solubilized membranes from SOY223 (lane 4) or SOY319 (lane 1) as a marker for the amount of Srp101p and Srp102p that are in each of the starting material. SRα and SRβ are indicated

with arrows. Antibody chains that were eluted after immunoprecipitation, and detected by the secondary antibodies used during the Western blot are indicated with filled (IgG light chain) or open circles (IgG heavy chain).

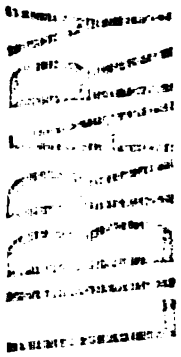

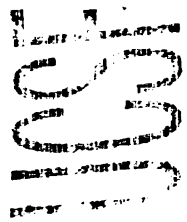

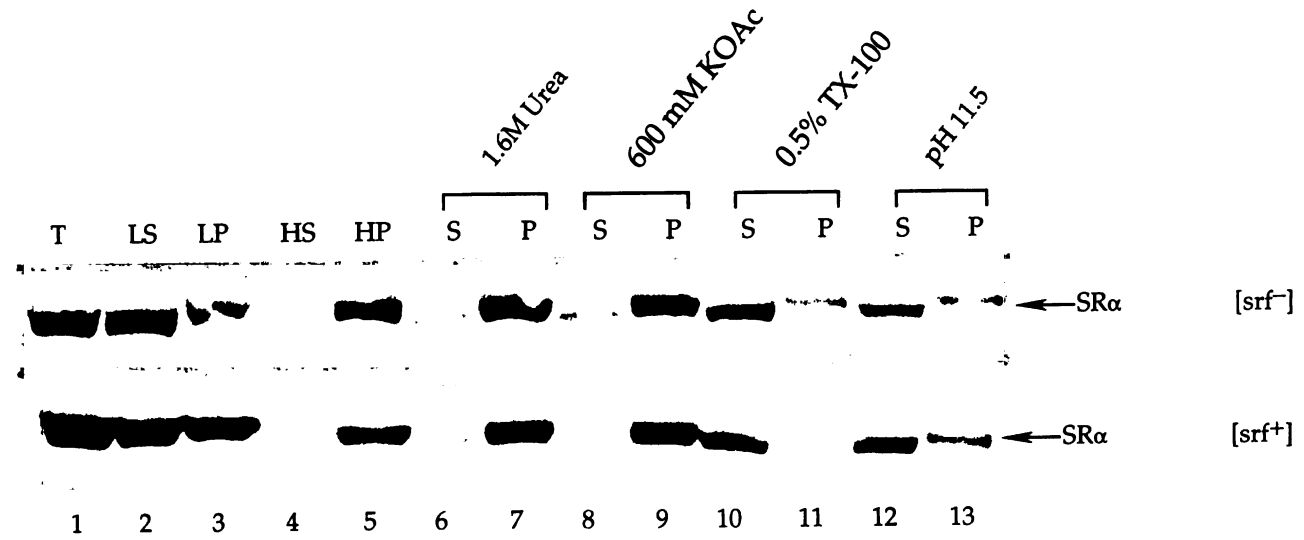
1.6M Urea
600 mM KOAc
0.5% TX-100
pH 11.5
T
LS
LP
HS
HP
S
P
SRα
[srf⁻]
[srf⁺]
1 2 3 4 5 6 7 8 9 10 11 12 13

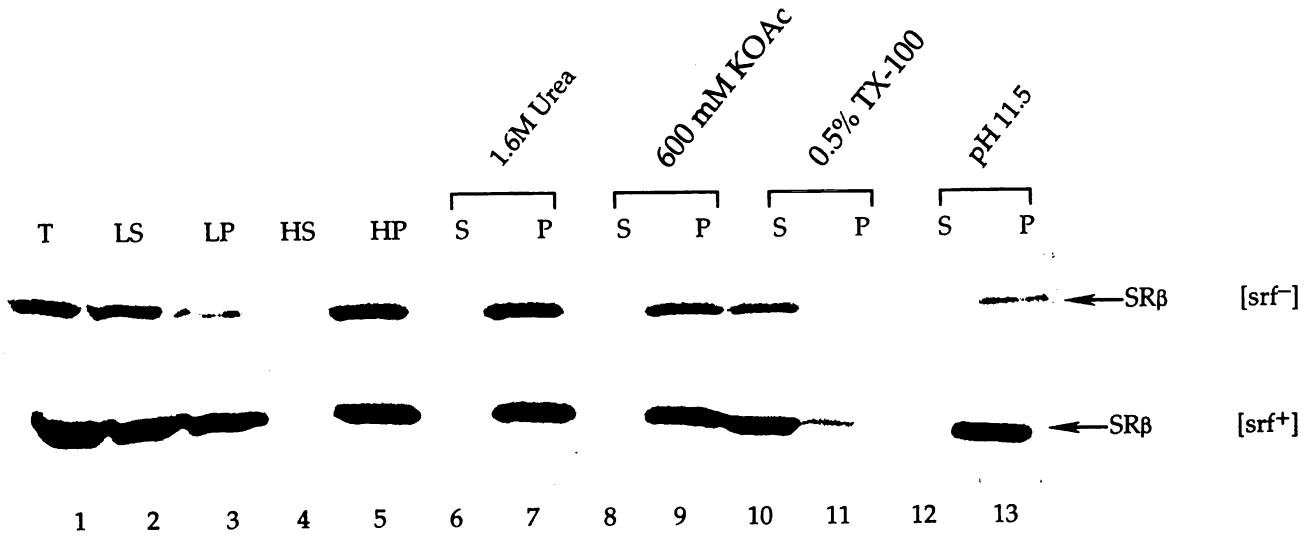
1.6M Urea
600 mM KOAc
0.5% TX-100
pH 11.5
T
LS
LP
HS
HP
S
P
SRβ
[srf⁻]
[srf⁺]
1 2 3 4 5 6 7 8 9 10 11 12 13

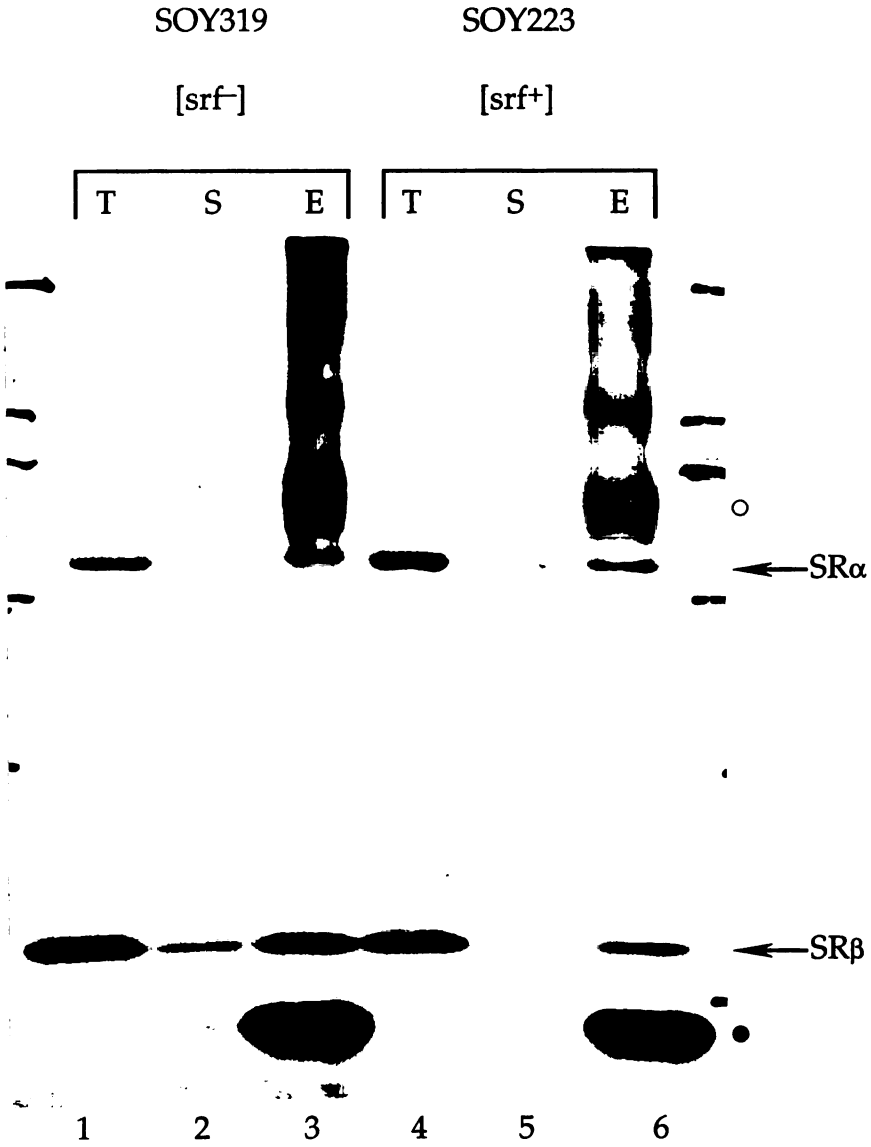
SOY319
[srf−]
SOY223
[srf+]
T
S
E
T
S
E
SRα
SRβ
1
2
3
4
5
6

for characterization). Each fraction is then analyzed by Western blot for the presence of endogenous Srp101p and Srp102p-HA expressed from the plasmid. As expected and described previously, Srp101p fractionates as a peripheral membrane protein and Srp102p fractionates as an integral membrane protein. Roughly equivalent amounts of both Srp102p and Srp101p are present in the total cell lysate from either [srf$^+$] or [srf$^-$] strains (compare Fig. 3A, lanes 1 top panel to bottom panel), suggesting that pSO459 can supply the missing Srp102p, and that the biochemical defect causing the [srf$^-$] phenotype is not at the level of protein expression. Importantly, the pattern of fractionation is identical between the [srf$^+$] and the [srf$^-$] strain (Fig. 3A lanes 1-13, compare the two strains within each panel). This suggests that in [srf$^-$] strains, to a first approximation, the Srp102p that is being expressed from the reintroduced plasmid is properly localized and able to recruit Srp101p to the membrane.

We have previously shown that Srp101p and Srp102p are found associated with one another in the ER membrane (see Chapter 3). The two proteins can be coimmunoprecipitated from native detergent extracts of yeast microsomes. Given the apparently normal expression and localization of Srp102p in [srf$^-$] strain SOY319, we asked whether Srp101p and Srp102p could be coimmunoprecipitated from this strain. Fig 3B shows that Srp101p and Srp102p are associated in the [srf$^-$] strain (SOY319). We immunoprecipitated Srp102p-HA with anti-HA antibodies from extracts prepared by detergent solubilization of yeast microsomal membranes under non-denaturing conditions. Anti-HA antibodies were coupled to protein A-Sepharose beads to allow the isolation of immune complexes. Immune complexes were subsequently solubilized in SDS sample buffer and subjected to SDS-PAGE

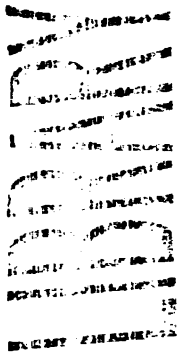

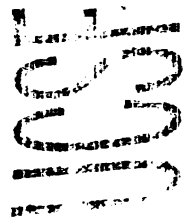

Table IV

Estimate of Switch Frequency. Two independent cultures of [srf$^-$] strain SOY319 were grown exponentially for 50 hours. At time = 0h and at time = 50h, aliquots of each of the cultures were diluted and plated at a density of approximately 500 colonies per plate. Three plates at each time point from each culture were utilized to get an accurate count. Colony size was used as an indicator of the [srf] state. Small colonies were considered [srf$^-$], while big colonies would have been considered [srf$^+$]. In no cases after 50 hours of growth do we observe switching of a [srf$^-$] cell to a [srf$^+$] cell. After growth of the cultures, we noticed some variation in the size of colony formed on a plate. About 10% of the colonies were of intermediate size (90% small), restreaking 30 of these intermediate colonies gave rise to streaks containing both small and medium sized colonies, therefore we conclude that the original 10% growing into medium sized colonies are still considered to be [srf$^-$].

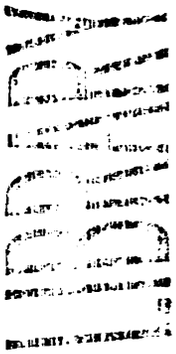

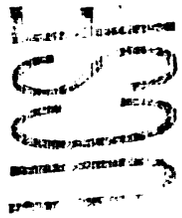

Table IV Switch Estimate

Culture	Number of cells plated at time = 0h		Number of cells growing fast at time= 0h	Number of cells plated at time = 50h		Number of cells growing fast at time= 50h
1	plate 1	367	0	plate 1	512	0
	plate 2	429	0	plate 2	832	0
	plate 3	396	0	plate 3	625	0
2	plate 1	555	0	plate 1	593	0
	plate 2	509	0	plate 2	657	0
	plate 3	586	0	plate 3	629	0

followed by Western blot analysis. The blots were probed with affinity-purified polyclonal antibody directed against Srp101p and monoclonal anti-HA antibodies. As a control we used a congenic [srf$^+$] strain. Starting from equivalent amounts of solubilized yeast microsomal membranes, roughly equivalent amounts of Srp101p are precipitated from both the [srf$^+$] and the [srf$^-$] strains (Fig. 3B, compare lane 3 to lane 6). Taken together, the data in Figure 3 and Table III suggest that the [srf$^-$] phenotype is not caused by such trivialities such as altered expression, or mislocalization of Srp102p. Unexpectedly, even in [srf$^-$] strains we find apparently normal complex formation between Srp101p and Srp102p, suggesting that both Srp101p and Srp102p are able to interact in a functional manner, even though the complex has minimal restorative properties on growth.

We wanted to know how stable the [srf$^-$] phenotype was. To assess this directly, we grew [srf$^-$] cells for many generations in liquid culture and then plated out these cells and asked what size colony they formed. We reasoned that if a cell had mutated to restore its growth rate to near wildtype levels, this change would be reflected in the cell's ability to form a large sized colony. To put a limit on the stability of this phenotype, we grew a culture containing [srf$^-$] cells until it reached mid log phase. At this point, 10^6 cells were diluted into fresh media and kept in log phase for 50 hours (see Materials and Methods for the calculation). We know that at time zero these 10^6 cells still remain [srf$^-$], because a sample plating at the time of dilution results in all of the plated cells giving the characteristic [srf$^-$] sized (small) colonies (Table IV). If, however, we assume that at the time we diluted these cells into fresh media (time = 0), one of the cells had undergone a mutation such that now it

Table V

Transfer of cytosol from a [srf$^+$] cell to a [srf$^-$] cell does not convert a [srf$^-$] cell to [srf$^+$]. Strains SOY327 [srf$^-$] and SOY328 [srf$^+$] were each mated to strain SOY326 (wt). Each of these strains also contain disruptions of the *KAR3* gene. This mutation does not prevent the plasma membranes of mating pairs from fusing, but blocks nuclear fusion, thus preventing the formation of diploids. Because the [srf$^-$] strain is also [rho$^-$], and the [srf$^+$] strain has been rendered [rho$^-$] (while the wildtype is [rho$^+$]), the rare cytoductant that results from the failed mating can be selected. Cytoductants were selected on plates containing only ethanol and glycerol as carbon sources and lacking adenine and uracil, in order to select for the *SRP101* disruption, and the plasmid containing wildtype *SRP101* gene from the [srf$^-$] strain (pSO211), and cytosol from the [srf$^+$] strain.

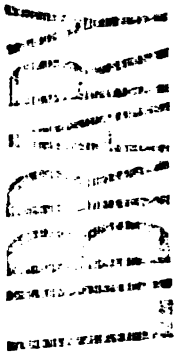

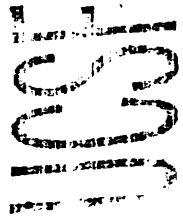

Table V **cytosol does not contain a factor that complements the [srf−] phenotype**

Mating	cytoductant colony size	
SOY326 X SOY327 [srf−]	1	small
	2	small
	3	small
	4	small
	5	small
	6	small
	7	small
	8	small
SOY326 X SOY328 [srf+]	1	wt
	2	wt
	3	wt
	4	wt
	5	wt
	6	wt
	7	wt
	8	wt

was growing with a near wildtype doubling time, we can calculate the time it should take for the offspring of that single cell to reach 50% of the population in the culture (time = 50 h, see methods). The results of this experiment are shown in Table IV. Even after prolonged exponential growth in liquid culture, none of the cells plated from any of the cultures examined had regained the ability to grow with near wildtype rates (i.e., all of the plated colonies grew with reduced rates, and were therefore [srf$^-$]). Thus, we can conclude that the frequency of switching from [srf$^-$] to [srf$^+$] is less than one in 10^6 cells.

Earlier, we postulated that the [srf$^-$] phenotype is due to a requirement for functional SRP receptor in the ER in order to promote the proper maturation of newly synthesized–but inactive–SRP receptor into functional SRP receptor. In [srf$^-$] cells, there is no preexisting SRP receptor to promote this conversion, thus, transformation of an SR encoding plasmid into a [srf$^-$] strain does not result in complementation of the growth phenotype. We wanted to know if we could provide functional SR to the [srf–] cells via an alternative method. We asked if we could provide functional SRP receptor in trans with the following genetic experiment. We selected cytoductants from a cross consisting of a [srf$^-$] strain to a wildtype strain. We reasoned that the ER/cytosol from the wildtype strain would provide functional SRP receptor to the plasmid expressed (but non-functional) SRP receptor in the [srf$^-$] strain. As a control we performed the same cross with a [srf$^+$] strain. To select cytoductants, all strains were deleted for the *KAR3* gene so that the cells would mate, but mating would not result in the production of diploids. We selected the *SRP101* gene deletion and plasmid from the [srf$^-$] or [srf$^+$] strain, and the cytoplasm from the wildtype strain. From a single mating, eight

Figure 4

A model to explain the [srf⁻] phenotype. In the wildtype ("[srf⁺]") situation, extant functional SR (SR^{active}) is required in a positive feedback loop to catalyze the formation of newly synthesized SR ($SR^{inactive}$) into SR^{active}. In the [srf⁻] situation, however, the continuity of the ER has been disrupted by deleting a component of the SR. In this scenario SR^{active} is lacking. Thus, providing new $SR^{inactive}$ does not restore the growth of the cells.

[srf–]

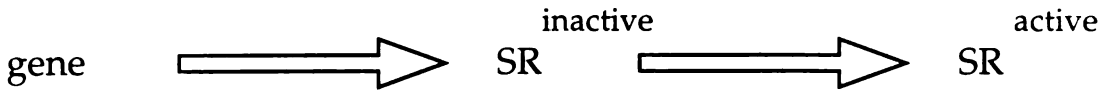

[srf+]

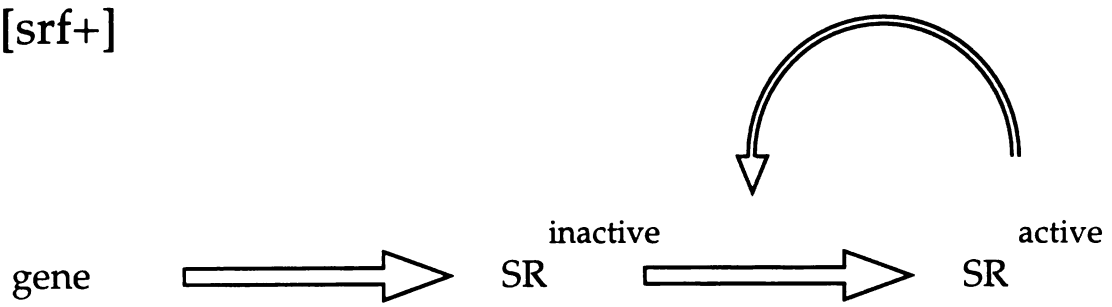

cytoductants were isolated from each cross. All 16 were verified to be haploid, contain the *SRP101* gene deletion, and plasmid expressing Srp101p. Cytoductants derived from the cross between the wildtype and [srf⁻] strains still grow with the characteristic [srf⁻] growth rate (Table V, "small"), even though these cells now contain cytosol from a wildtype strain (presumably containing functional SR). Two important conclusions can be drawn from this result. It suggests that the cytosol of a wildtype strain does not contain an activity capable of complementing the [srf⁻] phenotype. In addition, we have uncoupled the [srf⁻] phenotype from the rho⁻ phenotype. Because these strains were selected for their ability to grow on a carbon source containing only ethanol and glycerol, functional mitochondria can be maintained in these cells. Thus, the inability of the SR encoding plasmid to complement the SR gene deletion is not due to the loss of mitochondrial function.

Table I **Yeast Strains Used in This Study**

Strain	Genotype	Source
W303	MATα *ura3-1, ade2-1, trp1-1, leu2-3-112, his3-11 can1-100*	Deshaies and Schekman (1990)
SOY223	MATa *srp102::HIS3*, pSO459 [srf–]	This study
SOY319	MATa *srp102::HIS3*, pSO459 [srf+]	chapter 3
SOY100	MATα *srp101::ADE2* pSO211 [srf+]	chapter 2
SOY34	MATα/MATa *SRP101/SRP101::ADE2*	chapter 2
SOY36	MATα *srp101::ADE2*	chapter 2
SOY134	MATα/MATa *SRP102/SRP102::HIS3*	chapter 3
SOY324	MATα *srp101::ADE2* pSO211 [srf–]	This study
SOY326	MATa *kar3::LEU2*	This study
SOY327	SOY324 *kar3::LEU2*	This study
SOY328	SOY100 *kar3::LEU2* [rho–]	This study
WBY6	MATα/MATa *SRP54/SRP54::TRP1* pSRP54	This study
SOY162	*srp102::HIS3*	This study
SOY163	*srp102::HIS3*	This study
SOY167	*srp102::HIS3*	This study
SOY168	*srp102::HIS3*	This study
SOY170	*srp102::HIS3*	This study
SOY172	*srp102::HIS3*	This study

SOY175	*srp102::HIS3*	This study
SOY177	*srp102::HIS3*	This study

DISCUSSION

An epigenetic event confers a heritable phenotype that is not dictated solely on the basis of genotype. In this case, the heritable phenotype is the inability to reestablish growth in the presence of the wildtype protein. Other known examples of epigenetic inheritance include transcriptional silencing of the mating type cassettes (Pillus and Rine, 1989), as well as at chromosome telomeres in *Saccharomyces cerevisiae* (Gottschling et al., 1990), position effect variegation in Drosophila melanogaster (reviewed in Henikoff, 1990), and X chromosome inactivation (reviewed in Lyon, 1992) . We have established that complementation of the SRP receptor in the yeast *Saccharomyces cerevisiae* with a plasmid encoding the wildtype gene also falls into this category. We have described the phenomenon and now we are in a position to elucidate the proteins responsible for the phenotype.

Why are components of the SR only partially able to function when they are provided with seemingly wildtype constituents? Clearly something changes within the cells after they have been deprived of the SR. Whatever this change is, it must be epigenetic, as the entire system can be "reset" to the ground state simply by going through the diploid phase. We speculate that the difference between [srf$^+$] and [srf$^-$] cells is that the [srf$^-$] cells were at one point in their life, devoid of functional SR. As previously described, our model (Figure 4) interprets this and provides a satisfying hypothesis: active SR provides a "templating" function upon which newly synthesized–but inactive–SR can assemble into functional, active SR.

Alternatively, in the absence of any one of the components of the SRP dependent protein translocation pathway, other components may be down

regulated such that the alternative translocation pathway may assume the duties of translocation in the cell. That is, components needed for the SRP dependent translocation pathway may be coordinately regulated. Let's assume that this is the situation that exists upon deletion of one of the components of the SR. Reintroduction of one component of the SRP pathway, as a protein expressed from a plasmid, may not result in the other components becoming up-regulated. We would then have a situation where we have seemingly functional SR, but some other –as yet unknown– component of the pathway has become rate-limiting for growth and is not up-regulated in response to the return of the SR. This is not the case for deletion of SRP components, however, and this fact argues that the [srf] phenotype may be unrelated to adaptation (see below). In the case of an SRP deletion, we would envisage that the cell would be capable of restoring the SRP dependent translocation pathway upon restoration of the deleted component.

We already know of one thing that changes when the cells are deleted of SRP pathway components. In Chapter 2, I described "adaptation" as the ability of a cell that is missing part of the SRP pathway to change the way it translocates proteins. As a response to loss of the SRP pathway, cells can either upregulate limiting components of the alternative, SRP-independent translocation pathway, or increase a pathway for degrading the accumulated precursor proteins. This description arose from the observation that cells harboring an *srp101* gene deletion did not accumulate precursors to many of the proteins known to enter the secretory pathway. Depletion of Srp101p, under the control of a regulatable promoter, however, resulted in a much greater defect in translocation. Adaptation, like the [srf] phenotype is also an epigenetic state, not caused by mutation of any genes. Because there are two

translocation pathways into the yeast ER, it seems logical to propose that in the absence of the SRP dependent pathway (*SRP101* deletion) proteins can be shunted into the alternative translocation pathway. Perhaps adaptation and the [srf] phenotype are linked. Can we use this model to account for the [srf⁻] phenotype?

Our cytoduction experiment implies that not only is the cytosol devoid of a component that can complement the [srf⁻] phenotype, but during the aborted mating, ER from one mating partner does not mix with ER from the other mating partner. If it did, we would expect that SR^{active} would be transferred to the cytoductant, and the [srf⁻] phenotype would be complemented. It is interesting, therefore to note the cytological defect of the *kar3* disruption. In matings where both partners are *kar3* deletions, the plasma membranes fuse, but the nuclei fail to congress (Kurihara et al, 1994). Because in yeast, the ER is closely juxtaposed to the nucleus, it is tempting to speculate that in the *kar3* deletion we have prevented the ER from fusing. Perhaps if we would try the same experiment with a different KAR gene (one that would prevent diploid formation, but allow the congression of the nuclei, see (Kurihara et al., 1994)) we could complement the [srf⁻] phenotype.

As permeability barriers, membranes must be continuously maintained for the cell to remain in homeostasis. In addition, membranous organelles within the cell must be defined. If the organelles are defined by their steady state constituents, and these constituents in turn are targeted to the organelle through the action of a set of proteins, then it follows that the set of proteins required to target an organelle's components are ultimately responsible for defining the organelle. For example, in the present case, we have evidence that in the absence of the SR, the ER membrane becomes

undefined. So much so, that even after we restore SR expression it doesn't restore the growth of the cell. Because the SR is one of the steady state components of the ER, it may be the loss of the SR that causes loss of ER definition. Alternatively, we could say that the SR is required for the proper maintenance of the ER. This idea was first postulated by George Palade, who said:

> "Therefore, it can be logically postulated that membranes act as their own templates by the interplay of specific signals and specific signal receptors. Cellular membranes are endowed with spatial, temporal, and functional continuity." (Palade, 1977)

Spatial continuity is provided by the physical chemistry of the lipid bilayers. There are no discontinuities of membranes within the cell. Each membrane is continuous with itself. Temporal continuity is also a property of cellular membranes. Each daughter cell inherits from its mother, a complete set of cellular membranes. There are no membrane bound organelles which are regenerated after each round of cell division. Spatial and temporal continuity must exist to ensure functional continuity. With respect to the present situation, we infer that SR is required to ensure the functional continuity of the ER. The permeability barriers maintained throughout a cell's life are capable of being transmitted without interruption through many cellular generations.

REFERENCES

Brown, J. D., Hann, B. C., Medzihradszky, K. F., Niwa, M., Burlingame, A. L. and Walter, P. (1994). Subunits of the *Saccharomyces cerevisiae* signal recognition particle required for its functional expression. EMBO J. *13*, 4390-4400.

Gottschling, D. E., Aparicio, O. M., Billington, B. L. and Zakian, V. A. (1990). Position effects at S. cerevisiae telomeres: reversible repression of pol II transcription. Cell *63*, 751-762.

Guthrie, C. and Fink, G. R. (1991). Guide to yeast Genetics and Molecular Biology. Meth. Enz. *194*, 933 pp. Academic press, Inc, San Diego.

Hann, B. C. and Walter, P. (1991). The Signal Recognition Particle in *S. cerevisiae*. Cell *67*, 131-144.

Henikoff, S. (1990). Position effect variegation after 60 years. TIGS *6*, 422-426.

Kurihara, L. J., Beh, C. T., Latterich, M., Schekman, R. and Rose, M. D. (1994). Nuclear congression and membrane fusion: two distinct events in the karyogamy pathway. J. Cell Biol. *126*, 911-923.

Lyon, M. F. (1992). Some milestones in the history of X-chromosome inactivation. Annu. Rev. Genet. *26*, 16-28.

Ogg, S., Poritz, M. and Walter, P. (1992). The signal recognition particle receptor is important for growth and protein secretion in *Saccharomyces cerevisiae*. Mol. Biol. Cell *3*, 895-911.

Palade, G. 1977. Membrane biogenesis. Molecular specialization and Symmetry in Membrane Function Solomon, A.K. & Karnovsky, M., Eds. Harvard University Press, Cambridge. 3-30.

Pillus, L. and Rine, J. (1989). Epigenetic inheritance of transcriptional states in *Saccharomyces cerevisiae*. Cell *59*, 637-647.

Sambrook, J., Fritsch, E. M. and Maniatis, T. 1989 Molecular Cloning: a laboratory manual. Cold Spring Harbor Laboratory Press. Plainview. Pages pp.

Sherman, F. and Lawrence, C. 1974. *Saccharomyces*. Handbook of Genetics King, R.C., Eds. Plenum Press, New York. 359-393.

Tajima, S., Lauffer, L., Rath, V. L. and Walter, P. (1986). The signal recognition particle receptor is a complex that contains two distinct polypeptide chains. J. Cell Biol. *103*, 1167-1178.

Walter, P. and Johnson, A. E. (1994). Signal Sequence Recognition and Protein Targeting to the Endoplasmic Reticulum Membrane. Ann. Rev. Cell Biol.*10*, 87-119.

Chapter 6

Perspectives

Perspectives

In this thesis I describe the initial cloning and characterization of the yeast SRP receptor (Chapters 2 and 3). In addition, I describe some vignettes which began as intriguing, but unexplained observations (Chapters 4 and 5). I began this thesis with the intention of following a straight scientific line from point A (entering graduate school) to point B (graduating from graduate school) along a route that would be easy to follow. I reasoned that I would make the knockout of the *SRP101* gene, followed by random mutagenesis, followed by suppressor analysis. The suppressor analysis would lead to the identification of the SRβ, which I would characterize and then mutate, to dissect the contribution of the suspected SRβ–GTPase to translocation. What actually happened was something quite different. Finally, six years later, I am almost to point B, but the route has been a circuitous one. Several unexpected findings contributed to my wandering off the straight and narrow path. One unanticipated finding is described in chapter two, and is the phenomenon I call "adaptation". Another observation that required some amount of detour, finally became chapter four. Initially, we only knew that cycloheximide would suppress the growth defect of *sec65-1* cells. Visually, this was an impressive result, certainly worth pursuing (see Chapter 4, Figure 2). Yet another unexpected observation was that haploid yeast cells containing SR deletion could not be complemented by reintroduction of the deleted component. Again, this observation was expanded and strengthened, until it too became a chapter in this thesis (Chapter 5). Although the circuitous route may not have been the fastest, it was the most satisfying. We have learned many things about the SRP-dependent protein targeting pathway as a result of these several detours. None of which would have been uncovered if I had

worn blinders and forged ahead with my original plans. I believe that this work strengthens the case for the SRP pathway in yeast, as well as providing fertile ground for new experiments. Many questions remain unanswered, most importantly, how do three interacting GTPases (Srp54p, Srp101p, and Srp102p) contribute to targeting and translocation. Although the next experiments are clear, the challenge now is to decipher the meaning behind the observations that we already have that may tell us something about how the cell functions.